Regulation and pathomechanistic role of matrix metalloproteinases in Idiopathic Pulmonary Fibrosis.

Dissertation submitted in partial fulfilment of the degree of Doctor of Philosophy of Science in the Faculties of Veterinary Medicine and Medicine of the Justus-Liebig University Giessen.

by

Eusebius Henry Nkyimbeng Takwi,

from Mankon, Cameroon.

Department of Internal Medicine II

Universitätklinikum Giessen und Marburg GmbH

Giessen, 2008

Aus dem Medizinischen Zentrum für Innere Medizin

Medizinische Klinik und Poliklinik II

Direktor: Prof. Dr. Med. Werner Seeger

des Fachbereichs Medizin der Justus-Liebig-Universität Giessen

Dekan: Prof. Dr. Dr. Georg Baljer (Faculty of Veterinary Medicine)

Dekan: Prof. Dr. Wolfgang Weidner (Faculty of Medicine)

1. Gutachter: Prof. Dr. Andreas Günther

2. Gutachter: Prof. Dr. Jeanine D'Armiento

Prüfungsvorsitzender: Prof. Dr. Martin Diener

Beisitzer: Priv.-Doz. Dr. Konstantin Mayer

Tag der Disputation: 28th August, 2008

Index of figures

Index of Tables

1. INTRODUCTION

1.1 Physiology of the Lung

1.1.1 Functional anatomy of the lung

The primary function of the lung is to provide a sufficiently sized and highly efficient area for gas exchange. In addition, the lung also serves as a reservoir for blood, moves air to and from the exchange surfaces of the lungs, protects the respiratory epithelia from dehydration, temperature changes, or other environmental variations and defends the respiratory system and the organism from invasion by pathogens. Respiratory diseases frequently interfere with ventilation, blood flow and gas exchange and might ultimately lead to respiratory failure and death.

The respiratory tract consists of the airways that carry air to and from the exchange surfaces of the lungs. The *conducting airways* consist of a series of branching tubes that become narrower, shorter and more numerous as they penetrate deeper into the lung, eventually reaching the terminal bronchioles which are the smallest airways without alveoli. Their function is to lead inspired gas to the gas-exchanging regions of the lung. Since they lack alveoli and therefore take no part in gas exchange, the conducting airways form the *anatomic dead space*. The *respiratory portion* of the airways includes the delicate *respiratory bronchioles* and the *alveoli* where gas exchange occurs; it makes up most of the lung and has a volume of 2 to 3 litres in adult humans.

The cellular composition of the airways is complex, comprising nearly 50 distinct cell types, at least 12 of which are epithelial cells on the surface of the conducting airways, respiratory bronchioles and alveoli.

The lung has two well defined interstitial connective tissue compartments arranged in series: the parenchymal interstitium and the loose binding connective tissue (peribronchovascular sheaths, interlobular septa and visceral pleura)[1]. The parenchymal interstitium of the alveolar wall makes up about 33% of the total interstitial volume. These two compartments have significant anatomical and functional differences. For instance, collagen type IV is located mainly in the parenchymal compartment, the site where the extensive basement membrane of the capillary endothelium and alveolar epithelium are found; whereas the lymphatics are confined to the loose-binding connective tissue. The bulk of the lung interstitium is occupied by the ground substance and matrix of glycosaminoglycans[1, 2] as well as several different interstitial cells such as mast cells, plasma cells and occasional leukocytes, and fibres such as collagen, elastin and reticulin[3]. The ground substance constitutes a complex group of large polysaccharide molecules whose interactions impart a gell-like structure to the interstitium[2]. Thus the lungs are well designed to fulfill their major physiological role of gas exchange, whereby incoming fresh air is distributed through the branching airways, and in the terminal respiratory units, the mixing of gas occurs largely through molecular diffusion[4]. Incoming mixed venous blood flows through a series of branching arteries into a network of capillaries that provide a thin film of blood in close proximity to the gas in the terminal respiratory units[1]. Thus, the matching of inspired air (ventilation) with incoming poorly

oxygenated blood occurs at the level of the gas exchange units of the lung and thereafter, oxygenated (arterialized) blood flows through a series of pulmonary veins to the left heart for distribution to the tissues of the body[1]. Although gas exchange is nearly perfect in the lungs of healthy individuals, it is often impaired in patients with lung diseases because of hypoventilation, ventilation-perfusion mismatch, or right-to-left shunts[5, 6]. The lungs are also endowed with an elaborate system of nerves, lymphatics and specialized cells that regulate gas exchange, protect the lungs and contribute to host defense properties[7, 8].

1.2 Interstitial Lung Disease

Under physiological conditions, the interstitial space of the lung is a delicate and almost invisible space between the basement membrane of the alveolar epithelium and the alveolar capillary endothelium[9] (see Figure1).

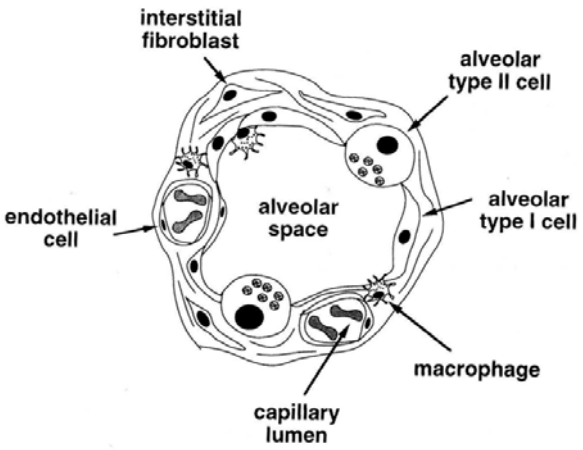

Figure 1: Schematic view of the lung parenchyma that surrounds an alveolar space showing the major cells that line and lie within the putative interstitial space.
(Adapted from Murray Nadel, Textbook of Respiratory Medicine, Volume 2)

Small numbers of interstitial macrophages, fibroblasts and myofibroblasts reside within this potential space. The matrix components of the lung, mainly collagen and related macromolecules, as well as noncollageneous proteins such as fibronectin and laminin[10, 11] make up the other components of the lung interstitium.

Interstitial lung disease (ILD) is a compound phrase for description of more than 100 entities that are causing diffuse parenchymal lung diseases, characterized by a non-malignant increase of the cellularity of the alveolar, interstitial and/or vascular spaces[9]. To some extent, these diseases possess similar clinical, radiographic, and pathophysiological features[12]. However, they are are distinct in view of their underlying etiology and molecular pathophysiology. Patients complain of dyspnea on exertion followed by dyspnea at rest[13-15]. In many ILDs the underlying trigger is unknown but it may, in principle, be due to chronic inflammation (for example, sarcoidosis, hypersensitivity pneumonitis), or a direct epithelial injury resulting in epithelial apoptosis[16]. Lung fibrosis then develops in response to chronic inflammation or repetitive injury of the distal lung epithelium. Regenerative and reparative processes take place at the epithelial and endothelial surfaces, ultimately leading to fibroblastic proliferation and excessive collagen deposition, the histologic hallmark of ILDs[14, 16-18]. The term diffuse parenchymal lung disease (DPLD) which is thought to more fully replace the term ILD, more accurately describes these entities as many DPLDs involve not only the alveolar interstitium but also the small airways of the lungs including the alveolar ducts, terminal and respiratory bronchioles, and lymphatics along the bronchovascular bundle and interlobular septae[9].

1.2.1 Classification of Interstitial Lung Disease

ILDs may develop in response to a variety of causes, e.g. in the frame of collagen/vascular diseases, in response to inorganic (asbestos, silicosis) or organic (hypersensitivity pneumonitis) dusts, or following medical interventions, such as chemo- or radiotherapy[19]. In contrast, the cause for the idiopathic interstitial pneumonias (IIP), (including non-specific interstitial pneumonia [NSIP] and idiopathic pulmonary fibrosis [IPF]), granuloma-forming ILD (sarcoidosis) and some rare forms such as eosinophilic pneumonia, pulmonary Langerhans cell histiocytosis and lymphangioleiomyomatosis, remains unknown up-to-date[19].

Currently, seven distinct subtypes of idiopathic interstitial pneumonias (IIPs) have been proposed by the American Thoracic Society/European Respiratory Society (ATS/ERS) as shown in Table 1[14].

Table 1: ATS/ERS classification of idiopathic interstitial pneumonias

Acute interstitial pneumonia (AIP)
Cryptogenic organizing pneumonia (COP)
Desquamative interstitial pneumonia (DIP)
Lymphoid interstitial pneumonia (LIP)
Nonspecific interstitial pneumonia (NSIP)
Respiratory bronchiolitis-interstitial lung disease (RB-ILD)
Idiopathic pulmonary fibrosis (IPF)

Figure 2: Schematic representation of the major categories of interstitial lung diseases (ILD), showing the overlap among various disorders.
Red = Most frequent forms of ILD in the Western World.

1.2.2 Prevalence of Interstitial Lung Disease

The prevalence and incidence of ILDs is often under-estimated: up to 750,000 patients may suffer from ILDs in the Western World[20], and almost 80% of these patients are diagnosed with sarcoidosis, idiopathic pulmonary fibrosis (IPF)/non-specific interstitial pneumonia (NSIP), or hypersensitivity pneumonia. In this regard, ILDs are less frequent than asthma, but more patients die from ILDs than from asthma each year, illustrating the severity of these diseases[20]. Although some forms of ILD show a generally favorable course (sarcoidosis, early hypersensitivity pneumonitis in case of strict antigen removal), others present with poor prognosis and may even exhibit a rapidly fatal progressive disease course. IPF, which alone may affect up to 150,000 patients in the European Community[20, 21] is characterized by an average survival time of 3-5 years upon diagnosis[14] and represents the most aggressive form of ILD.

1.3 Idiopathic Pulmonary Fibrosis (IPF)

Idiopathic pulmonary fibrosis (or cryptogenic fibrosing alveolitis) [IPF or CFA]
is a distinct type of idiopathic interstitial pneumonia of yet unknown etiology limited to the lungs and associated with a surgical lung biopsy showing a histological pattern of usual interstitial pneumonia (UIP)[13]. IPF is a severe and progressive disease[19, 22] and it is relatively rare. Although the exact prevalence is not known, a prevalence rate of 3 to 6 cases per 10,000 population is estimated[15].

IPF is more frequently diagnosed in men than women, (male: female prevalence ratio of 1.4:1 and a male: female incidence ratio of 1.3:1). Although there is a wide range in the age of IPF patients (35 to 70 years), a majority of patients are over 60 years old. In addition, cases of IPF have been reported in young children and infants[13, 14]. Following diagnosis, the mean survival time is 3.2 to 5 years[18, 19, 23].

1.3.1 Clinical and histological features of IPF

Patients with IPF typically complain of a dry, nonproductive cough and dyspnea for at least 3 to 4 months[13, 14]. Dyspnea is often associated with exertion early in the disease course, but usually progresses to shortness of breath at rest[18]. Physical exercise is progressively diminished and impossible in later stages, even with long-term oxygen treatment[13, 14]. On physical examination, 25% - 50% of patients have evidence of clubbing and bi-basilar, end-expiratory rales are observed in greater than 80% of patients[15]. Late in the course of the disease, cyanosis of the lips and fingers as well as signs of pulmonary hypertension may be seen[24]. Recurrent respiratory infections, in part due to a compromised pulmonary innate immune defense, are a frequent observation and fuel further aggravation of this disease (Guenther,A., personal communication). Faced with an ever diminishing quality of life, the only option for IPF patients is lung transplantation, the long-term outcome being largely limited by fibroproliferation as a result of chronic rejection processes (bronchiolitis obliterans)[25-27]. IPF thus represents a prototypic ILD with a disastrous outcome.

Specific laboratory tests for the diagnosis of UIP are not available. A restrictive pattern is the classic finding on pulmonary function testing in IPF[28]. Greater than 90% of patients with UIP will have abnormal chest radiographs at the time of diagnosis manifesting the characteristic pattern of diffuse bilateral interstitial or reticulonodular infiltrates in the basilar and subpleural regions of the lung [15, 18].

Employing high-resolution computed tomography (HRCT) in IPF reveals coarse reticular or linear opacities (intralobular and interlobular septal thickening) commonly found in the periphery and lower lobes of the lungs, honeycomb cysts, and traction bronchiectasis[29]. Ground glass opacities (ill-defined hazy zones representing active alveolitis or fibrosis of the intralobular and alveolar septae) may be locally present or completely absent [29-31]. Extensive honeycombing, septal thickening, and a lack of ground glass opacities reflect a poor prognosis[18].

A surgical lung biopsy showing a UIP pattern increases the diagnostic certainty of IPF[18]. Video-assisted thoracoscopic surgical (VATS) biopsy is the preferred method of obtaining lung tissue and is generally safe[32, 33].

1.3.2 Diagnosis of IPF

IPF is diagnosed on the basis of clinical, histological and radiological findings[13-15]. Usual interstitial pneumonia (UIP) is the typical histological pattern that characterizes patients with the clinical disease called IPF[12-14, 34]. UIP is characterized by temporal and spatial heterogeneity and the presence of fibroblast foci. These changes are readily seen with low power microscopy, with areas of normal appearing lung tissue

alternating with areas of peripheral fibrosis, inflammatory cells and distortion of the normal lung architecture resulting in the formation honeycomb cysts and fibroblast foci[14, 34, 35]. Honeycomb cysts are enlarged and distorted airspaces, lined by hyperplastic alveolar type II cells, resulting from destruction of the normal alveoli[18]. Fibroblast foci are areas with aggregates of fibroblasts/myofibroblasts and connective tissue located just beneath hyperplastic type II pneumocytes and found at the border between fibrotic and normal lung. The distribution of pathological changes is subpleural, paraseptal and prominent at the bases[14]. A UIP pattern may also be seen in other conditions apart from IPF such as Hermansky-Pudlack syndrome (HPS), hypersensitivity pneumonitis or asbestos-induced lung fibrosis.

1.3.3 The initial trigger of IPF

The alveolar epithelial type II (AECII) cell is thought to be at the center of a pathomechanistic concept for sporadic or familial IPF, and also for other ILDs, such as the Hermansky Pudlack Syndrome (HPS), amiodarone-induced pneumonitis, or irradiation-induced lung fibrosis[16, 36]. Both enhanced AECII cell apoptosis and hyperplasia have been reported in IPF specimen, ultimately inducing distorted epithelial-mesenchymal cross-talk, resulting in enhanced fibroblast activation and ECM synthesis. Ultrastructural studies have revealed the existence of proliferative alveolar epithelial cells immediately adjacent to injured epithelial cells[37-39], suggesting that epithelial apoptosis and proliferation and hyperplasia occur simultaneously during the process of fibrosis. According to this concept, chronic endoplasmic reticulum (ER) or lysosomal stress have been reported to induce AECII

cell apoptosis and thus set the stage for the development of lung fibrosis[37-39]. In detail, mutations in the *SFTPC* {Surfactant Protein (SP)-C}[40] and the *TR/TERT* (telomerase)[41] genes in familial forms of idiopathic interstitial pneumonias (mostly IPF and NSIP) provided initial evidence that ER-stress-induced apoptosis of AECII cells may represent an important pathogenetic trigger event[40]. Furthermore, activation of ER stress pathway components including endoplasmic reticulum to nucleus signaling 1 (ERN1) (by proof of X-box binding protein (XBP) 1 splicing) and activating transcription factor 6 (ATF6) was observed in sporadic IPF and NSIP, and found to result in a persistent and overwhelming ER stress response and induction of epithelial apoptosis via DNA-damage-inducible transcript 3 (DDIT3)[42]. Drawn against this background it seems noteworthy that respiratory infections represent a common phenomenon in IPF[43]. These respiratory infections frequently antecede the clinical appearance of the disease and also accelerate the clinical course. Consistent with these observations, bacterial[44], and – even more compelling – viral[45] infections can induce severe ER-stress. Thus, an intriguing and unifying concept for sporadic and familial IPF would consist of a genetic predisposition to an epithelial injury, a modifying environmental stimulus and a common downstream pathway resulting in fibrosis based on ER stress (or DNA damage) induced AECII cell apoptosis. Other diseases resulting in chronic AECII cell injury, such as HPS, amiodarone- or irradiation-induced lung fibrosis, might similarly result in epithelial apoptosis and subsequent fibrosis[46], and could thus be integrated into this concept.

1.3.4 Mediators of distorted epithelial-mesenchymal interactions in lung fibrosis

Balanced epithelial-mesenchymal interactions are of the utmost importance for proper lung development, in particular for regular definition of a proximal-distal axis and dichotomous branching[47]. In the adult lung, mesenchymal-epithelial interactions warrant proper lung function and are a prerequisite for the maintenance of the trophic alveolar unit, but impaired epithelial-mesenchymal crosstalk between AECII cells and subepithelial fibroblasts, as well as dysregulated precursor cell recruitment, have recently been shown to contribute to the pathobiology of IPF[17, 48]. It has been proposed that the AECII, by action of cyclooxygenase 2, releases PGE2, which then binds to the EP-2 receptor on fibroblasts, increases cAMP levels in the fibroblast and thereby inhibits the proliferation and transactivation of this cell [49]. In addition, several growth factors are released by the AECII cell that control the fibroblast phenotype, such as members of the Wnt, BMP, or TGF-β superfamilies[50]. In particular, enhanced secretion and/or activity of Wnt and TGF-β superfamily members have been documented in IPF[9, 51]. The fibroblast itself is a rich source of FGF-7, FGF-10, and HGF. HGF will be released by fibroblasts in dependency of cAMP levels and must be activated by extracellular serine proteases such as the HGF activator. FGF-7, FGF-10, as well as HGF are known to exert a marked influence on AECII cell proliferation, migration and survival[52] and at least HGF has been shown to be released to a much weaker extent from IPF fibroblasts as compared to fibroblasts from healthy lungs[52].Thus, loss of regenerative capacity of the resident AECII cell

population due to loss of FGF-7, FGF-10, or HGF may contribute to the pathogenesis of IPF.

1.3.5 Origin of activated (myo-)fibroblasts in IPF

While the initial injury in IPF is most likely affecting the AECII cell (see above), it is well accepted that the interstitial fibroblast/activated myofibroblast represents the key effector cell responsible for the increased ECM deposition that is characteristic for this disease[16, 36]. Fibroblast foci represent the hallmark lesions of IPF, as they constitute aggregates of activated myofibroblasts, which promote excessive ECM deposition[23]. The occurrence of fibroblast foci represents an important prognostic factor, since their numbers have been correlated with survival in IPF[53]. Fibroblast foci occur in subepithelial layers, close to areas of alveolar epithelial cell injury and repair. The number of smooth-muscle-actin-positive, activated (myo)fibroblasts is significantly increased in multiple forms of pulmonary fibrosis including IPF, but their origin remains to be elucidated. Currently, three major theories attempt to explain this hallmark of maladaptive cell activation. It has been demonstrated that resident pulmonary fibroblasts proliferate in response to fibrogenic cytokines and growth factors, thereby increasing the local fibroblast pool via local fibroproliferation[54, 55]. In addition, several recent studies have shown that bone marrow-derived circulating fibrocytes traffic to the lung during experimental lung fibrosis, and serve as progenitors for interstitial fibroblasts[56]. In particular, collagen I-positive fibrocytes have been shown to traffic to injured lungs in a chemokine-dependent fashion, integrate into the lung ECM, and contribute to enhanced collagen synthesis in fibrosis[56-58]. Third, it was recently proposed that AECII cells are capable of

undergoing the process of epithelial-to-mesenchymal transition (EMT), the phenotypic, reversible switching of epithelial to fibroblast-like cells, which is initiated by an alteration of the transcriptional and proteomic profile of AECII cells[59, 60]. EMT is a highly controlled process initially discovered and described in embryonic development and morphogenesis[59]. The orchestrated series of events initiating EMT include remodeling of epithelial cell-cell and cell-matrix adhesion contacts, reorganization of the actin cytoskeleton, and induction of mesenchymal gene expression. EMT has gained wide recognition as a mechanism that facilitates cancer progression and metastasis, as well as the development of chronic degenerative fibrotic disorders of the kidney, liver, and lung[61-64]. Transforming growth factor beta (TGF-β) is a main inducer and regulator of EMT in multiple organ systems[65].

1.3.6 Major signaling pathways underlying matrix remodeling in the lung

As part of a primary wound healing response, activation of the coagulation cascade and suppression of the fibrinolysis system has been observed in patients with IPF [66, 67], and the cellular origin of these coagulation factors (alveolar macrophages and alveolar type II cells) was recently shown[68]. Analysis of bronchoalveolar lavage fluids (BALF) revealed substantial activation of the extrinsic coagulation pathway (tissue factor[TF]; FVII), alongside with pronounced suppression of antithrombotic (activated protein C) or fibrinolytic (Plasminogen Activator Inhibitor [PAI]-1) activities[66, 69]. These changes promote alveolar and interstitial fibrin deposition, forming a provisional matrix and thereby substantially contributing to lung fibrosis[70]. Moreover, several procoagulant serine proteases such as TF/FVII, factor X and thrombin

induce fibrotic events via the Protease activated receptor (PAR)-1 and PAR-2[71]. In response to the activation of this G-protein coupled receptor, increased ECM production and secretion and induction of profibrotic growth factors such as TGF-ß and PDGF can be observed[71]. Vice versa, the urokinase system has repeatedly been shown to exert strong antifibrotic activity, most likely due to the activation of HGF and the removal of fibrin and ECM[72]. Persistent suppression of urokinase by PAI-1 overexpression, as seen in IPF patients and in animal models of lung fibrosis, would thus contribute to the development of lung fibrosis[72, 73]. Alveolar deposition or overexpression of urokinase, knock out of PAI-1 or inhibition of the procoagulant pathways by heparin, factor Xa antagonists, direct thrombin inhibitors or activated protein C were shown to result in a substantial suppression of the fibrotic response in the bleomycin model of lung fibrosis, whereas knock out of urokinase or alveolar PAI-1 overexpression induced the opposite effect[73, 74].

With respect to scar formation as aberrant alveolar/interstitial wound healing response, there is currently no doubt that the TGF-β family represents the pivotal mediator system[75-78]. In vitro, TGF-β induces fibroblast chemotaxis, proliferation and transdifferentiation into myofibroblasts, and it largely promotes the production and secretion of extracellular matrix compounds, mainly collagen. Application of TGF-β encoding adenoviral vectors to the distal lung induces a progressive and severe lung fibrosis[79]. Likewise, application of these vectors to the pleural space induces pleural fibrosis and subpleural lung fibrosis as seen in IPF. Increased TGF-β signaling is also observed in other animal models of lung fibrosis, such as the

bleomycin model, where collagen deposition is reduced by TGF-β antibodies and soluble TGF-β receptors[80]. In lungs of IPF patients, increased expression of TGF-β has been observed in close proximity to areas of increased ECM deposition[81]. Apart from TGF-β, there are also other growth factors such as PDGF (platelet-derived growth factor), CTGF (connective tissue growth factor), members of the Wnt pathway, or IGF-I (insulin-like growth factor I) and endothelin, which may significantly contribute to the pathogenetic sequelae of IPF[75].

Apart from the proliferation of fibroblasts, the excessive deposition of matrix is a key feature of IPF and, most likely, is the result of excessive production of ECM compounds and a local imbalance between the matrix metalloproteinases (MMP) and their inhibitors (TIMP). In general, increased expression of TIMPs -1, -2 -3 and -4 and virtual absence of the collagen I specific MMP-1 has been observed in the lungs of IPF patients[82], thus contributing to collagen deposition. In view of the coexistence of fibrotic scars and honeycomb cysts in the lungs of IPF subjects, it is yet not settled, if a spatial disarrangement of the collagenases (largely MMP-1) and the TIMPs may be the primary reason for the development of this structural heterogeneity[82, 83]. In contrast, the two gelatinases MMP 2 and 9, known for their ability to destruct the basement membrane and thus to impair epithelial regeneration, were found to be increased in lung fibrosis[84]. Matrilysin (MMP-7) was also found to be highly upregulated in IPF[85, 86] and NSIP[85] by oligonucleotide microarray analysis and immunohistochemistry[87]. In addition, MMP-7 knock out mice were protected from the bleomycin induced lung fibrosis[86] thus suggesting that

MMP-7 is a key regulatory molecule in the pathogenesis of IPF and that it may directly or indirectly actively participate in pulmonary fibroproliferation[88] . In contrast, MMP-9 KO mice showed decreased alveolar bronchiolization after bleomycin-induced lung fibrosis[89] and MMP-12 KO mice were not protected from bleomycin-induced lung fibrosis[90]. Taking these together, underscores the important contribution of single MMPs in the dynamic regulation of the ECM and of remodeling processes in the lung[91].

1.3.7 Influence of genetic background in IPF pathogenesis

Familial forms of IPF occur in approximately 10-20% of all IPF cases and are characterized by variable penetrance[41, 92, 93]. The following gene mutations have been disclosed.

1.3.7.1 Surfactant Protein C mutations

Two families carrying separate mutations in the surfactant protein (SP)-C gene were reported with progressive pneumonitis and lung fibrosis[40]. SP-C is hydrophobic protein and a normal component of alveolar surfactant. It is synthesized in a proform requiring C-terminal proteolytic processing for proper folding, assembly with lipid, and secretion[40, 94, 95]. Childhood onset of interstitial pneumonitis and pulmonary fibrosis was reported in a family carrying an SP-C mutation[40, 41, 92, 96]. The mutation results in a truncated form of SP-C that accumulates in the endoplasmic reticulum of type II alveolar epithelial cells[40, 96]. A mutation, L188N, in the C-terminal SPC region

was found in some family members affected with disease, and also in two unaffected obligate heterozygote family members[97]. Expression of the mutant SP-C protein in murine alveolar cells resulted in accumulation of proSP-C and cell toxicity, suggesting that misfolded SP-C, through induction of ER stress, may cause AECII cell apoptosis and lung fibrosis[97].

1.3.7.2 Telomerase mutation

Telomerase, a specialized polymerase that adds telomere repeats to the ends of chromosomes has two essential constituents: telomerase reverse transcriptase (hTERT) required for catalysis and an RNA component called hTR[98, 99]. Dyskeratosis congenita is a rare hereditary disorder initially described on the basis of a triad of mucocutaneous manifestations: skin hyperpigmentation, oral leukoplakia, and nail dystrophy[100]. Twenty percent of patients manifest with pulmonary fibrosis, which is the second most common cause of death[41]. Armanios and colleagues recently reported a pedigree with autosomal dominant dyskeratosis congenita that carried a null *hTERT* allele. Idiopathic pulmonary fibrosis was the only manifestation of disease in a patient with a carrier mutation[100]. The presence of pulmonary fibrosis in dyskeratosis congenita, along with the presence of telomerase mutations in some families with IPF[41], suggests that the fibrotic lesion in patients with short telomeres is provoked by a loss of alveolar cells[41]. Therefore, damage of epithelial cells leads to a remodeling response that manifests as UIP/IPF.

1.3.8 Treatment of lung fibrosis- translational approaches

In striking contrast to the field of PAH, a disease previously characterized by a similarly poor outcome, the therapeutic approach to patients with IPF has not changed dramatically over the last 10 years[101, 102]. Apart from standard care, including long-term oxygen treatment, aggressive and early treatment of respiratory infections, and early listing for lung transplantation if suitable, all recently finished phase II/III trials exhibited unsatisfactory results[18, 102]. Interferon-γ was definitely proven to be ineffective in IPF, Pirfenidone (targeting the TGF-β pathway), as well as bosentan (targeting the endothelin pathway), have provided initial hope, but failed to significantly affect primary study endpoints[102, 103]. The only larger trial in IPF with a significant improvement in the primary study endpoint, albeit with a high drop out rate (1/3 of all patients), was the IFIGENIA trial, in which n-acetyl cysteine was tested against placebo and was found out to attenuate the loss of lung function[102]. In the meantime, an encouraging increase in clinical trials in the field of IPF can be observed. Most of these studies are addressing secondary processes forwarding fibrosis *per se*. An overview is given in figure 3 outlined below.

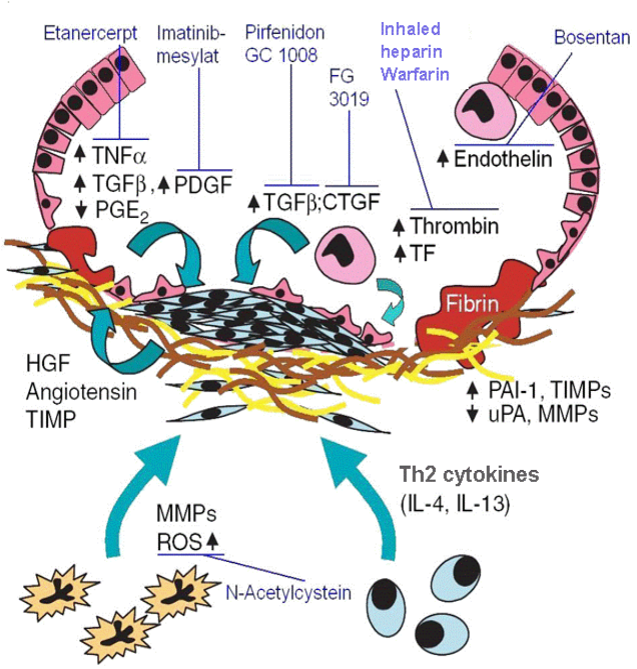

Figure 3: Overview of some of the key pathogenetic mechanisms and new treatment modalities in UIP/IPF.

(Adapted and modified from White, Lazar and Thannikal, 2003[18])

1.4 Animal models of IPF

In order to study the evolution of human pulmonary fibrosis and the cellular and other profibrotic mediators involved in the disease several animal models have been developed. In a recent review, Moore and Hagaboam[104] have extensively discussed the characteristics, advantages and disadvantages of these animal models as summarized in Table 2.

Table 2: Advantages and disadvantages of various animal models of fibrosis[104]

Model	Advantages	Disadvantages
Bleomycin	• Most well-characterized • Can be delivered intratracheally, intravenously, intraperitoneally or intranasally • Clinically relevant • Time frame for development of fibrosis is 24-28days	• Fibrosis is reported to be self-limiting after 28days in the intratracheal model • Development of fibrosis is limited in Balb/c mice • Expense
FITC	• Ability to visualize areas of lung injury by characteristic green fluorescence • Time frame for development of fibrosis is 14-28days • Fibrotic response persists for at least 6 months • Used in C57Bl/6 and Balb/c mice • Persistent nature of fibrotic response makes it amenable to studying viral exacerbations of fibrosis post-FITC	• Response can vary depending on the lot of FITC • Solution must be fresh each day and vortexed before each injection • Model is not clinically relevant
Irradiation	• Clinically relevant • C57Bl/6 mice are iradiation-fibrosis prone	• Fibrosis can take more than 30weeks to develop • Expensive per diem costs • C3H/HeJ and CBA/J mice are irradiation-fibrosis resistant
Silica	• Fibrotic nodules resemble those seen in humans exposed to occupational dusts and particulates • Persistent fibrotic stimulus	• Fibrosis can take 12-16 weeks to develop • Balb/c mice are resistant • Special instrumentation is needed if delivered via aerosol
Transgenic	• Can study the overexpression of a particular molecule • Can be expressed under inducible promoters, which allows expression only in adult mice	• Compensations can occur in mice that constitutively express a transgene throughout development • Amount of product produced may not be physiological

Viral vectors	• Can be used to deliver fibrotic or antifibrotic mediators • Lentivirus vectors can infect many cell types	• Immune response may prevent repeated dosing with adenoviral vectors • Adenoviral vectors have tropism only for epithelial cells
Adoptive transfer of human fibroblasts into immunodeficient mice	• Can study fibroblast from various human fibrotic diseases	• Expense of immunodificient mice required for adoptive transfer of human cells

1.5 Matrix metalloproteinases

Matrix metalloproteinases (MMPs) belong to the family of zinc-containing endopeptidases collectively assigned to the "MB clan" of metalloproteinases and the metzincin superfamily[105-108]. The metzincin superfamily comprises enzymes with similar metalloproteinases domains; this superfamily is further subdivided into four multigene families: astacins, seralysins, ADAMs/ADAM-TS, and MMPs [109, 110].

The metzincins are distinguished by the so-called metzincin fold and a highly conserved motif (HEXXHXXGXXH) containing three histidines, and a conserved "methionine turn" (XXMXP) that sits beneath the active site. The third histidine is bound to a zinc atom at the catalytic site[110-112].

The founding MMP family member was interstitial collagenase (MMP-1), first discovered in 1961 by Gross and Lapière in the tail skin of a tadpole *(Xenopus)*

undergoing metamorphosis[113]. The most recent member, epilysin (MMP-28) was reported separately by the groups of Parks and Stronginin in 2001[114, 115].

Currently, 26 related but distinct vertebrate MMPs are known, of which 24 are found in mammals[116]. They have both a descriptive name generally based on a preferred substrate and a MMP numbering system based on order of discovery[107, 116, 117] (Table 3). MMPs were initially characterized by their extensive ability to degrade extracellular matrix proteins including aggrecan, collagens, elastin, enactin, fibronectin, gelatin, laminin, proteoglycans, tenascin, and vitronectin[107]. More recently, it has been recognized that MMPs cleave many other types of peptides and proteins and have many other important functions that may be independent of proteolytic activity[106, 109, 116]. There is, however, little consensus about the grouping of MMPs and different authorities in the field classify MMPs based on their structural similarities, substrate specificity or tissue expression[118, 119]. One clear division is between secreted MMPs and those attached to the cell surface by the intrinsic motifs: a transmembrane (TM) domain, a glycosylphosphatidylinositol (GPI) anchor or an amino terminal signal anchor (SA)[116, 120]. Based on their substrate specificity, sequence similarity and domain organization, vertebrate MMPs are divided into six groups (Table 3, Figure 4).

Table 3: The family of Matrix Metalloproteinases

Enzyme	MMP	MW (kD) Latent/ active	ECM and other Substrates[120-136]
Collagenases			
Collagenase 1 *ColA[137] *ColB[137]	1	55/45	Collagens I, II, III, VII, X, XI; aggrecan, α_2-macroglobulin, C1q, casein,gelatin, fibronectin, myelin basic protein, link protein, SPARC, vitronectin, laminin, entactin, versican; autolytic, proMMP-1, proMMP-2, proMMP-9
Collagenase 2	8	75/58	Collagens I, II, III; aggrecan, α_2-macroglobulin, C1q, casein,gelatin, fibrinogen; autolytic, angiotensin I & II, bradykinin, plasmin C1 inhibitor
Collagenase 3	13	60/48	Collagens I, II, III, IV,VII,IX, X, XIV; aggrecan,α_2-macroglobulin, C1q, casein, collagen telopeptides, gelatin, fibronectin, perlecan, large tenascin-C; autolytic, proMMP-9
Collagenase 4 *(Xenopus)*	18	70/53	Rat collagen I
Gelatinases			
Gelatinase A	2	72/66	Denatured collagens (gelatin), collagens I, II, III, IV, V, VII, X, XI; aggrecan, decorin, elastin, entactin, fibronectin, laminin, myelin basic protein, link protein, SPARC, tenascin, vitronectin ; autolytic, α_2-macroglobulin, proTNFα, latent TGFβ, MCP-3, FGFR1, IGFBP-3, IL1-β1, big endothelin-1, plasminogen, proMMP-1, proMMP-2, proMMP-9, proMMP-13
Gelatinase B	9	92/86	Denatured collagens (gelatin), collagens IV, V, XI, XIV; aggrecan casein, decorin, elastin, laminin, myelin basic protein, link protein, SPARC, vitronectin ; autolytic, α_2-macroglobulin, angiotensin I & II, IL1-β1, IL-2Rα, carboxymethylated-transferrin, plasminogen, proTNFα, proTGFβ2, VEGF
Stromelysins			
Stromelysin 1	3	57/45	Collagens III, IV, V, VII,IX, X, XI; aggrecan, casein, collagen telopeptides, decorin, gelatin, elastin, entactin, fibrin, fibrinogen, fibronectin, fibulin, laminin, myelin basic protein, link protein, perlecan, SPARC, tenascin, versican; autolytic, α_2-macroglobulin, E-cadherin, proTNFα, IGFBP-3, IL1-β1, osteopontin, plasminogen, u-PA[138], PAI-1[139], proMMP-1, -3, -7, -8, -9, -13.
Stromelysin 2	10	57/44	Collagens III, IV, V; aggrecan, casein, gelatin, elastin, fibronectin, link protein; autolytic, proMMP-1, -7, -8, -9

Stromelysin 3	11	51/44	Collagen IV, casein, gelatin, fibronectin, laminin; IGBFP-3, α_2-macroglobulin, PAI-2
Matrilysins			
Matrilysin 1	7	28/19	Collagens I, IV; aggrecan, casein, decorin, gelatin, elastin, fibronectin, fibulin, laminin, link protein, myelin basic protein, SPARC, tenascin, versican; autolytic, α_2-macroglobulin, osteopontin, plasminogen, proMMP-1, -2, -7, -9
Matrilysin 2	26	28/19	Gelatin, fibronectin, vitronectin; Fas-L, α_2-macroglobulin, fibrinogen, proMMP-9
Membrane type MMPs			
(A)Transmembrane domain-bound MMPs			
MT1-MMP	14	66/56	Collagen I, II, III; aggrecan, gelatin, entactin, fibronectin, laminin, perlecan, vitronectin; α_2-macroglobulin, factor XII, fibrin, fibrinogen proTNFα, proMMP-2, proMMP-13
MT2-MMP	15	72/60	Aggrecan, fibronectin, entactin, laminin, perlecan, proTNFα, proMMP-2
MT3-MMP	16	64/52	Collagen III, casein, gelatin, fibronectin, laminin, victronectin; α_2-macroglobulin, proMMP-2
MT5-MMP	24	-/62	Chondroitin and dermatan sulphate proteoglycan, gelatin, fibronectin, proMMP-2
(B)GPI-anchored MMPs			
MT4-MMP	17	57/53	Fibrin, fibrinogen, gelatin, proTNFα[140, 141]
MT6-MMP	25	-	Collagen IV, gelatin, chondroitin and dermatan sulphate proteoglycan, fibrinogen, fibrin, fibronectin, proMMP-2
Other MMPs			
Macrophage elastase	12	54/45 and 22	Collagen I, IV, V; aggrecan, gelatin, fibronectin, elastin, entactin, laminin, myelin basic protein, osteonectin, vitronectin; α_2-macroglobulin, casein, factor XII, proTNFα, fibrinogen
No trivial name	19	54/45	Collagen IV, aggrecan, COMP, fibronectin, gelatin, entactin, laminin, large tenascin-C; autolysis, fibrinogen, fibrin,
Enamelysin	20	54/22	Aggrecan, amelogenenin, COMP; autolysis

XMMP*(xenopus)*	21	70/53	Aggrecan, casein, gelatin
CA-MMP	23	-	Gelatin, casein, fibronectin
CMMP *(Gallus)*	27	51/42	Gelatin, casein; autolysis
Epilysin	28	-	Casein

ColA and ColB = Collagenase-like proteins A and B, respectively, are probably the murine homologues of MMP-1, COMP = cartilage oligomeric matrix protein, GPI = glycosylphosphatidylinositol, SPARC = secreted protein acidic and rich in cysteine.

1.5.1 Structure and Function of MMPs

Each MMP consists of a specific domain sequence with several domain motifs. MMPs are active at neutral pH and are generally secreted as the inactive proenzyme in the extracellular space or anchored to the plasma membrane[142].

Consequently, they generally consist of a signal peptide, a propeptide domain, a catalytic domain, hinge region and a C-terminal hemopexin-like domain (Figure 4)[116]. The hinge region and hemopexin-like domain are absent in MMP-7 and -26, the so-called minimal domain MMPs[116, 118]. In addition, more complex MMPs possess other features such as fibronectin-like repeats, a collagen type V-like domain, furin cleavage site, vitronectin inserts or cysteine array motif[116, 118]. These are discussed in more detail in the following sections.

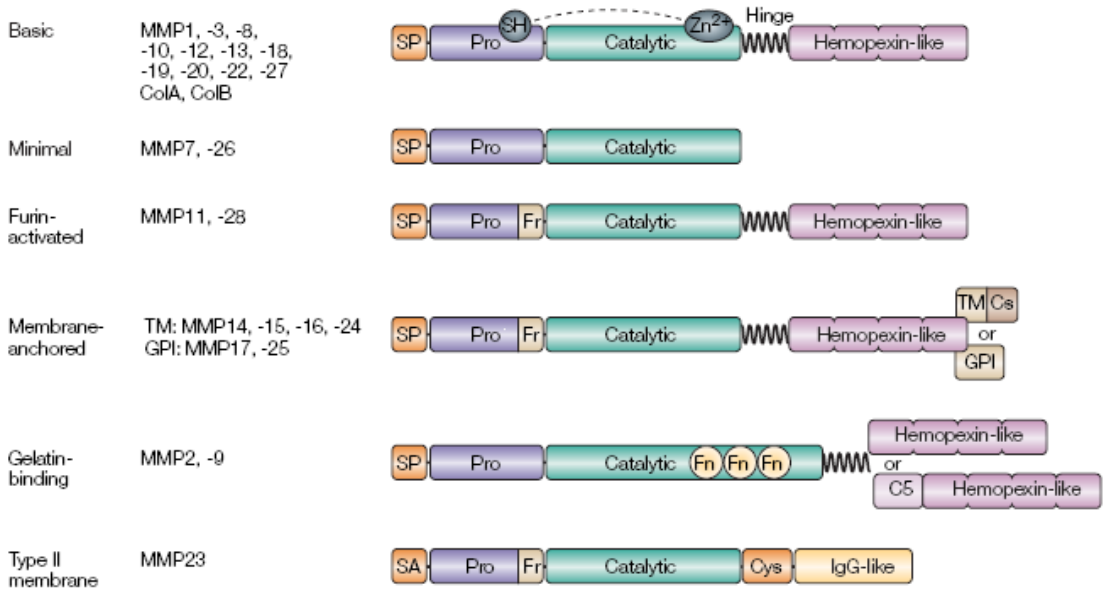

Figure 4: Domain structure of the mammalian MMP family.

Nine MMPs, including all of the cell membrane-anchored enzymes have a furin cleavage domain. C5, collagen-type-V-like domain; Col, collagenase-like protein; Cs, cytosolic; Cys, cysteine array; Fn, fibronectin repeat; Fr, furin-cleavage site; Pro, propeptide domain; SH, sulfurhydryl (thiol) group; SP, signal peptide; Zn, zinc (Adapted and modified from Parks, W.C., Wilson, C.L. and López-Boado, Y.S., 2004 [116]).

1.5.1.1 Propeptide domain

The propeptide (pro-) domain of a typical MMP contains approximately 80 amino acids with a hydrophobic residue at the amino terminus. It also contains the consensus sequence PRCG(V/N)PD, where the thiol group of the cysteine residue at position 73 (the "cysteine switch") ligates with the zinc ion that is held by the histidine residues in the catalytic domain of the MMP[142]. The structure of the propeptide domain of MMP-2, MMP-3 and MMP-9 is known to consist of three α-helices and connecting loops[120]. A peptide region after the third helix extends to the substrate-binding cleft of the catalytic domain (of MMPs) that contains a conserved cysteine, which forms a 4th ligand to an active site zinc ion. In this conformation, the enzyme is stable and inactive and is known as a zymogen[143, 144]. The exception is MMP- 23, where the crucial cysteine residue is found in a distinct amino-acid sequence[128, 145]. In addition MMP-11 [146], MT-MMPs [147], MMP-21, MMP-23 [128] and MMP-28 [114] have a pro-protein processing sequence RX(K/R)R (where X denotes any amino acid), at the C-terminal end of the prodomain[106] which is a target sequence for pro-protein convertases or furins[116].

1.5.1.2 Catalytic domain

The catalytic domain of MMPs contains approximately 160 -170 amino acid residues, including the binding motifs for three structural calcium (Ca^{2+}) ions, one structural zinc (Zn^{2+}) and one catalytic Zn^{2+} (hence the prefix “metallo”) in the active site, which are required for the stability and the expression of enzymatic activity[142]. The 50 - 54 residues at the C- terminus of the catalytic domain include a highly conserved HEXXHXXGXXH sequence (where X denotes any amino acid)[111, 116]. The three histidines coordinate the active site Zn^{2+}. On the carboxy side of the zinc active site, MMPs have a conserved methionine residue which is part of a 1,4 - β-turn or “Met-turn” that loops the polypeptide chain beneath the catalytic Zn^{2+} and forms a hydrophobic base for the Zn^{2+}-binding site. A water molecule is the fourth ligand of the catalytic Zn^{2+}[118, 144, 148]. The carboxyl group of the glutamate residue (E) [which is adjacent to the first histidine] serves as a general base and facilitates the nucleophilic attack of the water molecule on the carbonyl carbon of the peptide scissile bond[120] and histidine residues that coordinate the Zn^{2+}. The side chain of a substrate docks into a pocket to the right of the active site Zn^{2+} known as the specificity or S1’ pocket[142]. The size of the S1’ pocket, one major determinant of substrate specificity, varies among the MMPs[142]. Structurally, the catalytic domain consists of a 5-stranded β-pleated sheet, three α-helices and bridging loops[111, 142]. These backbone structures including the Met turn are similar to those of the members from other metalloproteinases families: the astacins, reprolysins (ADAMs) and serralysins[111]. In addition, MMP-2 and MMP-9 have 3 repeats of fibronectin-type

II domain inserted in the catalytic domain that interact with collagens and gelatins[149, 150].

1.5.1.3 Hinge region, hemopexin domain and other domains

With the exception of MMP7, -23 and -26, MMPs have a flexible proline-rich hinge and a C-terminal hemopexin-like domain, which functions in proper substrate recognition, activation of the enzyme, protease localization, internalization anddegradation[151, 152]. Structurally, the hemopexin domain encodes a 4- bladed β-propeller structure that is known to mediate protein-protein interactions[153].

Other domains found in MMPs are restricted to subgroups of enzymes[118]. For example, the four membrane type (MT)-MMPs (MMP14, -15, -16 and -24) have type 1 transmembrane (TM) and cytosolic domains, whereas MMP-17 and - 25 have C-terminal hydrophobic extensions that function as glycosylphosphatidylinositol (GPI)-anchoring signals[116]. The gelatinases (MMP-2 and MMP-9) have three repeats of type II fibronectin- like domains that bind to collagen, gelatin and laminin[154, 155].

1.6 MMP gene arrangement

In addition to a common three-dimensional structure, MMPs have a similar gene arrangement, indicating that they probably arose by duplications of an ancestor gene[156]. At least eight of the known human MMP genes (MMP-1, -3, -7, -8, -10, -12, -13 and -20) are clustered on chromosome 11 at 11q21- 23, whereas other MMP genes are ‘scattered’ along chromosomes 1, 8, 12, 14, 16, 20 and 22 [157].

1.7 Activation of MMPs

MMPs are secreted in latent form as proenzymes, which require activation. MMPs become activated following a disruption of the bond between the thiol group of the conserved cysteine moiety (Cys73) of the propeptide domain and the active site Zn^{2+} of the catalytic domain (cysteine switch mechanism)[144]. A water molecule then binds to the Zn^{2+} ion and replaces the cysteine residue after the dissociation. The noncatalytic zinc is then switched to a catalytic one resulting in an intermediate active enzyme[148, 158]. In addition, the propeptide domain of the MMP is removed by autolytic cleavage or by other proteases. This cleavage causes a reduction in molecular mass by 8 -10 kDa and results in a fully active enzyme[158].

MMPs are generally activated by other proteinases *in vivo*. Several MMPs contain a furin cleavage site (RXKR or RRKR) between the propeptide and catalytic domains, which functions as a target sequence for pro-protein convertases or furins[116]. The cell-surface activation of proMMP2 by active MMP14, non-furin proMMP activation mechanism has been described in detail[159-162].

In vitro, MMPs are also activated by chemical and physical agents such as amino-phenylmercuric acetate (APMA), low pH, and heat treatment [106, 120, 148]. Additionally, it has been demonstated *in vitro*, that during inflammation oxidants generated by leukocytes or other cells can both activate MMPs (through oxidation of the propeptide domain thiol group) and subsequently inactivate MMPs (through

modification of amino acids that are crucial for catalysis), providing a mechanism to control huge surges of proteolytic activity[163, 164].

1.7.1 Regulation of MMP activity

The catalytic activity of MMPs is tightly regulated at multiple levels including gene expression (transcription and translation), compartmentalization, zymogen activation, inhibition by their endogenous inhibitors, the TIMPs and substrate availability and affinity[109, 120, 165-167]. Recently, epigenetic modifications have been shown to contribute to MMP regulation[168].

MMPs are expressed at very low levels in normal healthy tissues. In contrast, MMP expression can be detected in all repair or remodelling processes, in all diseased or inflamed tissues and in all cell types grown in culture[116]. As a result of these different patterns and levels of MMP expression, it is expected that activated cells either in a tissue or culture express MMPs. The transcript levels are regulated by specific signals that are temporally limited and spatially confined[116].

Latent MMPs are kept in a catalytically inactive state by the sulfurhydryl bond between the conserved cysteine moiety (Cys^{73}) of the propeptide domain and the active site Zn^{2+} of the catalytic domain. By the “cysteine switch mechanism”[144] pro-MMPs are converted to active enzymes. After the propeptide domain has been cleaved, the active MMPs can be inhibited by their natural inhibitors, the TIMPs and internalization[169].

Compartmentalization (that is, where and how in the pericellular environment an MMP is released and held) is important for regulating the specificity of proteolysis and the affinity of the enzyme-substrate interaction[116]. Some MMPs are anchored to the cell membrane, thereby maintaining a high enzyme concentration locally and targeting their catalytic activity to specific substrates in the pericellular space[116]. In addition, specific cell–MMP interactions have been suggested to function as accessory factors that mediate the activation of the pro-enzyme and the binding of both substrate and MMP, thereby increasing the probability of proteolysis[116]. For example the binding of MMP2 to the $\alpha_v\beta_3$-integrin[170], MMP1 to the $\alpha_2\beta_1$-integrin[171, 172], MMP9 to CD44[173] and MMP7 to surface proteoglycans[174, 175].

1.8 Genetic knockout of MMPs in mice

MMPs have distinct but often overlapping substrate specificities *in vitro*[176], inferring possible genetic redundancy *in vivo*[152]. At least 14 mouse MMP mutants have been generated: *Mmp-2, 3, 7, 8, 9, 10, 11, 12, 13, 14 19, 20, 23, 24,* and *28.* The initial characterization of these knockout mice has shown obvious postnatal phenotypes, with all MMP-knockout lines surviving to birth (reviewed by Page-McCaw, Ewald and Werb,2007[152]). Mouse MMP double mutants have also been generated for *Mmp2/Mmp-9*[177], *Mmp2/Mmp14*[178] and *Mmp13/Mmp9*[179]. The functional role of MMP-13 in liver fibrosis and skeletal development has been studied employing MMP-13 KO mice[180-184]. Liver fibrosis was attenuated in MMP-13 KO mice[180], however MMP-13 null mice showed profound defects in growth plate cartilage,

delayed endochondral ossification and bone remodelling[181, 182, 184]. However, the role of MMP-13 in lung fibrosis remains to be established.

1.9 Tissue inhibitors of metalloproteinases

Tissue inhibitors of metalloproteinases (TIMPs) are specific regulators of MMP activity that bind and inhibit their specific active MMPs in a 1:1 stoichiometry[120]. The TIMP family consists of four members (TIMP-1, TIMP-2, TIMP-3, and TIMP-4) that have been identified in vertebrates[185]. Their expression is regulated during development and tissue remodeling. TIMPs have been shown to bind to the proenzyme forms of MMP-2 [186, 187] and MMP-9 [150, 187] with high degree of specificity, an interaction that provides an extra level of regulation by preventing activation. Moreover, TIMP-1 and TIMP-2 are capable of inhibiting the activities of all known MMPs and as such play a key role in maintaining the balance between extracellular matrix deposition and degradation in different physiological processes[185]. Under pathological conditions associated with unbalanced MMP activities, changes of TIMP levels are considered to be important because they directly affect the level of MMP activity[188].

1.9.1 Structure and Biological Functions of TIMPs

TIMPs (21 to 29 kDa) have an amino (N)-and carboxy (C)-terminal domain of approximately 125 and 65 amino acids, respectively, with each containing three conserved disulfide bonds[189, 190]. The N-terminal domain folds as a separate unit and is capable of inhibiting MMPs[189]. In 1994, the structure of the N-terminal domain of TIMP-2 was first resolved by nuclear magnetic resonance (NMR)[191]. The complete structure of TIMP-1 and of its mechanism of inhibition was determined in 1997 by X-ray crystallographic studies of the TIMP-1–MMP-3 complex[192], and that of the TIMP-2–MT1-MMP complex was determined soon after this[193]. The overall shape of the TIMP molecule is like a wedge, which slots into the active-site cleft of an MMP in a manner similar to that of the substrate[193].

TIMP-1 is also called erythroid potentiating activator (EPA), fibroblast collagenase inhibitor or collagenase inhibitor[194]. It is a 184 amino acid glycoprotein of 28.5 kDa. It has 41% sequence homology with the non-glycosylated 21.5 kDa TIMP-2 protein[119, 195, 196]. TIMP-1 has been located in the nucleus of fibroblasts, or shown to bind to the cell surface of MCF-7 breast carcinoma cells and subsequently translocates to the nucleus[197, 198]. It is expressed by all cell types and as such is more widely distributed than the other TIMPs[194]. It forms a non-covalent, stoichiometric complex with both latent and active MMPs and inhibits the activity of all active MMPs [196]. TIMP-1 preferentially binds and inhibits proMMP-9 ($K_d \approx 35nM$)[187]. Its binding to MMP-9 occurs via a reversible non-covalent binding to the catalytic domain of the MMP protein[187]. It is not cleaved by the binding process and may be recovered with full

activity from complexes with MMP-3 [192]. In addition to its MMP-inhibitory role, TIMP-1 has also been demonstrated to have erythroid-potentiating [194, 199] and cell growth - promoting activities[200].

TIMP-2 (also called CSC-21K) is a 194 amino acid unglycosylated protein of 21.5 kDa that has 41% and 44% sequence homology to TIMP-1 and TIMP-3, respectively[119, 195, 196]. It is expressed by a variety of cell types, forms a non-covalent stoichiometric complex with both latent and active MMPs, inhibiting all active MMPs, showing a preference for MMP-2. It regulates the activation of proMMP-2 by binding to its C-terminal domain ($K_d \approx 5nM$) [186]. Likewise to TIMP-1, TIMP-2 also has erythroid - potentiating activity and cell growth–promoting activities [194, 199] and both TIMP-1 and TIMP-2 have been shown to have anti-apoptotic activity[201-203]. TIMP-2 equally inhibits endothelial cell growth induced by basic fibroblast growth factor[204].

TIMP-3 is a 27 kDa glycoprotein (24 kDa unglycosylated), constitutively expressed by many cells in culture and has a markedly high expression in the eye[205]. It has a more basic K_i than other TIMPs and differs from them because it is localized to the extracellular matrix [196, 206]. TIMP-3 also forms a non-covalent stoichiometric complex with both latent and active MMPs, and inhibits the activation of proMMP-2 by MT5-MMP (MMP-15) [207]. Sorsby's fundus dystrophy, an autosomal dominant form of blindness due to macular degeneration, is reported to be caused by mutation in the gene encoding TIMP-3. Mutations are all found in the C-terminal domain and include the substitution of a residue for a cysteine, a nonsense mutation, or a splice

mutation, resulting in the deposition of the mutant TIMP-3 in Bruch's membrane [208-210]. In addition, TIMP-3 has pro-apoptotic activity, possibly through the stabilization of TNF-α cell receptor 1, Fas, and TNF-related apoptosis, inducing ligand receptor-1, as shown for some tumor cells [211, 212]. Furthermore, overexpression of TIMP-1, TIMP-2, and TIMP-3 reduces tumor growth [213]. These activities are also distinct from MMP inhibition and their mechanisms of action are yet to be resolved.

TIMP-4 is a 24 - 29 kDa glycoprotein. It shows 37 % amino acid homology to TIMP-1 and 51 % homology with TIMP-2 and TIMP-3 [214]. TIMP-4 is secreted extracellularly, predominantly in heart and brain tissue. It may function in a tissue specific fashion in extracellular matrix homeostasis. TIMP-4 binds to the proMMP-2 hemopexin-like domain and inhibits MT1-MMP but unlike TIMP-2 it neither forms a trimolecular complex nor activates pro-MMP-2 [189, 215]. TIMP-4 has a strong inhibitory effect on the invasion of human breast cancer cells across reconstituted basement membranes suggesting that TIMP-4 may have an important role in inhibiting primary tumor growth and progression[216, 217].

1.10 Hypothesis

The expression level and spatial distribution of MMPs, especially the collagenases, largely determines the collagen deposition and the ultrastructural changes in fibrotic lung diseases.

1.10.1 Aims and Objectives

This study aims to define the spatial expression and the nature of MMP activity in IPF versus donor lungs, the contribution of TIMPs in the local inhibition of MMPs and the relative contribution of single MMPs in the process of fibrotic repair.

In this light, the first goal was to characterize the cell-specfic distribution and expression, and the activation status of MMPs [collagenases, gelatinases, matrilysin, macrophage metalloelastase, membrane type matrix metalloproteinases (MT-MMPs)] and TIMPs in lungs from IPF patients and from organ donors.

The second goal of the study was to further investigate the pathomechanistic role of collagenases in fibrotic lung diseases. Mice lack the orthologue of human MMP-1. Therefore, we further investigated the relevance of MMP-13 in context of fibrotic lung diseases by examining the fibrogenic response to bleomycin in MMP13$^{-/-}$ mice and their wild type littermates.

2. MATERIALS

2.1. Chemicals

1-Propanol	Merck KGA, Darmstadt, Germany
2-mercaptoethanol	Sigma-Aldrich, St.Loius, MO, USA
2-methoxyethanol, ReagentPlus®	Sigma-Aldrich, St.Loius, MO, USA
3,4-Dehydro-DL-proline ($C_5H_7O_2$ FW113.1)	Sigma-Aldrich, Germany
Acetic acid	Merck KGA, Darmstadt, Germany
Acetone	Merck KGA, Darmstadt, Germany
Acetonitrile (Lichrosolv®) for HPLC	Merck KGA, Darmstadt, Germany
Acrylamide-Bisacrylamide	BioRad Laboratories, Hercules,CA, U.S.A
Agarose	Sigma-Aldrich, St.Loius, MO, USA
Ammonium persulphate	Sigma-Aldrich, St.Loius, MO, USA
Bovine serum albumin Fraction V	Carl Roth GmbH & Co.,Germany
Bromophenol blue	Fischer Scientific, NJ, U.S.A
BSA Protein assay Kit	Pierce, Rockford, IL, U.S.A
Calcein-AM, C3099	Molecular Probes, Oregon, U.S.A
Calcium Chloride dihydrate	Merck KGA, Darmstadt, Germany
Captopril	Fagron GmbH, Barbüttel
Chloramine -T hydrate	Sigma-Aldrich, St.Loius, MO, USA
Dabsyl chloride (DABS-Cl)	Sigma-Aldrich, Germany
Deoxycholic acid sodium salt	Fluka AG Chemicals, Germany
Dimethylsulfoxide	Merck KGA, Darmstadt, Germany
Dodecyl sodium salt (SDS)	Sigma-Aldrich, St.Loius, MO, USA

Enhanced Chemiluminescence (ECL)™ Plus reagents	GE Healthcare Ltd, Buckinghamshire, United Kingdom
Ethanol	Carl Roth GmbH & Co., Germany
Gelatin type A from Porcine skin	Sigma-Aldrich, St.Loius, MO, USA
Glycin	Carl Roth GmbH & Co., Germany
Heparin	Roche, Basel, Switzerland
LMP-Agarose (ultra pure)	Roche, Basel, Switzerland
L-Proline	Sigma-Aldrich, Germany
Methanol	Merck KGA, Darmstadt, Germany
N,N - Dimethylformamide HPLC Gr	Merck KGA, Darmstadt, Germany
Normal Goat Serum	Alexis Biochemicals, Grünberg, Germany
ortho-Phthalaldehyde (OPA)	Sigma-Aldrich, Germany
p-amino phenyl mercuric actetate	Calbiochem, USA
Ponceau S solution	Fluka AG Chemicals, Germany
Porcine Gelatin for electrophoresis	Sigma-Aldrich, St.Loius, Missouri, USA
Potassium chloride for analysis	Merck KGA, Darmstadt, Germany
Potassium dihydrogen phosphate	Merck KGA, Darmstadt, Germany
Protease Inhibitor cocktail	Roche Applied Sc., Minneapolis, USA
Rat tail collagen type 1	BD Biosciences, MA, U.S.A
Restore™ W. Blot Stripping Buffer	Pierce, Rockford, IL, U.S.A
RNeasy® Mini Kit	Qiagen, Valencia, CA, U.S.A
SERVA Blue G	SERVA Biochemika, Heidelberg, Germ.
Skimmed milk powder	BioRad Laboratories, CA, U.S.A
Sodium azide (ultra pure)	Merck KGA, Darmstadt, Germany

Sodium Chloride	Carl Roth GmbH & Co., Germany
Sodium Citrate	Sigma-Aldrich, St.Loius, MO, USA
Sodium dihydrogen phospahate	Fisher Scientific GmbH, Germany
Sodium hydrogen carbonate	Merck KGA, Darmstadt, Germany
TEMED	BioRad Laboratories, Hercules,CA, U.S.A
Trans-4-hydroxy-L-proline	Sigma-Aldrich, Germany
Triethylamine	Sigma-Aldrich, St.Loius, MO, USA
TRIS-HCl	Carl Roth GmbH & Co., Germany
Triton-X-100	Sigma-Aldrich, St.Loius, MO, USA
Tween-20	Sigma-Aldrich, St.Loius, MO, USA
Zinc Chloride	Sigma-Aldrich, St.Loius, MO, USA

2.2 Injecting solutions and substances

Solution/ Substance	**Manufacturer**
Albumin, FITC conjugate from bovine	Sigma-Aldrich, St.Loius, MO, USA
Bleomycin sulphate ®	Sigma-Aldrich, St.Loius, MO, USA
Enrofloxacine (Oral solution Baytril 2,5%®)	Bayer Vital GmbH, Leverkusen, Germany
Isofluorane Forene®	Abbott, Wiesbach, Germany
Physiological saline solution	Baxter S.A.,München, Germany

2.3 Consumables

Material	Manufacturer/Supplier
0.5ml, 1ml, 1.5ml , 2ml Eppendorf tubes	Eppendorf, Germany
1.8ml brown glass vials with caps	VWR International, Darmstadt, Germany
10ml,15ml, 50ml Falcon tubes	Becton Dickinson Biosciences, Germany
2ml, 5ml, 10ml, 25ml disposable pipettes	Becton Dickinson Biosciences, Germany
5ml, 10ml VWR vials with screw cap	VWR International, Darmstadt, Germany
Combi-Stopper	Intermedica GmbH Kliein-Winternheim, Germany
Gauze 5 x 4 cm Purzellin®	Lohmann und Rauscher Rengsdorf, Germany
Gauze balls size 6	Fuhrman Verrbandstoffe GmbH Much, Germany
Heating pad Thermo-Lux®	Witte und Suttor, Murrhardt, Germany
Hybond-C polyvinylidene difluoride (PDVF) membrane	Amersham Biosciences, GE Healthcare, Buckinghamshire, United Kingdom
Medical adhesive bands Durapore®	3M Company, St. Paul, MN, USA
Pyrex glass tubes (15ml)	VWR International, Darmstadt, Germany
Napkins	Tork, Mannheim, Germany
Needles 26G (0,9mm x 25mm)	Becton Dickinson Biosciences, Germany

BD Microlance 3®	
Perfusor-tubing 150 cm Original-Perfusor®-tubing	Braun, Melsungen, Germany
Respirator N95 Particulate	3M Canada Company, Ontario, Canada
Single use gloves Transaflex®	Ansell, Surbiton Surrey, UK
Single use syringes 1ml, 2ml, 5ml, 10ml Inject Luer®	Braun, Melsungen, Germany
Surgical instruments	Martin Medizintechnik, Tuttlingen, Germany
Centricon® Centrifugal Filter devices Centricon YM-10	Millipore Corporation, Bedford, MA, U.S.A
Surgical threads non-absorbable Size 5-0 ETHIBOND EXCEL®	Ethicon GmbH Norderstedt, Germany
Surgical threads with needle Size 5-0, 6-0 and 7-0 ProleneTM	Ethicon GmbH, Norderstedt, Germany
Threads Nr. 12	Coats GmbH, Kenzingen, Germany
Tracheal cannula, 20G	Becton Dickinson/ MEDEX Inc. Carlsbad, CA, U.S.A

2.4 Histology

Material	Company
Automated Cryotome	Leica Microsystems, Nussloch, Germany
Automated microtome RM 2165	Leica Microsystems, Nussloch, Germany
Cooling plate EG 1150C	Leica Microsystems, Nussloch, Germany
Cover slips 24x36mm	VWR, Menzel, Germany
Digital Camera Microscope DC 300F	Leica Microsystems, Nussloch, Germany
Eosin Y solution, alcoholic	Sigma Diagnostics®,St. Loius, MO, U.S.A
Flattening bath for paraffin sections HI 1210	Leica Microsystems, Nussloch, Germany
Flattening table HI 1220	Leica Microsystems, Nussloch, Germany
Formaldehyde alcohol free ≥37%	Roth, Karlsruhe, Germany
Graded Ethanol 70%, 95%, 99,6%	Fischer, Saarbrücken, Germany
Histological glass slides Superfrost Plus®	R. Langenbrinck, Emmendingen, Germany
Hydrogen peroxide 30% pro analysi	Merck Darmstadt, Germany
Isopropanol (99,8%)	Fluka Chemie, Buchs, Swiss
Kernechtrot Aluminium sulfate	Chroma, Münster, Germany
Mayer's Hematoxylin solution	Sigma-Aldrich, St. Loius, MO, U.S.A
Methanol, HPLC Grade	Fischer Scientific, New Jersey, U.S.A
Microtom blades S35	Feather Safety Razor Co.Ltd, Japan
Mounting medium Pertex®	Medite GmbH Burgdorf, Germany
Paraffin	Allegiance Health Care, Corp. IL, U.S.A

Paraffin embedding medium Paraplast Plus®	Sigma Aldrich,Steinheim, Germany
Picric acid	Fluka Chemie, Buchs, Swiss
Resorcin Fuchsin	Chroma, Münster, Germany
Roti-Histol (Xylolersatz)	Roth, Karlsruhe, Germany
Shandon Cytospin 4	Thermo Electron Corporation, Waltham, U.S.A
Stereo light microscope DMLA	Leica Microsystems, Nussloch, Germany
Tissue embedding machine EG 1140H	Leica Microsystems, Nussloch, Germany
Tissue processing automated machine TP 1050	Leica Microsystems, Nussloch, Germany
Universal-embedding cassettes	Leica Microsystems, Nussloch, Germany
Urine pots with covers, 100ml	Corning Incorporated, Mexico
Van Giesson's solution	Polyscientific, Bay Shore, NY, U.S.A
Xylene	Fischer Scientific, New Jersey, U.S.A

2.5 Antibodies

Antibody	Catalogue Number & Description	Company
Anti-ß-actin (AC-15), mouse monoclonal	AB6276; loading control; recognizes 42kDa human ß- actin	Abcam, Germany
Actin (C-11), loading control, goat polyclonal	SC1615; recognizes actin isoforms of human/mouse	Santa Cruz Biotechnology, Inc, U.S.A
Anti-MMP-1 (Ab-1) ; monoclonal, mouse anti-human	IM35L; recognizes both latent (57/52kDa) and active (46/42kDa) MMP-1	Calbiochem, Darmstadt, Germany
Anti-MMP-2 (468-483) (Ab-3) ; monoclonal mouse anti-human	IM33L; recognizes both latent (72kDa) and active (66kDa) MMP-2	Calbiochem, Darmstadt, Germany
Anti-MMP-7 (Ab-4) ; rabbit polyclonal	PC492; recognizes the ~ 28 kDa latent and the ~ 18 kDa active forms of MMP-7	Calbiochem, Darmstadt, Germany
Anti-MMP-8 (Ab-1) ; mouse monoclonal antibody (115-13D2)	IM38L; recognizes the ~ 85kDa latent and the ~ 64kDa active MMP-8 protein.	Calbiochem, Darmstadt, Germany
Anti-human MMP-9 ; goat polyclonal antibody	AF911; recognizes human and mouse pro (92kDa) and active (86kDa) MMP-9.	R&D Systems GmbH, Germany.

Anti-MMP-13 (Ab-4) ; mouse monoclonal antibody (VIIIA2)	IM78; recognizes both the ~ 60 kDa latent and the ~ 48 kDa active forms of MMP-13 protein	Calbiochem, Darmstadt, Germany
Anti-TIMP-1 (Ab-1) ; mouse monoclonal antibody (7-6C1)	IM32L; recognizes the ~ 28kDa TIMP-1 protein	Calbiochem, Darmstadt, Germany
Anti-TIMP-2 (Ab-2) ; mouse monoclonal antibody (67-4H11)	IM56L; recognizes the ~ 27kDa TIMP-2 protein	Calbiochem, Darmstadt, Germany
Anti-TIMP-3; mouse monoclonal antibody (136-13H4)	IM43L; recognizes both the ~ 27kDa glycosylated and the ~ 24kDa unglycosylated forms of TIMP-3.	Calbiochem, Darmstadt, Germany
Anti-human TIMP-4; (HOM01), goat polyclonal antibody	AF974; recognizes human TIMP-4 protein (~29kDa glycosylated & ~24kDa non-glycosylated forms).	R&D Systems GmbH, Germany

2.6 Machines, systems and software

Machine/System/Software	Company
Agilent HewLettPackard Series 1100 HPLC system	Agilent Technologies Waldbronn, Germany
Applied Biosystems' 7500 Real-Time PCR System	Applied Biosystems, Foster City, CA, U.S.A
Biorad 200/2.0 electrophoresis power supply	BioRad, Hercules, CA, U.S.A
BioRad iCycler™ 96 well Reaction Module	BioRad, U.S.A
Computer Q 550 IW	Leica Microsystems, Nussloch, Germany
Consort EV 231 Elect. Power Supply	Belgium
Eppendorf BioPhotometer	Eppendorf, Hinz GmbH, Germany
Eppendorf Centrifuge 5417R	Eppendorf, Hinz GmbH, Germany
Fluorochem™ 8900	Alpha Innotech, San Leandro, CA, U.S.A
Gel Logic 2000 Imaging System	Carestream/Kodak Molecular Imaging System, CT, U.S.A
H1221 pH meter	HANNA INSTRUMENTS GmbH, Kehl am Rhein,Germany
Heraeus Instruments, (Oven/Dessicator)	Hanau, Germany
Hettich Zentrifugen Universal 30 RF	Tuttlingen, Germany
HP Chem Station for LC and LC/MS systems	Agilent Technologies Waldbronn, Germany

Intrapulmonary Aerosolizer: Series IA-1C Microsprayer™ with series FMJ-250 High-Pressure Syringe	Penn-Century, Inc, Philadephia, PA, U.S.A
Labnet Shaker 35	Labnet International Inc, NJ, U.S.A
Lichrosorb RP18 RP-HPLC column	Merck KGA, Darmstadt, Germany
LYPH.LOCK6 Freeze Dry System	Labconco Corp., MO, U.S.A
Mettler Toledo AB 54 Balance	Mettler Instrument Corp., Switzerland
Mettler Toledo AG 285 Balance	Mettler Instrument Corp., Switzerland
Mettler Toledo MX5 Balance	Mettler Instrument Corp., Switzerland
Mettler Toledo PB 801 Balance	Mettler Instrument Corp., Switzerland
PowerPac Basic, BioRad	BioRad, Hercules, CA, U.S.A
Primer Express® Software Version 3.0	Applied Biosystems, Foster City, CA, U.S.A
Scotsman's Ice machine	Scotsman Ice Sytems, IL, U.S.A
Software Q Win V3	Leica Microsystems, Nussloch, Germany
SPOT ™ 2.3.0 software	Diagnostic Systems Inc, MI, U.S.A
Tecan Spectra Fluor⊕, Magellan™	Tecan Austria GmbH
TJ 25 Centrifuge	Beckman Coulter™, U.S.A
Trans-Blot SD Semi-dry Transfer Cell	BioRad, Hercules, CA, U.S.A
VLM EVA 2 metal block thermostat	VLM GmbH, Bielefeld, Germany

3. METHODS

3.1 Human Lungs

3.1.1 Study Population and Specimen Collection

The study was approved by the local ethics committee, and informed consent was obtained from all study subjects. Explanted lungs (n=16 for sporadic IPF) or non-utilized donor lungs or lobes fulfilling transplantation criteria (n=6; human donors, HD) were obtained from the Dept. of Thoracic Surgery in Vienna, Austria. All IPF diagnoses were made according to the Consensus Conference criteria[14] and a UIP pattern was proven in all IPF lungs. All IPF subjects experienced progress under a preceding course of steroids.

All lungs or lobes of normal tissue were taken from donors who died from brain death. The lungs fulfilled selection criteria for organ transplantation but were not transplanted due to technical reasons. Donor lobes were obtained when donor lungs needed to be reduced by size in order to be compatible with recipient's anatomical dimensions. Informed consent was obtained at the time of transplant evaluation. Donor lungs had no evidence of active infection, chest radiographic abnormalities, and no past medical history of underlying systemic or lung disease. Two additional control samples were purchased: a pool of total RNA from six normal lungs obtained from CLONTECH and total RNA from one normal lung from AMBION.

IPF and donor lungs were transferred from Vienna (Department of Thoracic Surgery, Vienna General Hospital, Vienna, Austria) to Giessen (Univerisity of Giessen Lung Center) on crushed ice, after being flushed with preserving solution. In addition, at the surgical theater in Vienna, samples were obtained and snap-frozen in liquid nitrogen. In Giessen, the lungs were processed following a predefined algorithm and samples were stored at -80°C.

Lung tissues were dissected according to the scheme shown in figure 5.

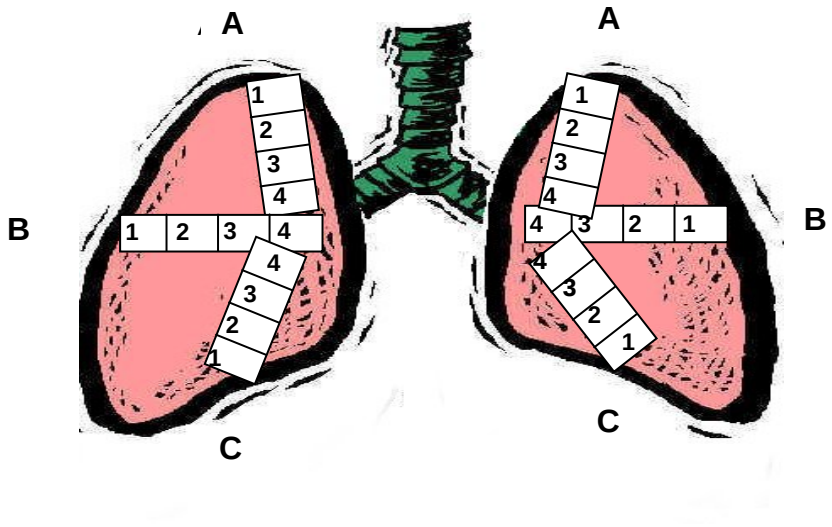

Figure 5: Schematic diagram showing IPF lung tissue dissection.

A= the apical region, B = the hilar region, and C= the basal region

Table 4 depicts which lung tissues were used as controls for the specific analysis.

Table 4: Overview of control specimen used in this study

Method	IPF	Control
Histology	C1 - C3	Vienna donor lung/lobe
Hydroxyproline	C1 - C3	Vienna donor lung/lobe
PCR Semi-quantitative Quantitative	 C1 C1	 Vienna donor lung/lobe Commercial RNA from Ambion and Clontech
Western blot	C1	Vienna donor lung/lobe
Gelatin zymography	C1	Vienna donor lung/lobe
Collagenase activity	C1	Vienna donor lung/lobe
Immunohistochemisty	C1	Vienna donor lung/lobe
In situ zymography	C1	Vienna donor lung/lobe

3.2 Animals

MMP-13$^{-/-}$ and wild type littermates were generated from the intercross between heterozygous MMP-13 $^{+/-}$ mice in a C57BL/6J and 129/Sv hybrid background. Generated MMP-13$^{-/-}$ mice were genotyped by Southern blotting and by PCR analysis as described elsewhere[180]. Mice received food and water *ad libitum*, and were kept under controlled light (12/12-hours light/dark cycle) and temperature (16° - 25°C) throughout the experimental period. All experiments were performed according to the protocol approved by the Institutional Laboratory Animal Care and Use Committee of Columbia University in the City of New York. Animals received humane care according to the criteria outlined in the “Guide for the Care and Use of Laboratory Animals”.

3.3 Induction of pulmonary fibrosis in mice by bleomycin treatment.

Eight to twelve week-old and gender-matched MMP-13$^{-/-}$ and wt littermates were used in the study. Pulmonary fibrosis was induced in mice by intratracheal administration of a single dose of bleomycin sulphate (5U /kg body weight), reconstituted in 0.9% NaCl solution. Control animals received 0.9% NaCl intratracheally. The solution was aerosolized by use of a microsprayer at a volume of 200µl. For the analyses, mice were euthanized 7, 14 and 28 days after bleomycin or saline administration. Unless otherwise specified, for every variable analyzed, five control and experimental mice were used. The experimental protocol for the mouse experiments is shown in Figure 6.

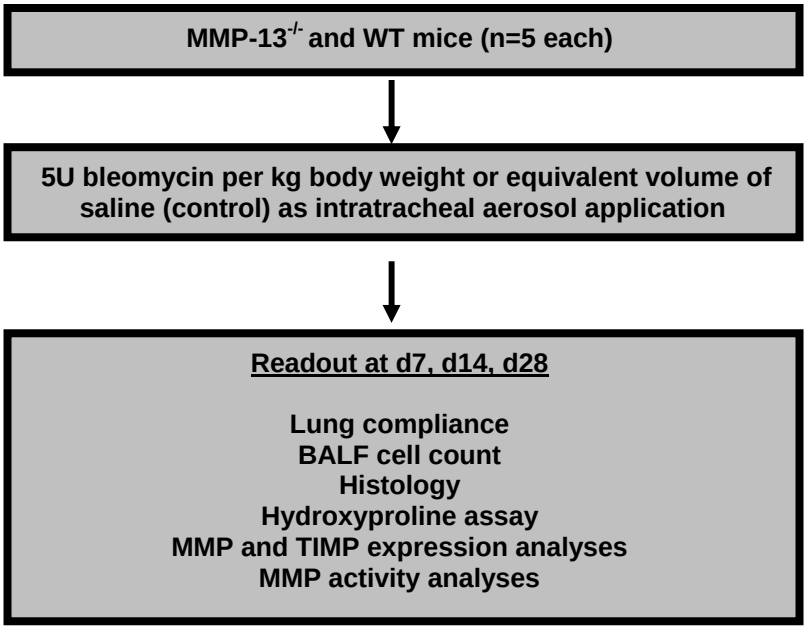

Figure 6: Schematic protocol for mouse experiments. Mice were euthanized at d7, d14 and d28 after bleomycin or saline administration. Samples were retrieved for analyses; n= number of mice in the group.

3.4 Quasi-static lung compliance

To determine the pulmonary compliance of the lung, an open-chest model was used as previously described [218] and the quasi-static lung compliance was measured using the Flexivent apparatus (SCIREQ, Inc. Montréal, Québec, Canada). Briefly, mice were euthanized by CO_2 asphyxia and after a careful tracheotomy; a 20-gauge catheter was inserted into the trachea and secured with a silk suture. A mediastinal dissection was performed, and the anterior chest wall was completely resected. Before lung compliance measurements, the Flexivent apparatus was calibrated for a transpulmonary pressure-volume (PV) of 30cm H_2O; a water manometer was connected in circuit with a tube that was inserted into the three-way stopcock into which the flexivent's plastic tubing had also been inserted. The flexivent plastic tubing was inserted into the tracheal cannula and an attached 10ml syringe was used to install the desired volume of air. Three measurements were taken per animal with a 30s interval between each measurement. The quasi static pressure-volume curve for each measurement was digitally converted by the instruments software. Data from each pressure-volume curve were collected, and pooled mean pressure-volume (quasi-static expiratory compliance (E_{cst}) parameters were obtained for each animal.

3.5 Bronchoalveolar lavage

Euthanized mice with a tracheal cannula inserted as described above were carefully lavaged with 1ml of PBS twice, so that ~ 2ml of bronchoalveolar lavage fluid (BALF) were recovered from each mouse. The BALF was centrifuged at 300g for 10 minutes at 4°C, and the supernatant was aliquoted and frozen at -80°C until analysis. Total cell counts were performed on the cell pellets employing an improved Neubaur hemocytometer. Cells were then cytospun at 700 r.p.m for 3 minutes (Cytospin 3®, Thermo Shandon, Ltd, Astmoor, United Kingdom) and stained with a modified Wright's stain (DiffQuik, American Scientific Products, McGaw Park, IL). Differential cell counts were performed on 200 cells using standard morphological criteria as described elsewhere[90].

3.6 Processing of human and murine lungs

Shock-frozen tissue and paraffin sections were prepared from explanted human lungs immediately after retrieval. For paraffin sections, human tissues were fixed by submersion for 72h at RT and murine lungs were perfused via vasculature at 25 cmH_2O followed by submersion for 24h at RT in 10% neutral buffered formalin. Sections were dehydrated through a series of graded ethanol and xylene, and embedded in paraffin. 3µm thick paraffin sections were cut, transferred onto glass slides and incubated overnight at 37°C. For frozen sections of human lungs, the lung samples were snap-frozen in liquid nitrogen already at the surgical theatre and stored at -80°C. For frozen sections, murine lungs were distended to total lung capacity with Tissue-Tek® OCT compound, removed en bloc, snap-frozen in liquid

nitrogen and stored -80°C. 10µm thick sections were cut by cryostat, transferred onto superfrost glass slides, air dried and stored at -20°C.

3.7 Gelatin zymography in murine BALF samples

Bronchoalveolar lavage fluid (BALF) was pooled from experimental animals at the indicated time points, concentrated five-fold using YM-10 Centricon centrifugal filters and the total protein concentration was measured with the BCA protein assay kit. 50µg of BALF total protein was mixed with 4x Laemmli sample buffer without ß-2-mercaptoethanol and in absence of boiling, and the proteins were separated in non-reducing, 10 % polyacrylamide gel copolymerized with 1 mg/mL of porcine skin gelatin. After electrophoresis (100V, 1h) SDS was removed from the gels by two washes in 2.5% Triton X-100, 30 minutes each time. Subsequently, the gels were equilibrated in developing buffer (50 mM Tris [pH 7.4], 10 mM $CaCl_2$, 1µM $ZnCl_2$, 1% Triton-X-100) for 30 minutes, then incubated in fresh developing buffer at 37°C for 18 hours. The gel was stained with 0.5% Coomassie Blue R-250 for 1 hour, followed by destaining (20% methanol, 20% ethanol, 7% acetic acid). Gelatinolytic activity was detected as clear bands on a dark blue background. The protein molecular weight marker and specific recombinant gelatinases were included in the gel for identification. Control gels were incubated in buffer containing 20mM EDTA.

3.8 Macrophage Chemotaxis to BALF samples

BALF that served as the chemoattractant was retrieved from experimental animals at d7. Fluorescently labeled alveolar macrophages (AMJ2-C11 macrophage cell line [ATCC]) served as the target cells. BALF was diluted 8-fold and 29µl was placed in the bottom chamber of a 96 well chemotaxis chamber (101-5, Neuroprobe, Inc.) and 28 µl of serum-starved macrophages at 1.5 x 10^4 cells/ml was placed on top of the filter above its corresponding well so that beads were formed. After 1 hour of incubation at 37°C at 5% CO_2 the number of macrophages that migrated into the lower chamber was determined by reading the fluorescence intensity using a fluorescent plate reader (Ex/Em = 485/530nm). Results are reported as the directed versus random migration ratio; i.e, the ratio of the intensity of fluorescence in the test wells to that of the blank (wells containing only media).

3.9 Analysis of collagenase activity in human lung homogenates

Collagenase activity in human lung homogenates was determined using the EnzChek® Gelatinase/Collagenase assay kit from Molecular Probes, with some modifications. As substrate, the DQ™ collagen, fluorescein conjugate called D-12060 collagen, in which heavy labeling with fluorescein results in quenching of fluorescence was used. Briefly, a serial dilution of standard stock solution (500 U/ml) of collagenase, type IV from *Clostridium histolyticum,* was prepared in 1X reaction buffer (50mM Tris, 150mM NaCl, 5mM $CaCl_2$, pH 7.6). 50µg protein in each lung homogenate was diluted to100µl in 1X reaction buffer. Wells of a black flat-bottom 96-well optical bottom microtiter plate were coated (50 µl per well) with 100µg/ml of DQ-collagen in low gelling agarose, in the dark. After the agarose solidified, 100µl of

standards and 100µl of sample were added to the wells in triplicates followed by 100µl 1X reaction buffer. For controls (blanks), 200µl 1X reaction buffer was added to coated and uncoated wells. Samples were incubated at 25°C, protected from light for 2 hours. The fluorescence intensity was read in a fluorescence microplate reader at Ex/Em of 495/515nm. For each standard and sample background fluorescence was corrected by subtracting values derived from the blanks. A standard curve was obtained from the standard to confirm the linearity between collagenase activity and substrate degradation. Collagenase activity was calculated by the computer software (Magellan) and expressed as unit of activity per unit sample volume (mU/ml).

3.10 Hydroxyproline determination in human lungs

Hydroxyproline levels in human lung tissues were determined following the protocols of Ikeda[219] and Sormiachi[220]. Human lung tissues in 1000µl of distilled H_2O (dH_2O) were thoroughly homogenized employing a Potter homogenizer. 500µl of each lung homogenate were transferred into pre-weighed and labeled 2ml eppendorff tubes and then dried for 12 h employing a speed vaccum and the lung dry weight was measured. The dry lung was hydrolyzed with 500µl of 6N HCl at 116°C for 16 h[221]. After cooling, a 1:10 dilution of each hydrolysate (10µl hydrolysate + 90µl dH_2O) was prepared and 10µl of diluted hydrolysates were transferred to 1.8ml brown glass vials. External standard solutions (in duplicate) containing trans-4-hydroxy-L-proline and L-proline were prepared in 1.8ml brown glass vials at concentrations and volumes shown in Table 5.

Table 5: Trans-4-hydroxy-L-proline and L- proline external standards

No.	Hydroxyproline	Proline
1	50µl of 0.1µmol/ml	50µl of 0.1µmol/ml
2	20µl of 0.1µmol/ml	20µl of 0.1µmol/ml
3	10µl of 0.1µmol/ml	10µl of 0.1µmol/ml
4	50µl of 0.01µmol/ml	50µl of 0.01µmol/ml
5	20µl of 0.01µmol/ml	20µl of 0.01µmol/ml
6	10µl of 0.01µmol/ml	10µl of 0.01µmol/ml
7	5µl of 0.01µmol/ml	5µl of 0.01µmol/ml

For derivatization, 20µl of triethylamine and 20µl of 0.1µmol/ml 3, 4-dehydro-DL-proline (internal standard) were added to the diluted hydrolysates and external standards, and mixed. Then all the samples were frozen with liquid nitrogen and were dried under vacuum. To block the primary amino group, 20µl of 14.9 mM *ortho*-pthalaldehyde (OPA) solution were added to the dried samples (lung hydrolyates or external standards), and mixed thoroughly. The solution was incubated for 5 min at room temperature, and then 20µl of dabsyl-Cl in acetonitrile (1.3mg/ml) were added to all samples solutions and mixed well. Dabsylation was performed for 20min at 70°C with all vials capped. After 10 min at RT, 60µl of 50% acetonitrile in dH_2O were added to the samples, mixed well and stored at 4°C until RP-HPLC analysis. The detection of dabsylated amino acids (secondary amino groups) was carried out at 279.8nm and 436.8nm on the column, Merck Lichrosorb RP 18 (4.6 x 150mm, particle size 5µm). The column was maintained at 50°C and eluent flow-rate was

1.5ml/min.The gradient elution programme and mobile phases used for separating hydroxyproline, dehydroproline and proline are given in Table 6.

Table 6: Gradient elution program for separation of hydroxyproline[219, 220]

Time (min)	*Solvent A (%)*	*Solvent B (%)*
0 - 3	55 (isocratic)	45
3 - 8	40	70
8 -12	33	67
12 -13	0	100
13 -15	0 (isocratic)	100
15 -15.5	55	45

Solvent A: 40mM Na_2HPO_4 adjusted to pH 3.0 with ortho-phosphoric acid.
Solvent B: 4% (v/v) dimethylformamide in acetonitrile-dH_2O (4:1).

A standard curve was obtained from the external standards. The hydroxyproline content of the lung hydrolysates was calculated using the HP Chem Station for LC and LC/MS systems software and expressed as microgram hydroxyproline per milligram lung dry weight (µg/mg).

3.11 Hydroxyproline determination in murine lungs

Hydroxyproline levels in murine lungs were determined following the protocol of Woessner[222]. The mouse lung tissue was homogenized in 500µl of distilled H_2O (dH_2O), then lyophilized for 12 h and the lung dry weight was measured. The dry lung was hydrolyzed with 4 ml of 6N HCl at 116°C for 16 h. 2ml of the hydrolysate were evaporated and the powder was then reconstituted with 2ml of dH_2O and then

re-evaporated. This powder was then reconstituted with 2 ml of dH_2O and the pH adjusted to pH 7.0. Standard solutions containing 3, 4 D-L- hydroxyproline (Sigma) were made at concentrations of 0, 1, 2, 3, 4, 5, 6, 7, 8, 9 and 10 µg/ml. Sample solution (2 ml) was taken and oxidized with 1 ml of Chloramine-T (Sigma) for 20 min. The reaction was then stopped with 1 ml of 3.15 M perchloric acid. After 5 min, 1 ml of *p*-dimethylaminobenzaldehyde solution was added. The sample was thoroughly vortexed until appearing lucent, incubated in a 60°C bath for 20 minutes, and then cooled under tap water for 5 min. The absorbence of the solutions was determined at 557 mm. The hydroxyproline content of the lung samples was calculated from the standard curve and expressed as mg hydroxyproline per lung dry weight.

3.12 Quantitative real time reverse transcription- polymerase chain reaction (RT-PCR) analysis.

Total RNA was extracted from lung tissue using the Qiagen RNeasy® Mini kit, according to recommendations from the manufacturer. Briefly, snap frozen lungs were homogenized in buffer RTL containing 1% v/v ß- mercaptoethanol. After full speed centrifugation for 3 min, supernatants were collected and mixed with an equal volume of 70% ethanol (RNase-free). The mixture was added to an RNeasy mini column and centrifuged again. RNase-free DNase I was added to the filter membranes for ≥ 15 min at 20-30°C in order to eliminate contaminating genomic DNA. Following washes of the column RNA was eluted two times from the filter using 40µl of RNase free water each time. The RNA concentration and quality were assessed by measuring the A_{260} and A_{260}/A_{280} respectively.

2 µg of total RNA was reverse-transcribed using a first-strand cDNA kit with random hexamers (Applied Biosystems, Foster City, CA) according to the manufacturer's recommendations. Two negative controls, one without the RNA template and other lacking reverse transcriptase were included. Human *MMP-1, MMP-2, MMP-7, MMP-8, MMP-9, MMP-12, MMP-14, TIMP-1, TIMP-2, TIMP-3,* and *TIMP-4* as well as murine *Mmp-7, Mmp-8, Mmp-13, Timp-1, Timp-2, Timp-3*, and *Timp-4* mRNA transcripts were quantified using Power SYBR Green® PCR and with human and mouse smooth muscle actin *(mACTB)* as internal controls respectively for human and murine samples. Each sample was run in triplicates. The negative control reactions were also included. The PCR reaction and analyses were carried out using the ABI Prism 7500 Sequence Detector and software. The relative abundance of the target genes was obtained by calculating against a standard curve and normalized to an internal control. PCR primers were purchased from ABI TaqMan Gene Expression Assays (Applied Biosystems) and QuantiTect® Primer Assays (Qiagen).

Table 7: Primers used for the amplification of cDNA from human lung tissue by Power SYBR Green® PCR

cDNA	Primer sequence (5' ⟶ 3') (F = Forward primer; R = Reverse primer)
hMMP-1	F: CCT CGC TGG GAG CAA ACA R: TTG GCA AAT CTG GCG TGT AA
hMMP-2	F: CGT CTG TCC CAG GAT GAC ATC R: ATG TCA GGA GAG GCC CCA TA
hMMP-7	F: GCT GGC TCA TGC CTT TGC

	R: TCC TCA TCG AAG TGA GCA TCT C
hMMP-8	F: CCC AAC TAT GCT TTC AGG GAA A R: GCC TGA ATG CCA TCG ATG T
hMMP-9	F: GGA CGA TGC CTG CAA CGT R: CAA ATA CAG CTG GTT CCC AAT CT
hMMP-12	F: TGC ACG CAC CTC GAT GTG R: GGC CCC CCT GGC ATT
hMMP-13	F: TTC TTG TTG CTG CGC ATG A R: AGG GTC CTT GGA GTG GTC AA
hMMP-14	F: TCA GGG TTC CCC ACC AAG A R: AAC AGA AGG CCG GGA GGT A
hTIMP-1	F: CGC TGA CAT CCG GTT CGT R: TGT GGA AGT ATC CGC AGA CAC T
hTIMP-2	F: GGG CAC CAG GCC AAG TT R: CGC ACA GGA GCC GTC ACT
hTIMP-3	F: CCT GGC TAC CAG TCC AAA CAC R: TGC AGT AGC CGC CCT TCT
hTIMP-4	F: GCA CCC TCA GCA GCA CAT C R: CTG GAG ATT TTG GCC CGA AT
hß-actin *(hACTB)*	F: GCG CGG CTA CAG CTT CA R: CTT AAT GTC ACG CAC GAT TTC C

Table 8: Primers used for the amplification of cDNA from murine lung by Power SYBR Green® PCR

Gene	Assay name	Catalog number
Mmp -7	Mm_Mmp7_1_SG Quantitect Primer Assay(200)	QT00110012
Mmp -8	Mm_Mmp8_1_SG Quantitect Primer Assay(200)	QT00113540
Mmp -13	Mm_Mmp13_1_SG Quantitect Primer Assay(200)	QT00111104
Timp -1	Mm_Timp1_1_SG Quantitect Primer Assay(200)	QT00996282
Timp -2	Mm_Timp2_1_SG Quantitect Primer Assay(200)	QT00138558
Timp -3	Mm_Timp3_1_SG Quantitect Primer Assay(200)	QT00105469
Timp -4	Mm_Timp4_1_SG Quantitect Primer Assay(200)	QT00151844
mß-actin (mACTB)	Mm_Actb_2_SG Quantitect Primer Assay(200)	QT01136772

3.13 Western blot analysis of MMPs and TIMPs in human tissues

Human lung tissue samples were pulverized in liquid nitrogen and incubated in RIPA buffer (50mM Tris-HCl pH 7.5, 150mM NaCl, 1mM EDTA, 1% (v/v) Triton-X-100, 1% NP-40, 0.1% SDS, 1mM PMSF, Complete protease inhibitor cocktail [Roche]). Protein concentrations were determined with the BCA Protein Assay Kit (Pierce, Rockford, IL). 50 µg total protein per sample were mixed with denaturing Laemmli sample buffer, electrophoresed on a 10% denaturating SDS-polyacrylamide gel and transferred onto polyvinylidene difluoride (PVDF) membranes using a semi-dry transfer cell. Non-specific sites on the membranes were blocked for 2 hours at room temperature with 5% (w/v) non-fat dried milk in TBS/T (Tris-buffered saline [TBS; 50

mM Tris-HCl, pH 7.5, 50 mM NaCl], and 0.1 % Tween 20). Membranes were incubated with primary antibody in 5% (w/v) non-fat dried milk in TBS/T at 4°C, overnight, with gentle shaking. Primary antibodies used were purchased from Calbiochem except otherwise indicated as shown in Table 9. Membranes were washed 3 x 15 minutes in 1 × TBS/T and incubated for 1 hour at room temperature with respective horse-radish peroxidase-conjugated secondary antibodies to mouse, goat and rabbit IgGs (1:2000 in 5% (w/v) non-fat dried milk in 1x TBS/T.

Table 9: Antibodies and dilutions used in western blot

Antibody	Dilution used
Monoclonal anti- human MMP-1	1:1000
Monoclonal anti- human MMP-2	1:1000
Rabbit polyclonal anti-human MMP-7	1:5000
Monoclonal anti-human MMP-8	1:1000
Goat polyclonal anti-human MMP-9 (R & D systems)	1:1000
Monoclonal antibody to latent and active human MMP-13	1:500
Monoclonal anti-human TIMP-1	1:500
Monoclonal anti- human TIMP-2	1:500
Monoclonal anti-human TIMP-4 (R & D systems)	1:500
Monoclonal anti-human ß-smooth muscle actin (Abcam)	1:10,000

After four washes with 1xTBS/T, membranes were developed with the Enhanced Chemiluminescence (ECL) Plus detection system using radiographic film. The band

intensity of exposed film was analyzed by densitometric scanning and quantified using AlphaEase®FC Imaging System. The density of the protein of interest was related to the density of the housing-keeping gene (β-actin). Experiments were repeated three times per each patient sample.

3.14 Histopathology and Immunohistochemistry

Formalin fixed, paraffin-embedded human and murine lung tissue sections were routinely stained with haematoxylin and eosin (H & E) stain and with Masson-Trichrome stain in order to assess the histological phenotype and extent of collagen deposition. For each human patient or murine sample, 3 slides were analysed and 5 random fields were examined. Immunohistochemistry for human MMP-13 and for murine MMP-7 was also performed on paraffin sections. Monoclonal anti-human MMP-13 antibody (5μg/ml) and goat anti-mouse MMP-7 antibody (15μg/ml) were primary antibodies for human and murine sections respectively. After deparaffinization and rehydration, endogenous peroxidase activity was quenched by treating tissue sections in 3% H_2O_2 in methanol. Antigens were retrieved by microwaving for 20 minutes in 10mM citrate buffer, pH 6.0 and cooling at RT. Sections were washed with phosphate-buffered saline (PBS, pH 7.4) and immunohistochemistry performed using the Labeled-[strept] Avidin-Biotin (LAB-SA) method according to the manufacturer's recommendations. Briefly, non-specific background was eliminated by incubating sections with blocking solutions A and B for 30 min and 10 min, respectively, followed by overnight incubation at 4°C with mouse anti-human MMP-13 (5μg/ml) [human sections] or goat anti-mouse MMP-7

(15µg/ml) [murine sections]. After three washes in PBS, a biotinylated secondary anti-IgG was applied followed by the streptavidin-peroxidase conjugate. The presence of peroxidase was revealed by adding the chromogenic substrate solution. The formation of a brown deposit demonstrates the location of the antigen and the reaction was terminated by washing in distilled water. Stained sections were counterstained with haematoxylin; slides were dehydrated with graded series of alcohol, cleared in xylene and mounted in Histomount™. For negative control slides, the primary antibody was replaced by the corresponding non-immune serum.

3.15 Immunohistochemistry combined with in situ zymography

Immunohistochemical (IHC) localization of MMP-1 and MMP-9 protein was performed on 10µm cryostat sections of human lungs followed by in situ zymography (ISZ) in order to co-localize the MMP protein signal with the collagenolytic and gelatinolytic activity in the tissue. Briefly, cryostat sections were air-dried for 1 hour at RT and fixed with ice cold acetone for 10 min at RT. The IHC procedure for the desired antigen was performed according to standard procedures using a fluorescently labeled secondary antibody (rhodamine Red™-X-conjugated) with spectral properties other than FITC. Non-specific antigenic sites were blocked with 5% goat serum in TBS at 4°C for 1 hour. Sections were incubated at 4°C overnight with primary antibody in TBST containing 1% goat serum. Control sections were incubated with the corresponding non-immune serum. After 3 x 5min washes with TBS, sections were incubated at 4°C for 90min with rhodamine Red™-X-conjugated secondary antibody in TBST containing 1% goat serum. ISZ was then performed in order to localize collagenolytic and gelatinolytic activity in the lung tissue[223, 224].

Briefly, sections were overlaid with 1 % low gelling temperature (LGT) agarose containing 100µg/ml highly quenched FITC-labeled DQ-collagen or DQ–gelatin, covered with a coverslip and gelled at 4°C. Sections were incubated at 37°C for 12 hours and examined. Control incubations were performed on serial cryostat sections by adding 30mM Captopril to the incubation medium. The presence of auto-fluorescence in sections was tested by incubating in agarose-containing medium lacking DQ-collagen or DQ-gelatin. Nuclei were counterstained by adding 1 µg/ml 4', 6-diamino-2-phenylindole [DAPI] to the incubation medium. Sections were analyzed

by comparing: (a) the localization of the fluorescence of FITC (activity) with that of rhodamine red (antigen); (b) the fluorescence of FITC formed after incubation in the presence of the DQ substrate with that produced after incubation in the absence of DQ substrate or in the presence of the DQ substrate and MMP inhibitors.

In murine lung immunohistochemical detection of macrophages in 10µm cryosection slides was performed with a fluorescent detection method according to the manufacturer's recommendations. Macrophages were detected with purified rat anti-mouse Mac-3 monoclonal antibody and with rhodamine Red™-X-conjugated affinipure Fab fragment goat anti-rat IgG (H+L). ISZ was then performed as outlined above.

3.16 Data analysis

Data are expressed as the mean ± SEM. Statistical analyses were performed with Graphpad Prism 4.02 software. Means between two groups were compared with 2-tailed unpaired Student's T-test, Wilcoxon test and 2-way ANOVA. Furthermore, statistical comparisons between IPF and normal groups were performed using the nonparametric Kruskal-Wallis test. $P < 0.05$ was considered statistically significant.

4. RESULTS

4.1 IPF patient lungs manifest the typical UIP histological pattern with marked collagen deposition in the matrix.

As a prerequisite of our study the histological phenotype of our patient population was examined.

4.1.1 Histological phenotype of patient lungs

A well known histological hallmark of IPF is the presence of fibroblastic foci in areas of active tissue remodelling adjacent to areas of normal tissue architecture[225]. We showed by haematoxylin and eosin staining of lung sections the typical UIP histological pattern in our patient study population (Figure 7b, 7e).

Masson trichrome stain showed deposition of collagen and other matrix proteins in the pulmonary interstitium of IPF patients compared to control lungs (Figure 7d, 7f versus 7b).

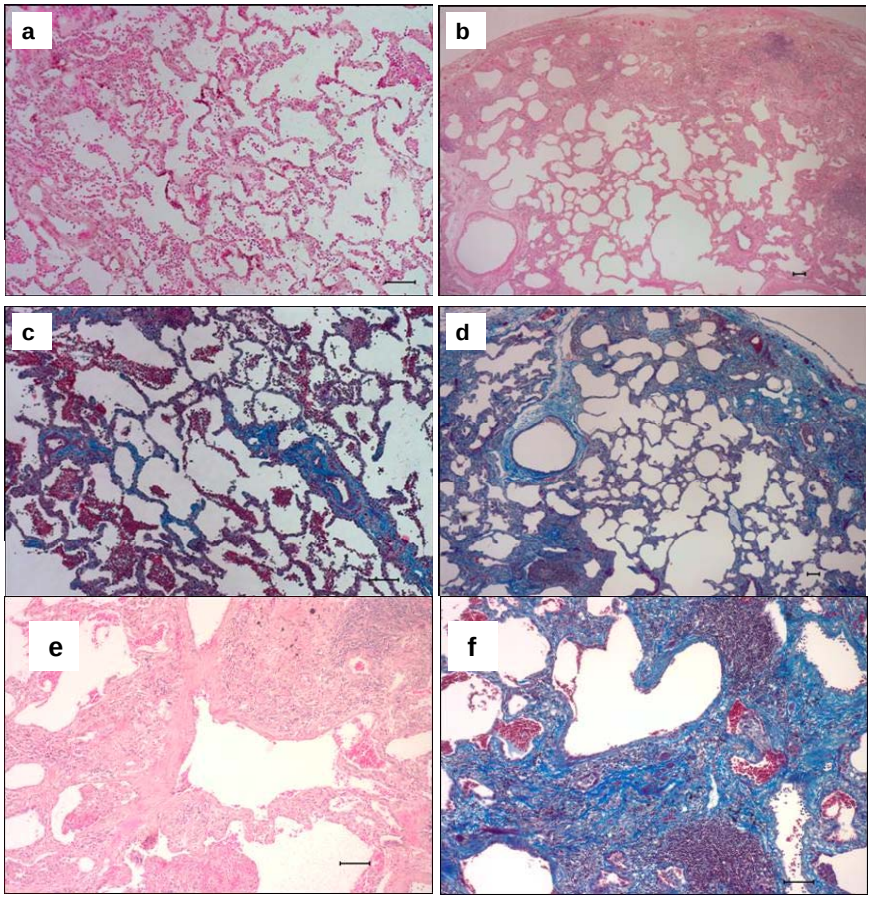

Figure 7: IPF lungs show the typical histological pattern of usual interstitial pneumonia and increased collagen deposition.

Paraffin sections from control and IPF lungs were stained with routine stains for histological assessment. Shown are representative lung sections from a control lung (a, c) and an IPF lung (b, d, e, f) stained with either haematoxylin & eosin (a, b, e) for general histological assessment and Masson trichrome for collagen and other matrix proteins (c, d, f). a & c,10X objective , scale = 100µm;

b & d, 4 x objective for IPF, scale = 250µm); e & f, 10x objective, scale = 100µm].

4.1.2 Hydroxyproline levels are increased in IPF lungs

Collagen deposition in IPF lung parenchyma was quantified by determining the hydroxyproline content (Figure 8) of lung tissues. Compared to control lungs we observed a moderate increase in lung hydroxyproline in two out of three different peripheral regions of the same lobe.The highest hydroxyproline content was encountered in the peripheral samples.

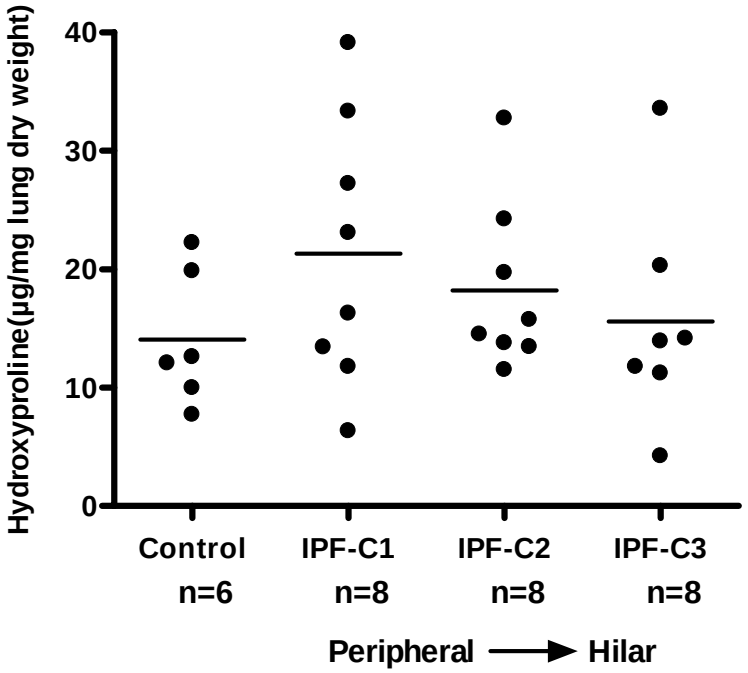

Figure 8: Hydroxyproline content of control and IPF patient lung tissues.
Lung tissue was taken from 3 different regions from the basal part of IPF lungs (n=8) and analysed for collagen deposition as described in the methods. Given are the hydroxyproline content in µg/mg lung dry weight. Comparison to control lung (n=6) was undertaken. Data are from three independent experiments and are presented as scatter dot-plot wherein the horizontal line within each group represents the mean hydroxyproline value.

4.2 Expression of MMPs and TIMPs in IPF and control lungs

The expression of MMPs and TIMPs at the transcriptional level was analyzed in homogenates from IPF and donor lungs and commercially available normal lung preparations (see Table 2 in Methods). In addition, MMP and TIMP protein expression was analyzed in IPF and donor lung homogenates and MMP-13 protein was localized in lung tissue. Furthermore, collagenolytic and gelatinolytic activities were analyzed.

4.2.1 mRNA expression of collagenases and matrilysin are upregulated in IPF lungs compared to control lungs

We first investigated MMP and TIMP expression at the mRNA level in IPF and control lungs by quantitative real time PCR. As compared to control lungs, mRNA expression of the collagenases MMP-1 and MMP-13 mRNA was greatly increased (44.8 fold and 57.1 fold, respectively). In addition, MMP-7 mRNA expression in the lungs of IPF patients was upregulated 11.8 fold (Figure 9). Expression of MMP -2, -8, -9, -12 and -14 was not significantly different between IPF and donor lungs. Among the TIMPs, only TIMP-4 was found to be significantly altered at the mRNA level, with a 2.5 fold reduction in expression in the IPF versus donor lungs.

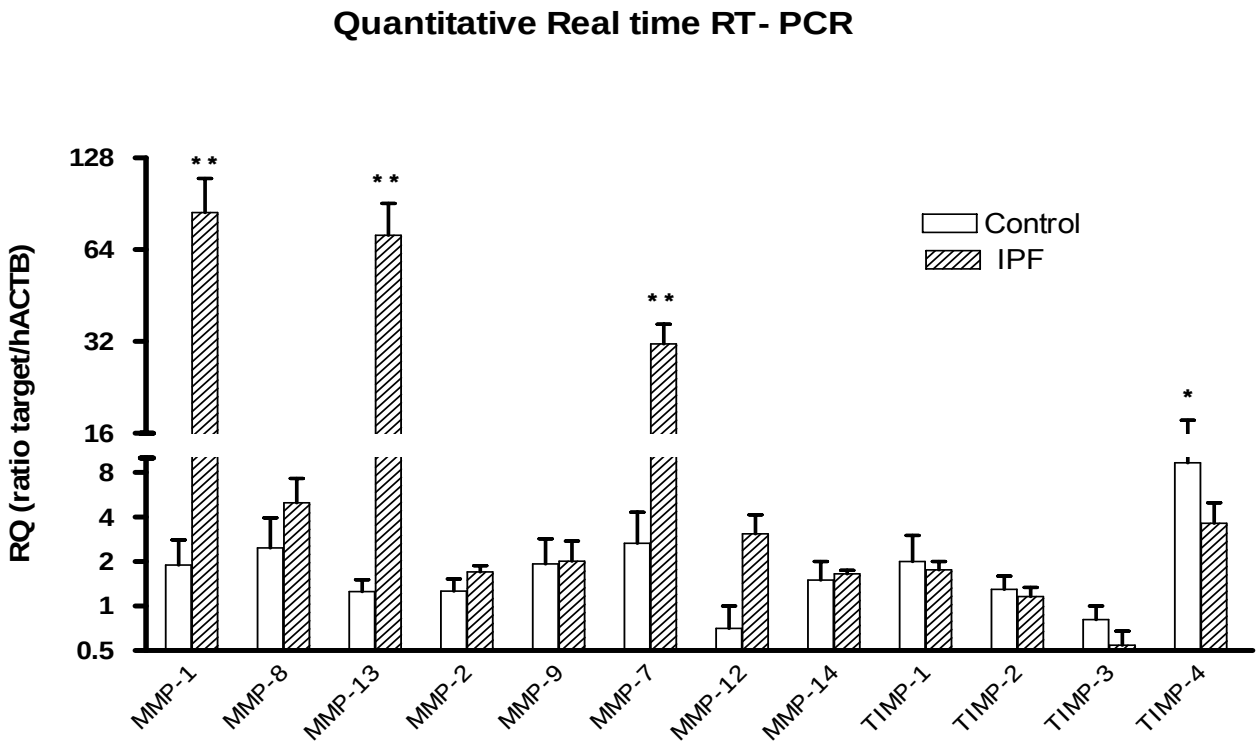

Figure 9: mRNA expression in control lungs and IPF patients.

Total RNA from control (n =7) and IPF patients (n =14) was reversed transcribed as described in the methods. mRNA transcripts of MMPs and TIMPs were quantified by quantitative RT-PCR and normalized as a ratio to human ß-actin as housekeeping gene. Data presented is the average quantification of 2 independent experiments. *p<0.05, **p < 0.01 compared to the control.

4.2.2 Increased protein content of MMP-1,-2, -7, -9, -13 in IPF lungs compared to controls

We employed western blot analysis to determine the expression of MMPs and TIMPs at the protein level. After densitometric analysis of the protein band intensities (Figure 10a), significant upregulation of protein in IPF versus control lungs was observed for MMP-1 (~2 fold), MMP-2 (~2 fold), MMP-7 (5.5), MMP-9 (~2 fold) and MMP-13 (~2 fold). In contrast, MMP-8 protein levels were reduced in IPF. None of the TIMPs showed significantly different expression at the protein level. We became interested in MMP-13 because among the MMPs analyzed the mRNA was increased the most. However, there was a lower level of protein than was anticipated from the mRNA expression data. We then examined the protein expression utilizing antibodies specific for the pro-and active form of MMP-13. We clearly demonstrated a high abundance of active MMP-13 protein in the IPF versus donor lungs (Figure 10b). To further corroborate these data and to identify the cellular source of MMP-13, immunohistochemistry was performed. Weak MMP-13 immunoreactivity was detected in the normal lung tissue (Figure 10c). However, in the lungs of IPF patients immunoreactive MMP-13 was easily detected in macrophages, in the alveolar and bronchiolar epithelial cells, alveolar septae and in the interstitial space (Figure 10d and 10e).

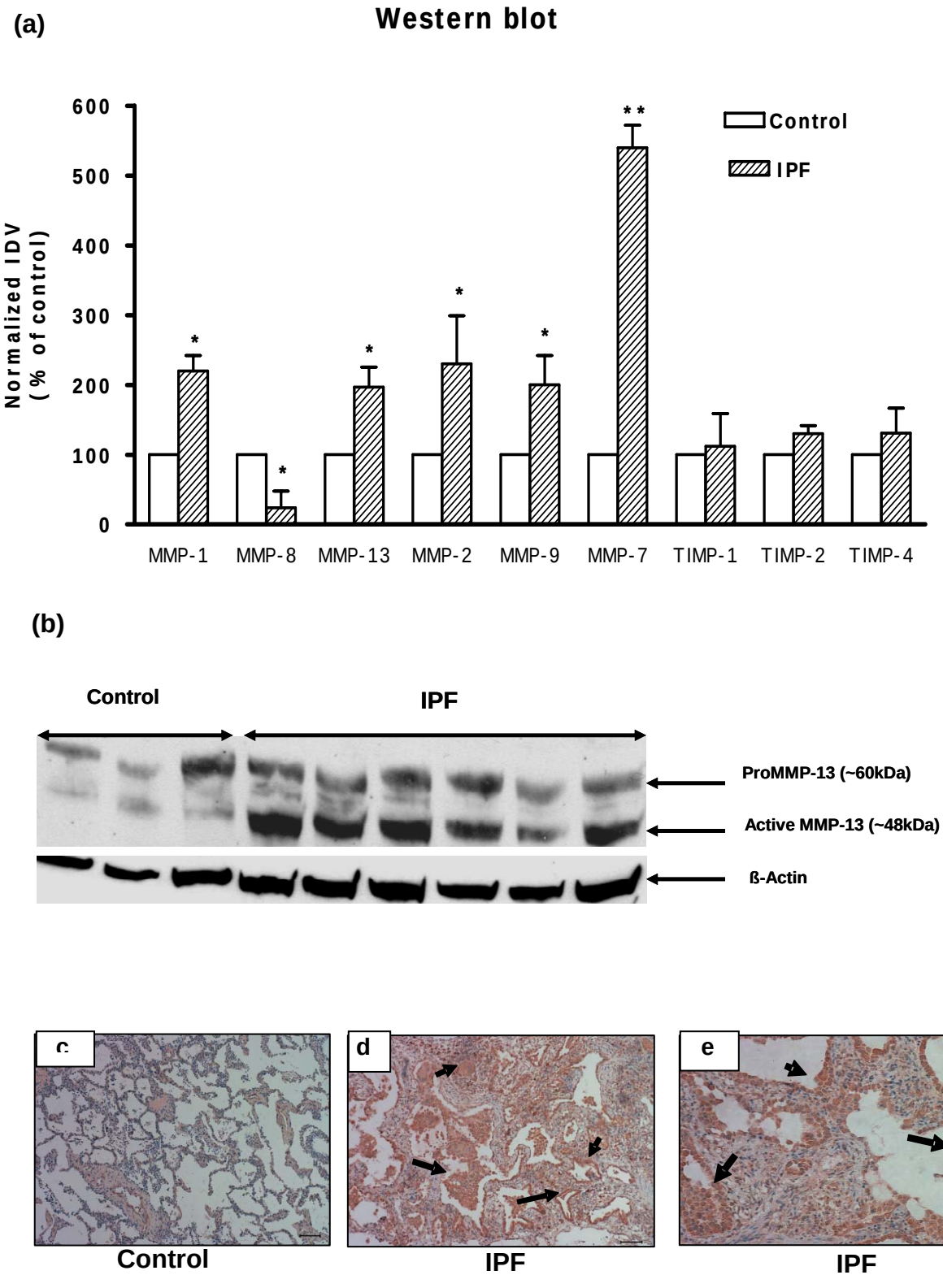
(a)
Western blot
Normalized IDV (% of control)
600
500
400
300
200
100
0
Control
IPF
MMP-1
MMP-8
MMP-13
MMP-2
MMP-9
MMP-7
TIMP-1
TIMP-2
TIMP-4
(b)
Control
IPF
ProMMP-13 (~60kDa)
Active MMP-13 (~48kDa)
ß-Actin
c
d
e
Control
IPF
IPF

Figure 10: MMP-13 protein expression is upregulated in IPF lungs

(a) Protein expression of MMPs and TIMPs were analyzed by Western blot and data are shown as the normalized integrated density value (IDV) to that of actin as loading control. Data presented are from three independent experiments. *$p< 0.05$ and ** $p<0.001$ compared to control. (b) Representative Western blot demonstrating increased protein expression of both the latent and active form of MMP-13 in IPF versus control.(c) Only weak MMP-13 immunoreactivity was observed in the control lungs, 10x objective, scale = 100µm. (d) MMP-13 immunohistochemistry confirms increased MMP-13 expression in IPF lungs. MMP-13 localized mainly to alveolar, bronchiolar epithelia cells (arrow), and alveolar macrophages; 10x objective, scale = 100µm. (e) Higher power view of showing abundant MMP-13 immunoreactivity (arrows); 20X objective, scale =50µm.

4.2.3 Increased collagenase and gelatinase activity in IPF versus control lungs

We further investigated if the increased protein levels of the collagenases and gelatinases would result in an increased activity. Collagenase activity in lung homogenates was measured by a fluorescence substrate assay and gelatinase activity was assessed by gelatin substrate zymography. Increased collagenase activity was observed in IPF compared to control lungs (Figure 11a). However, due to the limited number of samples investigated, this change did not reach statistical significance. We observed no difference in MMP-9 activity between IPF and control

lungs, but MMP-2 activity was significantly increased in IPF as compared to controls (Figures 11b, 11c and 11d). Development of lytic zones could be fully inhibited in control gels which were incubated in the presence of EDTA (data not shown).

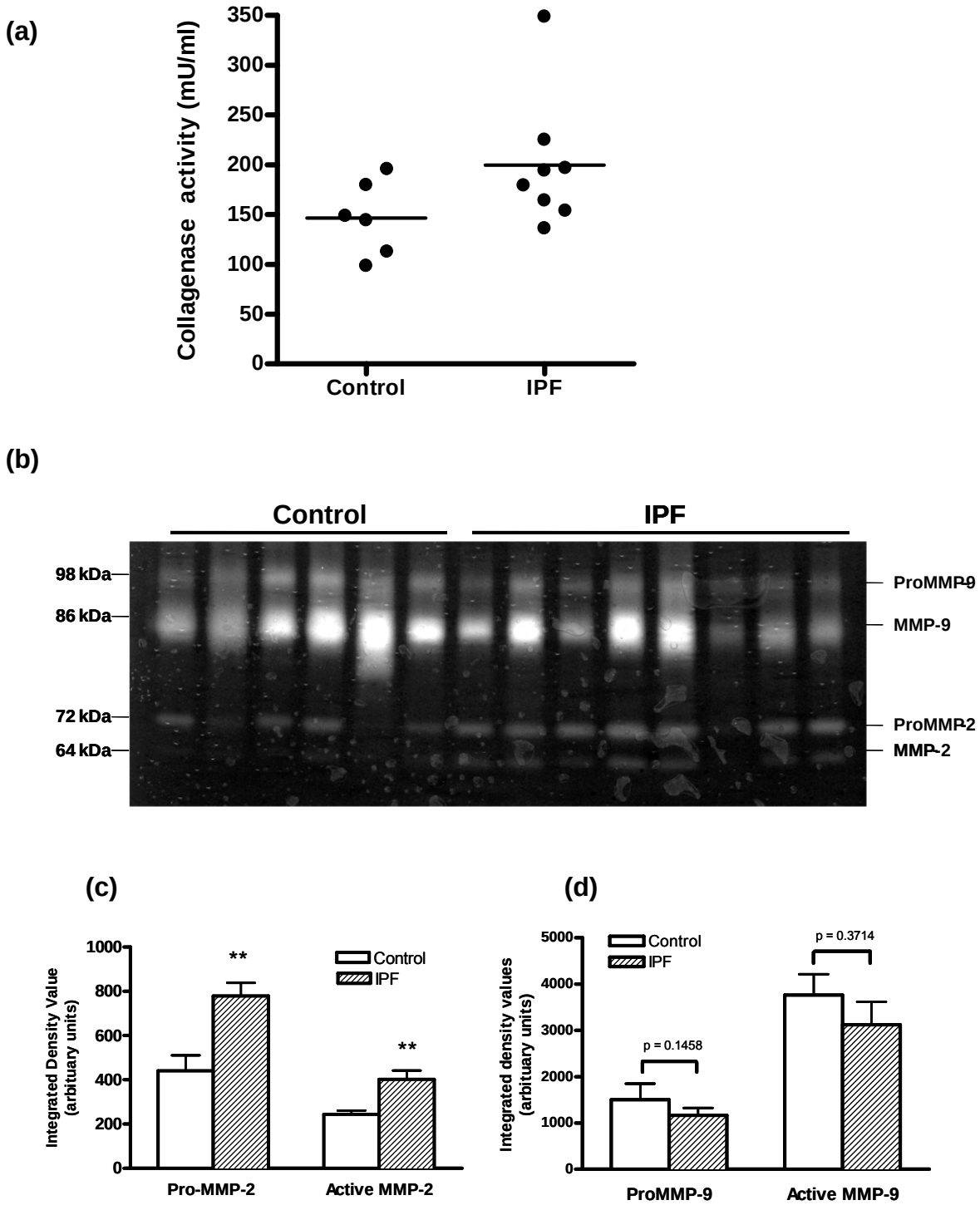

Figure 11: Increased collagenase and gelatinase activity in IPF versus control lungs.

(a) Microtiter plate based fluorescent substrate assay for collagenase activity in control (n=6) and IPF (n=8) lungs. Shown is a scatter-dot plot representing data from three independent experiments, wherein the horizontal line within each group represents the mean value. (b) Representative zymogram of gelatin substrate zymography of homogenates of control and IPF lungs; lytic zones of MMP-2 and MMP-9 activity appear white over the dark background. Densitometric analysis of pro- and active-MMP-2 activity (c); and of pro- and active MMP-9 activity (d). ***p < 0.01 IPF* compared to controls.

4.2.4 Spatial distribution of MMP antigen signal and collagenolytic and gelatinolytic activity in IPF and controls

In order to better judge on the spatial distribution of MMP protein signal and activity and in face of overlapping substrate specificities[118, 120], we employed collagen in situ zymography (ISZ) alongside with MMP-1 and -13 immunohistochemistry in order to correlate MMP-1 and -13 with collagenase activity. In addition, gelatin in situ zymography was performed simultaneously with MMP-2 immunohistochemistry in order to correlate MMP-2 with gelatinase activity. Whereas minimal activity and protein expression were observed in control lung tissue (Figure 12), we observed abundant MMP-1 and MMP-13 protein staining and partial co-localization with collagenase activity in alveolar epithelial cells lining fibroblastic foci and areas of dense fibrosis. We also found that MMP-2 protein and gelatinolytic activity co-localized in the endothelial and interstitial spaces of IPF lungs, but was not present

in the control lungs, thus underscoring the contribution of MMP-2 to the matrix remodelling process.

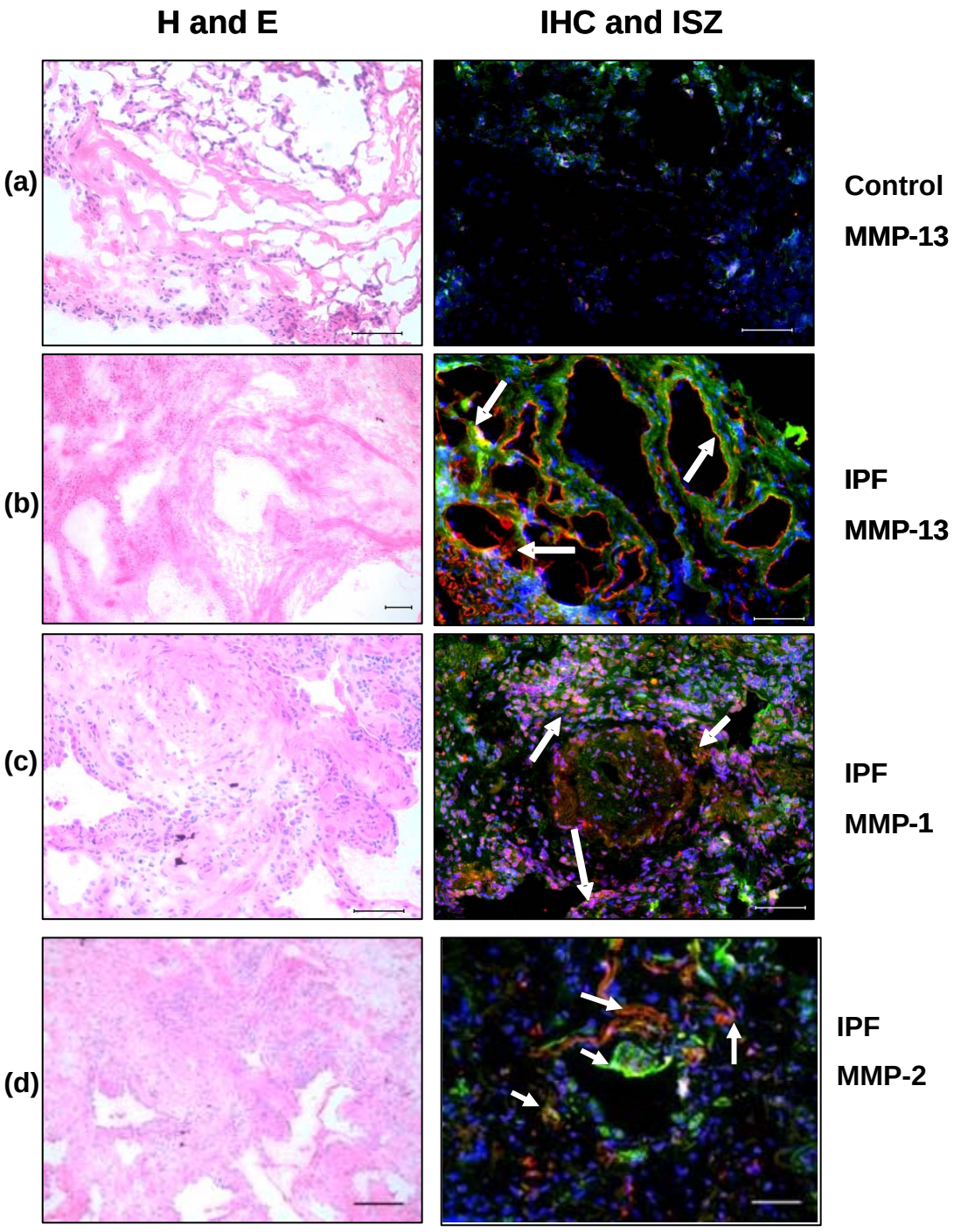

Figure 12: In situ zymography of MMPs in IPF.

Representative photomicrograph of in situ zymography combined with immunohistochemistry showing little collagenolytic activity and almost absence of MMP-1 (not shown) and MMP-13 protein signals in controlsl (a). In IPF tissues collagenolytic activity co-localized with MMP-13 (b), and MMP-1(c) in alveolar epithelial cells. Gelatinolytic activity co-localizes with MMP-2 (d). (Blue=nuclei, red = MMP-13 in (a) and (b), MMP-1 in (c), and MMP-2 in (d); green = collagenase activity (a, b, c) or gelatinase activity (d) 10X objective, Scale = 100µm.

4.3 Role of MMP-13 in the pathogenesis of fibrotic lung disease

As a result of our studies, we identified MMP-1 and MMP-13 as key collagenases upregulated in human IPF. Because rodents lack the orthologue of human MMP-1, we further investigated the relevance of the collagenase, MMP-13, in a murine model of bleomycin induced lung fibrosis. We examined the fibrotic response to bleomycin in MMP-13$^{-/-}$ and their in-bred wild type littermates.

In addition, we analyzed MMP activity in BAL fluid and expression of collagenases and TIMPs in lung homogenates pre- and post injury.

4.3.1 MMP-13$^{-/-}$ mice develop exaggerated inflammation following bleomycin challenge.

To characterize the bleomycin-induced inflammatory response in MMP-13$^{-/-}$ and wt littermates, we assessed total cell counts and cell differentials of cytospins from BALF at various time points after treatment (Figure 13a). Likewise to their littermate wt controls, MMP-13$^{-/-}$ mice showed a significantly elevated total cell count in response to bleomycin challenge which was caused largely by an influx of granulocytes and lymphocytes into the alveolar space of both mice. However, the extent of cell transmigration seemed to be much higher in the MMP-13$^{-/-}$ mice, reaching a significantly increased total cell count on d7 and d14 and a significantly increased relative number of neutrophils. Histological examination of lung sections from control MMP-13$^{-/-}$ and wt mice revealed an essentially normal lung architecture, with no differences between wt and MMP-13$^{-/-}$ mice (Figure 13b, 13e). 7d and 14d after bleomycin treatment, both, wt mice (Figure 13c and 13d, respectively) and MMP-13$^{-/-}$ mice (Figure 13f and 13g, respectively) developed patchy areas of inflammation throughout the lung parenchyma, with MMP-13$^{-/-}$ mice displaying a more severe and longer lasting inflammatory response to bleomycin. In accordance with the BALF findings, septal infiltration with lymphocytes and neutrophils was more prominent in MMP-13$^{-/-}$ as compared to wt mice, with some predominance in sub-pleural and peribronchial areas.

(a)

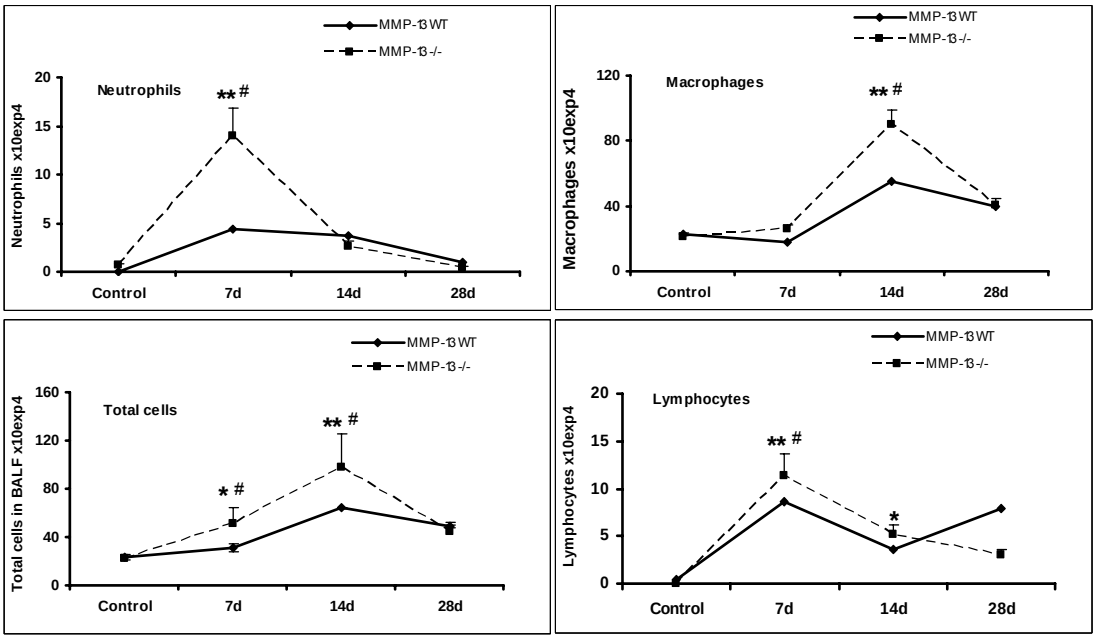
MMP-13 WT
MMP-13 -/-
Neutrophils
Neutrophils x10exp4
Macrophages
Macrophages x10exp4
Total cells
Total cells in BALF x10exp4
Lymphocytes
Lymphocytes x10exp4
Control
7d
14d
28d
** #
* #
*

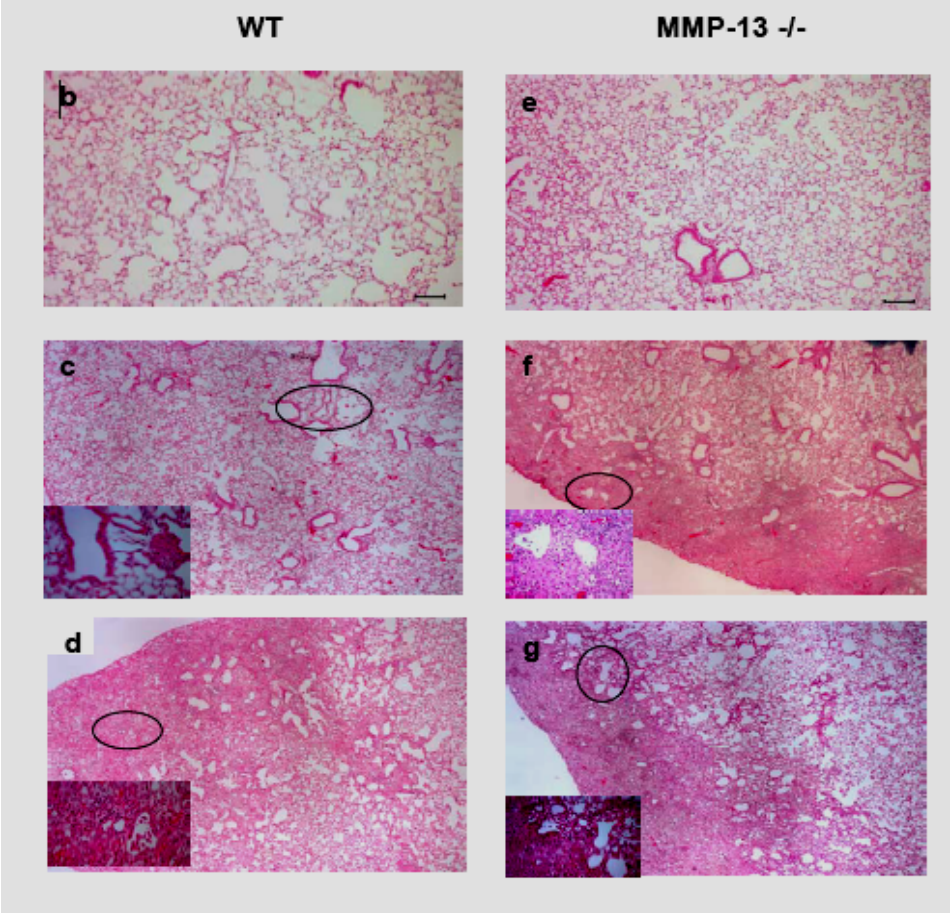
WT
MMP-13 -/-
b
c
d
e
f
g

Figure 13: Inflammatory changes in MMP-13$^{-/-}$ and wt mice after bleomycin challenge

Total cells and percentages of macrophages, neutrophils and lymphocytes were determined in BALF from wt and MMP-13 $^{-/-}$ mice, 7 days after saline application (control) and 7d, 14d, and 28d after bleomycin treatment (a). Results are presented as mean ± SEM, n = 4 - 5 per group. *$p< 0.05$ versus control, $^{\#}p < 0.05$ versus corresponding wt value. Histologic evaluation of lungs at 7 and 14 days postbleomycin challenge in wt and MMP-13$^{-/-}$ mice. Representative lung sections from wt (b, c, d) and MMP-13$^{-/-}$ (e, f, g) mice were H&E-stained. Inserts in (c) and (d) and (f) and (g) show phenotypic changes as marked. (Objective: a & b, x10; b, c, e, & f, x4; inserts, x20). Scale = 100µm.

4.3.2 Regulation of chemotatic activity in macrophages from MMP-13$^{-/-}$ mice

To better understand the sustained inflammatory reaction in MMP-13$^{-/-}$ versus wt mice in response to bleomycin, we performed a macrophage chemotaxis assay using BALF from MMP-13$^{-/-}$ and wt mice as the chemoattractant, and fluorescently labeled alveolar macrophages (AMJ2-C11 macrophage cell line) as responding cells. We noted that BALF from MMP-13$^{-/-}$ mice, obtained 7days after bleomycin challenge, exerted a slight, although significant, increase in chemoattraction to macrophages as compared to BALF from bleomycin or saline challenged wt mice (Figure 14).

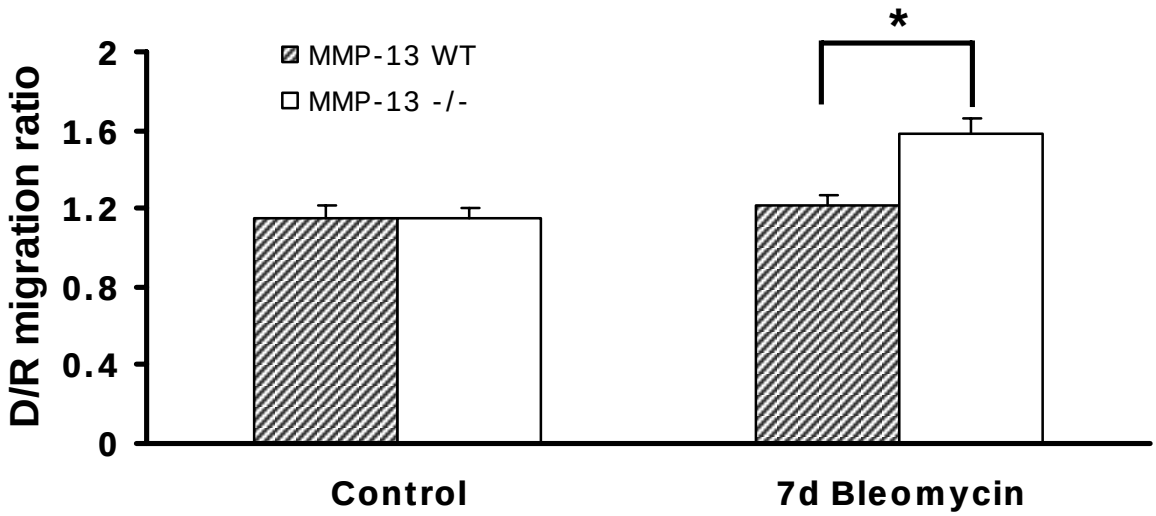

Figure 14: Increased macrophage chemotaxis to BALF from bleomycin challenged MMP-13$^{-/-}$ versus wt mice

BALF was obtained from control and bleomycin treated and MMP-13$^{-/-}$ and wt mice (n = 3 per group). The alveolar macrophage cell line AMJ2-C11 was used as responding cells. Data are presented as mean ± SEM, and are a representative of 2 independent experiments. * $p< 0.05$ comparing chemotaxis induced by 7d treated MMP-13$^{-/-}$ versus wt mice.

4.3.3 MMP-13$^{-/-}$ mice show more extensive lung fibrosis in response to bleomycin administration.

We then analyzed the lung collagen content and extent of lung fibrosis in bleomycin challenged MMP-13$^{-/-}$ and wt mice. Figure 15 shows representative Mason-Trichrome-stained lung sections (3 slides per lung and 5 random microscopic fields per slide examined) from control and bleomycin challenged wt (a & b) and MMP-13$^{-/-}$ (c & d) mice at d28. As evident from this figure, MMP-13$^{-/-}$ mice showed more extensive lung fibrosis and collagen deposition as compared to WT mice. Similar results were already observed at d14 (data not shown).

Analysis of lung hydroxyproline content (Figure 15e) revealed similar results: hydroxyproline levels were similar in control wt and MMP-13$^{-/-}$ mice in the absence of challenge, and challenge with bleomycin resulted in a significant increase in lung hydroxyproline content in wt and MMP-13$^{-/-}$ mice. However, hydroxyproline content of MMP-13$^{-/-}$ mice was significantly higher compared to the respective wt mice, 28d after bleomycin challenge.

In line with this observation, the lung compliance (Figure 16) of bleomycin challenged MMP-13$^{-/-}$ mice on d28 were significantly decreased as compared to bleomycin challenged wt mice.

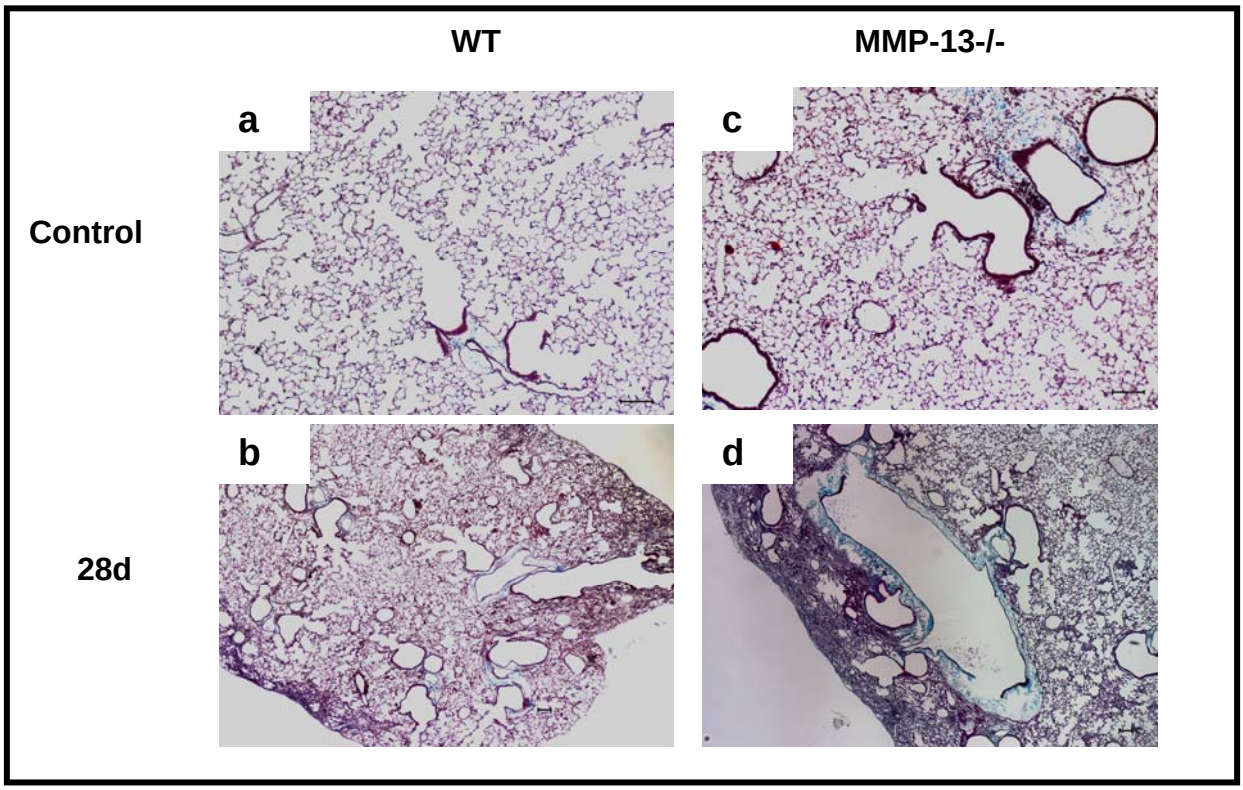
WT
MMP-13-/-
a
c
Control
b
d
28d

(e)

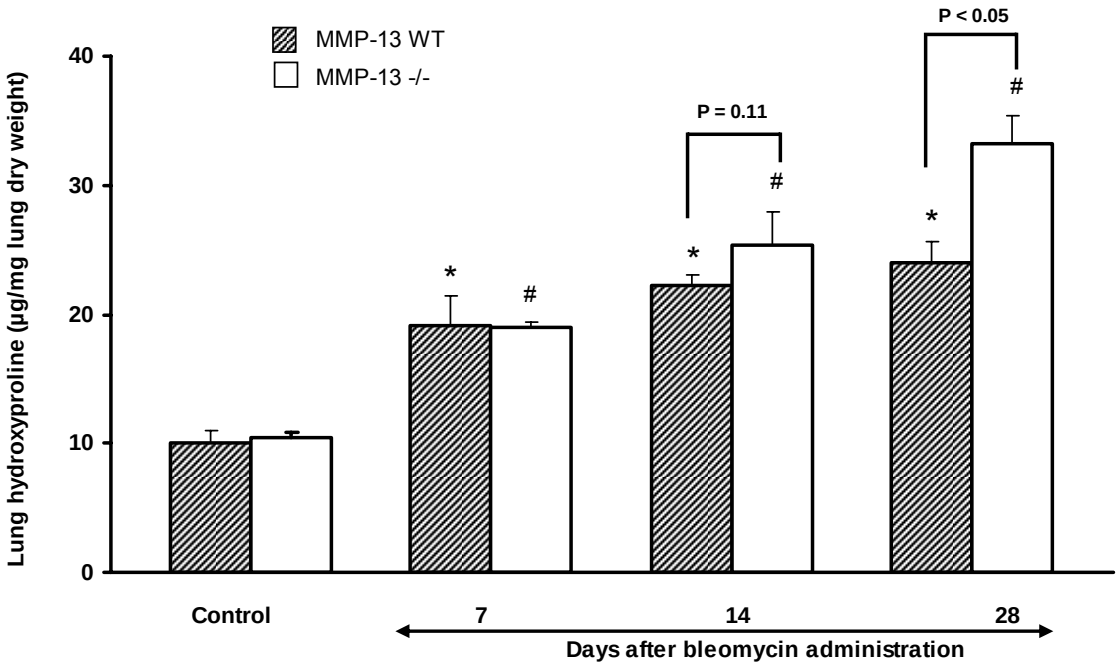
MMP-13 WT
MMP-13 -/-
P = 0.11
P < 0.05
Lung hydroxyproline (µg/mg lung dry weight)
40
30
20
10
0
Control
7
14
28
Days after bleomycin administration

Figure 15: Increased lung collagen content in MMP-13$^{-/-}$ versus wt mice in response to bleomycin treatment.

Representative lung sections from wt (a and b) and MMP-13$^{-/-}$ (c and d) mice stained with Masson-Trichrome stain for collagen and matrix proteins are given. (e) Hydroxyproline content in wt and MMP-13$^{-/-}$ lungs, control (saline) and at 7, 14 and 28d after bleomycin treatment, (n = 4-5 per group)

Data are representative of two experiments and presented as mean ± SEM.

p <0.05 compared to wt control; $^{\#}p<0.05$ compared to MMP-13$^{-/-}$ control.

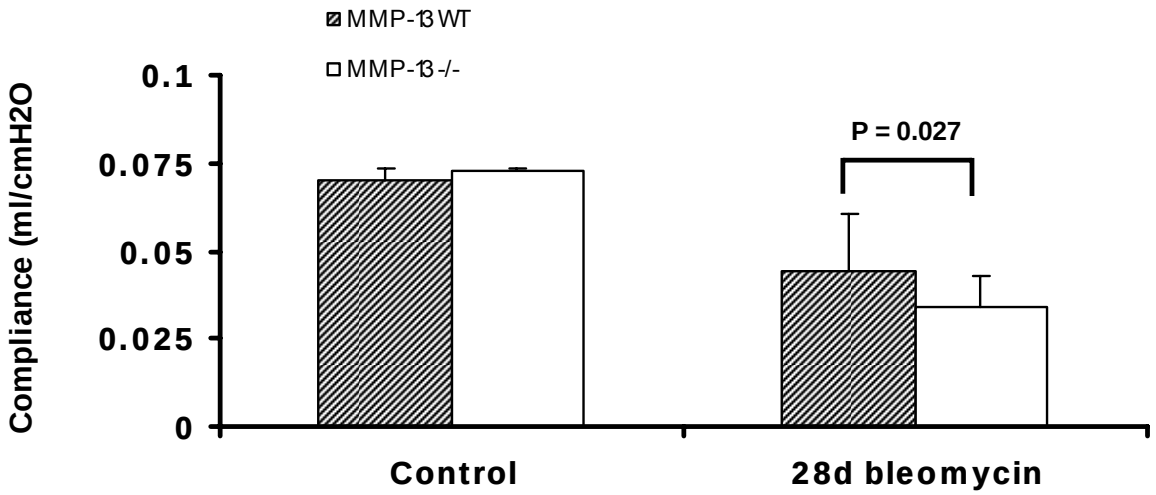

Figure 16: Lung compliance of control and d28 bleomycin treated MMP-13$^{-/-}$ and wt mice.

Lung compliance of mice (n = 3-5 per group) was measured as described in methods. Data are presented as mean compliance ± S.E.M, *p* value is indicated.

4.3.4 Expression of MMPs and TIMPs in MMP-13$^{-/-}$ and WT mice

We next assessed the effect of bleomycin on the expression pattern of MMPs and TIMPs and to identify a potential compensation for the loss of MMP-13 in MMP-13$^{-/-}$ mice. As depicted in Figure 17a, MMP-7 mRNA was upregulated in wt and in MMP-13$^{-/-}$ mice in response to bleomycin challenge (d28), however, MMP-7 mRNA was not different in wt versus MMP-13$^{-/-}$ treated mice and this was also encountered in lung specimen from the other time points post bleomycin challenge (data not shown). Such observation was further corroborated by immunohistochemistry of lung sections obtained d28 after bleomycin challenge: in here, MMP-7 immunostaining (Figure 17b) was absent in untreated lungs, but was found to be present in MMP-13$^{-/-}$ and wt mice (Figure 17b). In contrast, MMP-8 mRNA expression was found to be elevated in MMP-13$^{-/-}$ versus wt mice in absence of any challenge. In response to bleomycin challenge MMP-8 was induced in MMP-13$^{-/-}$ and wt mice, however, with much higher mRNA levels in the MMP-13$^{-/-}$ mice (Figure 17c). As expected, MMP-13 transcripts were not observed in the MMP-13$^{-/-}$ mice, whereas MMP-13 was found to be greatly induced in response to bleomycin challenge in wt mice (Figure 17d).

(a)

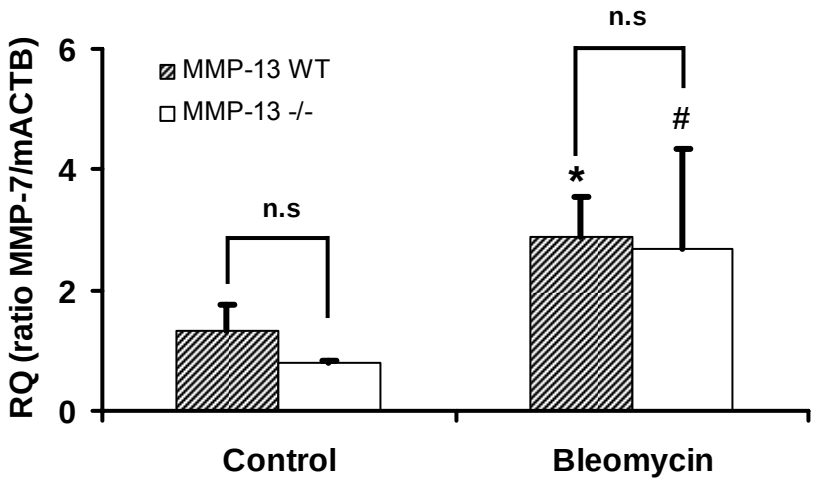
RQ (ratio MMP-7/mACTB)
6
4
2
0
MMP-13 WT
MMP-13 -/-
n.s
n.s
*
#
Control
Bleomycin

(b)

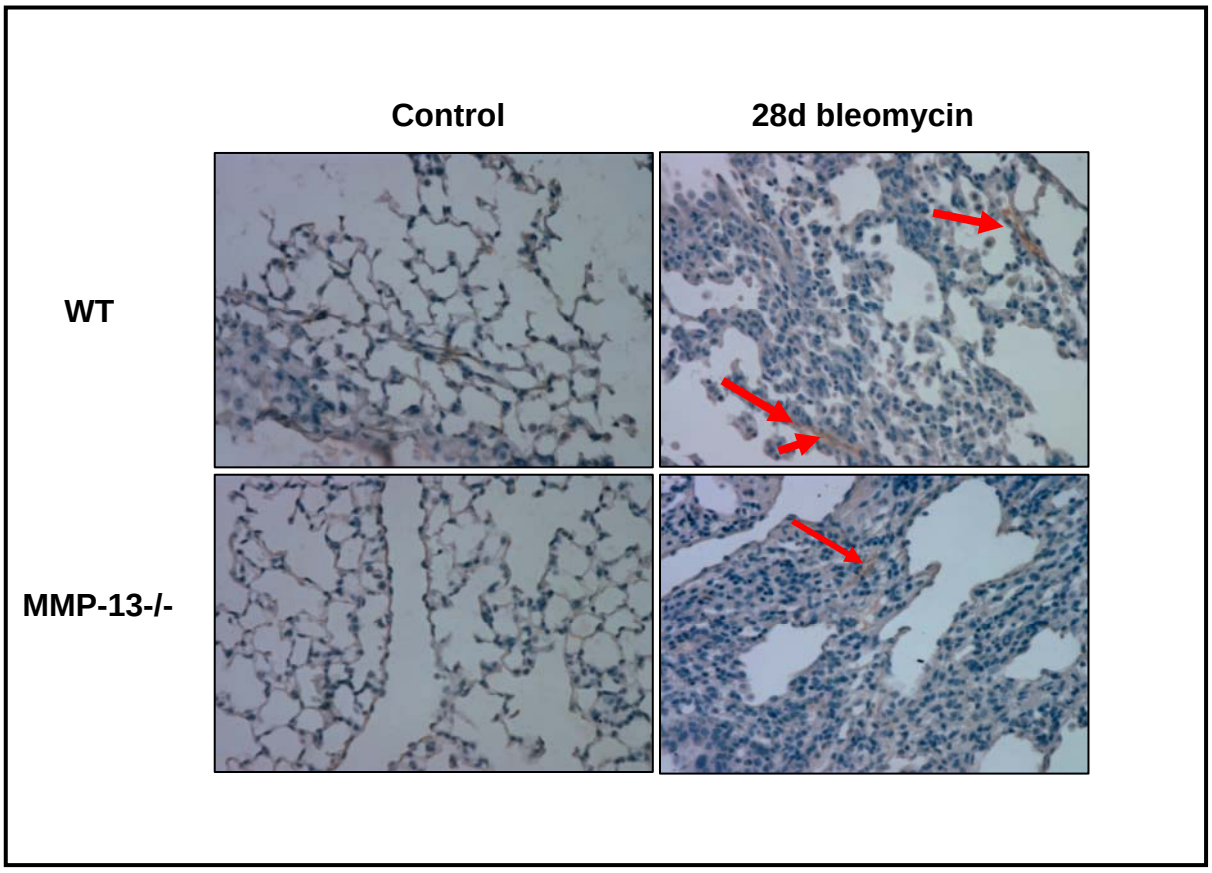
Control
28d bleomycin
WT
MMP-13-/-

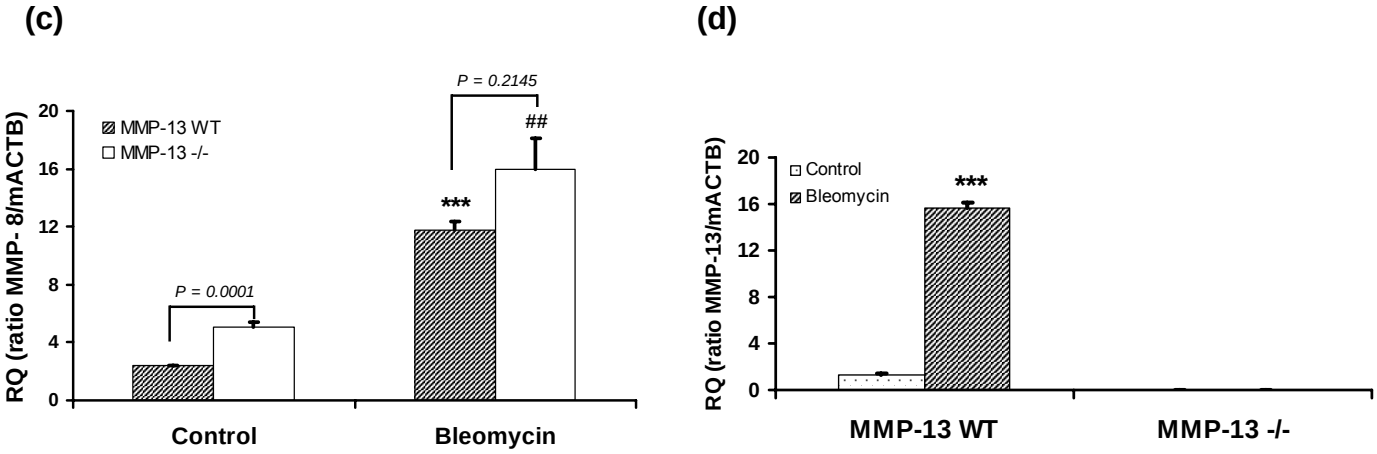

Figure 17: Expression of *Mmps-7, 8, 13* in lungs of wt and MMP-13$^{-/-}$ mice in response to bleomycin challenge.

Total lung RNA was obtained from saline treated (control, left bar) or bleomycin-treated (right bar) mice at d28 and analyzed for mRNA transcripts of *Mmp-7* **(a)**, *Mmp-8* **(c)**, *Mmp-13* **(d)** using quantitative RT- PCR and normalized as a ratio to *mouse ß-actin* as housekeeping gene. Data are shown as mean $ddC_t \pm$ SEM from 3-5 mice per treatment group. * *p< 0.05,* ** *p< 0.001,* ***$p< 0.0001$ compared to wt control; $^{\#}$ *p< 0.05,* $^{\#\#}$ *p< 0.001,* $^{\#\#\#}p< 0.0001$ compared to MMP-13$^{-/-}$ control.**(b)** MMP-7 protein immunostaining in distal airways of wt (upper panel) versus MMP-13$^{-/-}$ (lower panel) mice. No MMP-7 staining was observed in respective control lungs (left upper and lower panels).

We also analysed mRNA expression level of *Timp-1* (Figure 18a), *Timp-2* (Figure 18b), *Timp-3* (Figure 18c) and *Timp-4* (Figure 18d) in the lungs of wt and MMP-13$^{-/-}$ mice, control and 28d after bleomycin treatment. We observed significantly elevated levels of these mRNAs in MMP-13$^{-/-}$ versus wt mice in absence of bleomycin challenge (Figure 18) and significant induction of these TIMPs in response to bleomycin challenge (Figure 18)

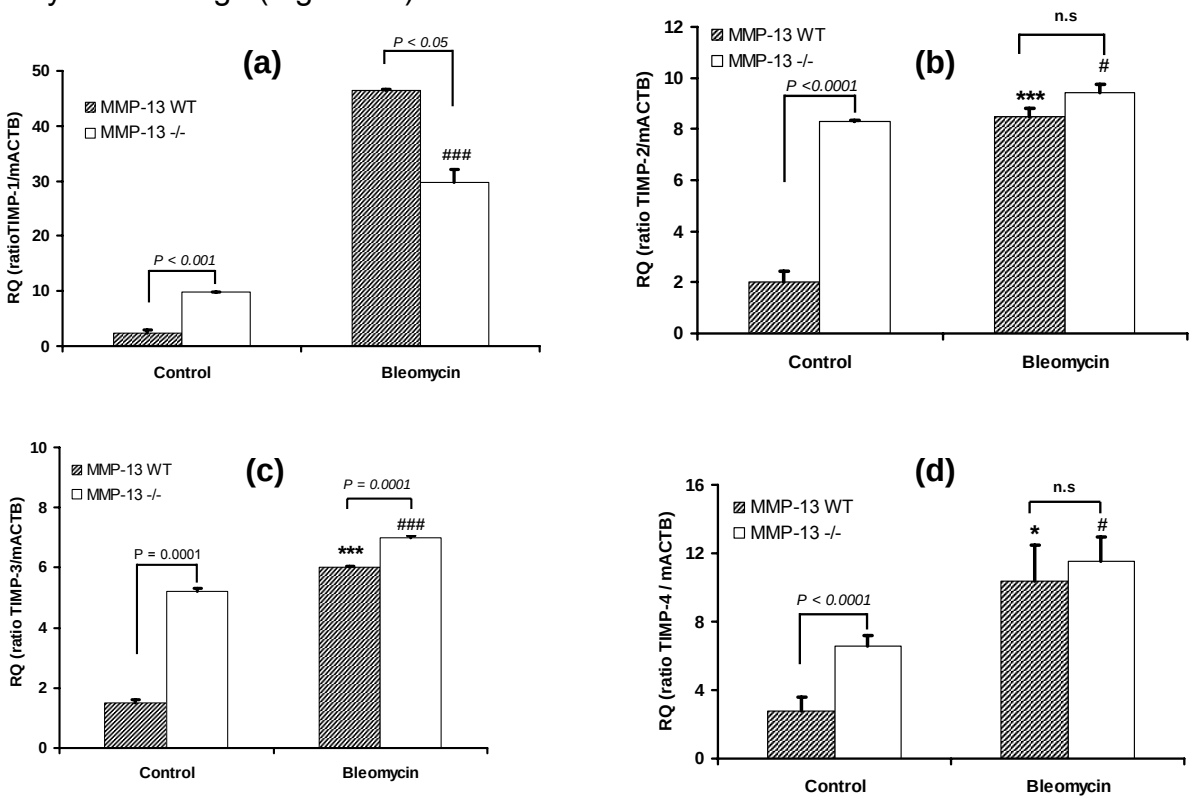

Figure 18: mRNA expression of *Timps* in wt and MMP-13$^{-/-}$ mice

mRNA expression of *Timps-1 (a)*, *-2 (b)*, *-3 (c) and -4(d)* was analysed by quantitative RT-PCR in lung specimen of saline treated (control, left bars) and bleomycin challenged (d28, right bars) mice. Data are shown as mean ddct ± SEM from 3-5 mice per treatment group.

* *p< 0.05, ** p< 0.001, ***p< 0.0001* compared to wt control;

$^{\#}$ *p< 0.05,* $^{\#\#}$ *p< 0.001,* $^{\#\#\#}$*p< 0.0001* compared to MMP-13$^{-/-}$ control.

5. DISCUSSION

5.1 Role of MMPs and TIMPs in Pulmonary Diseases

MMPs have been implicated in various pathologies. Redundant diseases associated with MMP regulation include: aortic aneurysms[226-229], atherosclerosis[230-232], rheumatoid and osteoarthritis[233, 234], nephritis[235-238], tumor growth and migration[239-241], and tissue ulcers[118, 120, 242, 243]. Dysregulation of MMP activity has been associated with lung diseases such as cancer, emphysema and fibrosis[91, 117, 244-248]. For this reason, MMPs have become an important focus for basic science studies and clinical investigations by lung biology researchers and are important players in the future diagnosis and treatment of lung disease involving excessive matrix remodelling.

Almost all of the MMPs can be identified in lung tissue. In view of the predominant extracellular matrix (ECM) compounds of the lung, in particular type I and II collagen and elastin, the collagenases, gelatinases, matrilysin and macrophage metalloelastase are of major interest. These MMPs are counterbalanced by the four TIMPs, among which TIMP 1 and 2 seem to play a major role in ILDs[249]. Under conditions of lung fibrosis a differential pattern of MMP and TIMP expression has been observed and suggested to contribute to the evolution of the disesase [250, 251]. In IPF, MMP 9 expression was found to be elevated [252], whereas in COP or NSIP, MMP 2 expression seemed to be preferentially upregulated [253]. The gelatinases (MMP-2 and -9)[253-255] and neutrophil elastase (MMP-8)[255] have been shown to be

elevated in the BALF and lungs of IPF patients. RNA and protein levels of MMP-7 in particular, have been shown to be increased in both human and experimental lung fibrosis[86]. In addition to MMP-7, increased MMP-1 expression levels were recently found in BALF and plasma of IPF patients[86, 256].

Recently, epigenetic modifications have been shown to contribute to MMP regulation [168]. Studies performed using transgenic or knock out mice also revealed the fundamental significance of MMPs in the development of emphysema[257,258] and lung fibrosis[86]. As an example, MMP-1 overexpressing mice do develop emphysema in spite of normal elastin content [257]. In parallel, increased collagenase (MMP-1) activity has been observed in BAL and lung parenchyma from emphysema patients and could be localized to alveolar type II cells[259]. Furthermore, MMP-12 KO mice were shown to have a normal lung phenotype even after exposure to cigarette smoke [260], and in yet another study, MMP-12 KO mice were not protected from bleomycin-induced lung fibrosis[90]. MMP-7 KO mice were shown to be protected from bleomycin-induced lung fibrosis[86] and MMP-9 KO mice showed decreased alveolar bronchiolization after bleomycin-induced lung fibrosis[89], thus underscoring the important contribution of single MMPs in the dynamic regulation of the ECM and of remodeling processes in the lung[91].

MMP-13 (also known as collagenase-3) is the major interstitial collagenase of rodents and has a high specificity for degrading insoluble fibrillar collagens especially type II and I collagens [180, 261]. The expression of MMP-8 and -13 were shown to be down-regulated in a model of pulmonary fibrosis induced in rats with

paraquat and hyperoxia [251]. MMP-13 was recently shown to play a role in the pathogenesis of liver fibrosis [180] but its role has never been studied in murine models of lung fibrosis such as the bleomycin-induced lung fibrosis model.

Less is known about the regulation of TIMPs under conditions of IPF. Under experimental conditions, it is observed that the concentration of TIMP-1 and TIMP -2 proteins was elevated more than 200 fold in bleomycin induced lung fibrosis, suggesting an imbalance of MMP and TIMP. In addition, Selman and colleagues reported increased TIMPs 1, -2, -3 and -4 expression levels in the lungs of IPF patients compared to normal lungs[82].

Taken together, elevated levels of MMPs have been implicated in the pathophysiology of various lung diseases, including acute respiratory distress syndrome, asthma, bronchioectasis, and cystic fibrosis. MMPs, EMMPRIN[257, 262], and TIMPs are produced by many of the resident cells in the lung, hence complicating the analysis of their role under disease conditions. Potential use of MMP inhibitors for treatment of these disorders in patients remains to be explored.

5.2 Regulation of MMP and TIMP expression and activity in human lungs.

In the present study, the expression pattern of several MMPs and TIMPs was analyzed in explanted IPF versus normal and donor lungs and the spatial distribution of MMP-13 and MMP-2 antigen signal correlated with the collagenolytic and gelatinolytic activity as assessed employing in situ zymography. Among all MMPs and TIMPs studied in lung homogenates, only the collagenases MMP-1 and MMP-13, and MMP-7 were found to be significantly upregulated on the mRNA and protein level and served as an explanation for the overall increased collagenolytic activity in IPF lung homogenates. Although the gelatinases MMP-2 and MMP-9 were unchanged on the mRNA level, a roughly 2 fold increase in these gelatinases was encountered at the protein level in IPF versus donor lung homogenates. Against our anticipation, TIMPs-1 - 4 were not found to be significantly increased in IPF homogenates, neither at the mRNA nor at the protein level. At a quick glance, this observation contrasts with the observed increase in hydroxyproline content, especially in the subpleural areas of IPF. Our data seem also not to support the previous suggestion of a far-reaching blockade of MMP activity by overwhelming TIMP levels[82] as the underlying principle of increased ECM content in IPF. Despite our restriction to only study MMP-1, -2 and -13 on the level of in situ zymography [224] and some theoretical limitations of assessing MMPs on the level of lung homogenate [263, 264], the most reasonable explanation for our observation is, however, that either production and deposition of ECM exceeds the capacity of the ECM degradation

machinery or that the spatial distribution of proteolytic activity is poorly distributed or both [265]. Indeed, our in situ zymography data do suggest that collagenolytic and gelatinolytic activities were not exclusively co-localizing with the respective MMP antigen signals in the lung tissues, suggesting free and overwhelming MMP activity within the airways and weaker activity in the scar regions. Such an observation may also serve as a potential explanation for the development of honeycomb cysts, an obviously inappropriate loss of lung architecture and puzzling feature of IPF and many other progressive forms of lung fibrosis [13, 14, 34, 266-268].

5.3 Upregulation of MMP-13 protein in human IPF lungs

A prominent and novel finding is our observation of the upregulation of pro- and active MMP-13 protein in IPF lungs. In lung tissue of IPF patients MMP-13 protein was found to be localized in alveolar and bronchiolar epithelial cells, alveolar macrophages, the alveolar septae and areas of remodelled interstitial lung tissue. This was an interesting finding, as the group of Selman[82] showed MMP-1, otherwise known as interstitial collagenase, to be localized in the bronchiolar epithelial cells but not in the interstitial space, where abundant extracellular matrix is found. Ortiz and colleagues[269] previously demonstrated MMP-13 overexpression in lungs of silica-treated TNF receptor-deficient mice and by in situ hybridization, showed that MMP-13 mRNA hybridized to the cytoplasm of macrophages inside silicotic nodules. Therefore, our results suggest that MMP-13 might be playing an important role in the pathogenesis of IPF especially at the level of tissue repair and remodeling.

5.4 Role of MMP-13 in pulmonary fibrosis

MMP-13 is the major proteinase that shows substrate specificity towards interstitial fibrillar collagens I, II, III and gelatin, preferentially cleaving type II collagen[179]. Drawn against this background and as MMP-13 had been recently shown to play a significant role in bone remodeling defects in skeletal diseases[179, 184], to reduce liver fibrosis[180], and to increase collagen accumulation in atherosclerotic plagues[270], we hypothesized that MMP-13 might also play a role in pulmonary fibrosis.

Employing the model of bleomycin induced lung fibrosis we investigated the role of MMP-13 in pulmonary fibrosis and firstly observed an exaggerated early inflammation in the MMP-13$^{-/-}$ mice. In detail, total BALF cell numbers of bleomycin challenged MMP-13$^{-/-}$ mice progressively and significantly increased during the first 14 days as compared to challenged WT littermates and this was found to be due to an exaggerated neutrophilic response in the MMP-13$^{-/-}$ mice. Contrary to our findings, previous studies reported less neutrophil accumulation in MMP-9$^{-/-}$ mice[89], and MMP-12$^{-/-}$ mice [90, 271] after bleomycin treatment whereas in WT mice a remarkable infiltration of neutrophils and lymphocytes characterized the initial inflammatory response to bleomycin. MMPs are known to proteolytically process chemokines and activate pro-inflammatory cytokines causing an increase in their chemotactic activity for inflammatory cells[258, 272, 273]. In spite of these known effects of MMPs, BALF from MMP-13$^{-/-}$ mice exerted a stronger chemoattraction toward macrophages. The underlying reason for the observed hyperinflammation in MMP-13$^{-/-}$ mice is currently not clear and deserves further studies. However, an

explanation for our observation could be a putative role of MMP-13 in the proteolytic inactivation of pro-inflammatory cytokines or chemokines.

Starting at d14 after bleomycin challenge, an augmented fibrotic response was encountered in the MMP-13$^{-/-}$ mice and it is currently unclear if this augmented fibrotic response was caused by the more extensive inflammation or the pure absence of MMP-13. This holds especially true when considering that MMP-7 was found to be similarly upregulated in both MMP-13$^{-/-}$ and wt mice, and the TIMPs were not dramatically altered in MMP-13$^{-/-}$ versus wt mice in response to bleomycin challenge. One intriguing interpretation of our experimental data would also be a compensatory, but insufficient upregulation of MMP-8 in order to substitute for missing MMP-13. Somewhat in line with such reasoning, Raulo and colleagues[274] had previously reported a positive correlation (in tracheal epithelial lining fluid [TELF] of horses) between immunoreactivity of MMP-8 and MMP-13 and the amount of degradation of type I collagen. Macrophages and epithelial cells were observed as the major cellular sources of MMP-8 and MMP-13 in the above study. Supporting the hypothesis of reciprocal compensation of MMP deficiency, Lindsey and colleagues[275] reported significantly lower levels of MMP-13 in the left ventricle of MMP-7$^{-/-}$ mice whereas pro-MMP-8 levels were elevated. Our data show increased fibrosis in MMP-13$^{-/-}$ mice in response to bleomycin, in contrast to MMP-7$^{-/-}$ mice that were shown to be protected from bleomycin-induced lung fibrosis[86]. Obviously, this differential and, indeed, opposite impact of knock out of single MMPs on the development of lung fibrosis indicates distinct roles of each MMP. Although purely

speculative at the present time, our observations alongside with unpublished data could suggest that MMP-13 and MMP-8 are regulated synergistically in fibrotic repair. However, further studies are required to define such a possible interaction.

We observed no difference in MMP-2 and MMP-9 activities between bleomycin-treated MMP-13$^{-/-}$ and wt mice. Since there was a robust increase in the BALF total cell count in MMP-13$^{-/-}$ versus wt mice, with a huge proportion of these cells being macrophages, it might be speculated that, following bleomycin administration MMP-13$^{-/-}$ mice would have more gelatinase activity being released as the enzyme is secreted into the alveolar lining layer. However, the lack of an increase in total gelatinolytic activity of the cell free BALF does not support such a concept. In addition, macrophages secrete the gelatinases into the alveolar lining layer but these enzymes may be diluted out at the time of lavaging and retrieving the BAL fluid from the lungs. Alternatively, a larger portion of the increase in the gelatinase post-bleomycin could originate from the epithelial cells and therefore, the difference in macrophage gelatinase becomes undetectable.

In summary, in an attempt to define the spatial expression and the nature of MMP activity in IPF, the contribution of TIMPs in the local inhibition of MMPs and the relative contribution of single MMPs in the process of fibrotic repair in IPF, we could show that

(a) TIMPs are not excessively upregulated as compared to MMPs in IPF lungs; the collagenolytic activity of IPF tissue homogenates is higher as compared to donor

lungs, thus the increase in collagen deposition seems to be largely due to excessive matrix synthesis and deposition rather than blockade of MMPs;

(b) collagenolytic and gelatinolytic activities do not colocalize completely with single MMP antigen signals in the lung tissues, suggesting a predominance of MMP activity within the airways and weaker activity in the scar regions (possibly providing one explanation for the process of honeycombing) and

(c) MMP-13 seems to play a significant role in IPF, as this collagenase is dramatically upregulated in lung tissue from IPF patients and as increased inflammation and excessive fibrosis are encountered in bleomycin challenged MMP-$13^{-/-}$ versus control lungs.

Our data therefore suggest that MMP-13 plays an important, (if not pivotal) role in the remodeling process in IPF, both in view of matrix deposition in the scarring areas, as well as in view of the development of honeycomb cysts, similar to the induction of emphysema formation in MMP-1 overexpressing mice[257, 276].

6. SUMMARY

Idiopathic pulmonary fibrosis (IPF) is a severe epithelial-fibroblastic disease with poor prognosis, characterised by excessive deposition of collagen in the pulmonary interstitium. Several matrix metalloproteinases (MMPs) and the tissue inhibitors of metalloproteinases (TIMPs) have been demonstrated to be strongly up-regulated in human and experimental lung fibrosis, thus underscoring their dynamic regulation of extracellular matrix and of remodeling processes in the lung. To investigate the spatial regulation, nature of MMP activity and the contribution of TIMPs in the local inhibition of MMPs in IPF, we examined IPF in comparison to donor lung tissue for regulation of MMPs and TIMPs, and the relative contribution of single MMPs to the fibrotic lung repair process.

We identified MMP-7 and the collagenases, MMP-1 and -13, as key proteases upregulated in human IPF. A prominent and novel finding of our work is the upregulation of pro- and active MMP-13 protein in IPF patients. MMP-13 protein was localized in alveolar and bronchiolar epithelial cells, the alveolar septae and extracellular matrix of remodelled lung tissue. TIMP proteins were not differentially regulated; an observation that somehow contrasted with the increased hydroxyproline content, especially in the subpleural areas of IPF. We have shown by a combination of immunohistochemistry and in situ zymography that collagenolytic and gelatinolytic activities did not exclusively co-localize with a single MMP antigen signal in the lung tissues, suggesting predominant MMP activity within the airways and weaker activity in the scar regions.

Since mice lack the orthologue of human MMP-1, we investigated further the relevance of MMP-13 in the context of fibrotic lung diseases by examining the fibrogenic response to bleomycin in MMP-13$^{-/-}$ mice and wt littermates. In response to bleomycin challenge and likewise to their littermate wt controls, MMP-13$^{-/-}$ mice were characterized by elevated total cell counts in BALF caused largely by an influx of granulocytes and lymphocytes. Seven and fourteen days after bleomycin treatment, both wt and MMP-13$^{-/-}$ mice developed patchy areas of inflammation throughout the lung parenchyma, with MMP-13$^{-/-}$ mice again displaying a more severe inflammatory response to bleomycin that persisted for a longer time period. Likewise, the extent of fibrosis was more prominent in MMP-13$^{-/-}$ versus wt mice, with increased levels of hydroxyproline and more significant histologic signs of fibrosis. It is currently unclear if this augmented fibrotic response was caused by the more extensive inflammation or the absence of MMP-13, especially when considering that MMP-7 was found to be similarly upregulated in both MMP-13$^{-/-}$ and wt mice and the TIMPs were not dramatically altered in MMP-13$^{-/-}$ versus wt mice.

In conclusion, in an attempt to define the spatial regulation and the nature of MMP activity in IPF, the contribution of TIMPs in the local inhibition of MMPs and the relative contribution of single MMPs in the process of fibrotic repair in IPF, we could show that (a) TIMPs are not excessively upregulated as compared to MMPs in IPF lungs; (b) the collagenolytic activity of IPF tissue homogenates is higher as compared to donor lungs, thus the increased collagen deposition seems to be largely due to excessive matrix synthesis and deposition rather than blockade of

MMPs, (c) collagenolytic and gelatinolytic activities do not colocalize completely with single MMP antigen signals in the lung tissues, suggesting the predominance of MMP activity within the airways and weaker activity in the scar regions (possibly providing one explanation for the process of honeycombing) and (d) MMP-13 seems to play a significant role in IPF, as this collagenase is dramatically upregulated in tissues from IPF patients and as excessive inflammation and fibrosis are encountered in bleomycin challenged MMP-13$^{-/-}$ mice versus control mice lungs.

Our data therefore suggest that MMP-13 plays an important, (if not pivotal) role in the remodeling process in IPF, both in view of matrix deposition in the scarring areas, as well as in view of the development of honeycomb cysts, similar to the induction of emphysema formation in MMP-1 overexpressing mice. However, the mechanism of action of MMP-13 together with related mediators remains a subject for further investigation.

7. ZUSAMMENFASSUNG

Die Idiopathische Interstitielle Pneumonie (IPF) ist eine interstitielle Lungenerkrankung, der eine gestörte epitheliale-mesenchymale Interaktion zugrunde liegt, und die aufgrund eines rasch-progredienten und therapierefraktären Verlaufs eine äußerst schlechte Prognose aufweist. Ein Charakteristikum der IPF ist die exzessive Deposition von Komponenten der extrazellulären Matrix wie z.B. Kollagen. Für verschiedene Matrixmetalloproteinasen (MMPs) und deren Inhibitoren (*tissue inhibitors of metalloproteinases*, TIMPs) konnte eine differentielle Regulation bei der Lungenfibrose gezeigt werden, die auf eine dynamische Regulation des Stoffwechsels der Extrazellulärmatrix und auf kontinuierlich ablaufende Umbauprozesse in der Lunge hinweisen. Anhand von Lungengewebe von IPF Patienten wurde in der vorliegenden Arbeit die kompartimentalisierte Regulation der MMPs, die Quelle und Eigenschaften der MMP Aktikivät und die Beteiligung der TIMPs bei der IPF näher untersucht. Darüberhinaus wurde die relative Beteiligung einzelner MMPs am bei der Lungenfibrose gestörten Wundheilungsprozess untersucht.

Wir konnten mit MMP-7 und den Kollagenasen MMP-1, MMMP-8 und MMP-13 wichtige Schlüsselenzyme identifizieren, die bei der IPF heraufreguliert sind. Dabei konnte in der vorliegenden Arbeit erstmals die gesteigerte Expression von MMP-13 (latentes und aktives Protein) im Lungengewebe von IPF Patienten gezeigt werden. MMP-13 wurde in alveolären und bronchiolären Epithelzellen, in Alveolarsepten und in der extrazellulären Matrix von bereits umgebautem Lungengewebe gefunden. Die

MMP Inhibitoren (TIMPs) hingegen zeigten keine differentielle Regulation, ein Befund, der im Widerspruch zu dem –vorallem in subpleuralen Gebieten der IPF Lunge- deutlich erhöhten Hydroxyprolin Gehalt steht. Mittels immunhistochemischer Verfahren in Kombination mit *in situ* Zymograhie konnte gezeigt werden, dass die gelatinolytischen und kollagenolytischen Aktivitäten nicht zwangweise mit einzelnen MMP Antigensignalen im Lungengewebe kolokalisiert waren; die prädominante MMP Aktivität wurde in den Atemwegen detektiert, in den fibrotischen Herden hingegen zeigte sich eine schwächere Aktivität.

Da orthologe knockout Mäuse für humane MMP-1 nicht verfügbar waren, lag der weitere Focus auf der Untersuchung der Rolle von MMP-13 bei der Fibroseentwicklung am Modell der Bleomycin-induzierten Lungenfibrose unter Verwendung vom MMP-13 knockout Mäusen. Hinsichtlich der Zahl und der prozentualen Zusammensetzung lavagierbarer Zellen im alveolären Kompartiment. zeigte sich sowohl bei MMP-13$^{-/-}$ wie auch bei Wildtyp Mäusen ein Anstieg der Gesamtzellzahl, der auf einen Einstrom von Granulozyten und Lymphozyten in den Alveolarraum zurückzuführen war. An Tag 7 und Tag 14 nach Bleomycinapplikation war histologisch bei beiden Mäusen eine Entzündungsreaktion des Lungenparenchyms mit unregelmäßigem Verteilungsmuster festzustellen, das bei den MMP-13$^{-/-}$ Tieren jedoch stärker ausgeprägt war und über einen längeren Zeitraum bestand hatte. Dabei zeigten die Septen der Knockout Tiere eine stärkere Infiltration mit granulozytären und lymphozytären Zellen, mit einer Akzentuierung subpleuraler und peribronchiolärer Areale. Derzeit ist allerdings unklar inwieweit die

verstärkt ablaufende Fibroseantwort auf die gesteigerte Inflammationsreaktion oder das Fehlen von MMP-13 zurückzuführen ist, insbesondere wenn man berücksichtigt, dass MMP-7 sowohl in MMP-13 $^{-/-}$ wie auch Wildtyp-Mäusen heraufreguliert war und die TIMPs in MMP-13 $^{-/-}$ im Vergleich zu Wildtyp Tieren nicht substantiell verändert waren.

Die wichtigsten Befunde dieser Arbeit lassen sich wie folgt zusammenfassen: (a) im Gegensatz zu MMPs werden deren Inhibitoren (TIMPs) in Lungen von IPF Patienten nicht überhöht exprimiert. (b) die kollagenolytische Aktivität im Homogenat von IPF Lungen ist höher als in Homogenaten von Donorlungen. Die erhöhte Kollagendeposition scheint daher eher durch eine überhöhte Synthese von Komponenten der extrazellulären Matrix als durch die Inhibition der Degradation (MMP Inhibition) zustande zukommen. (c) die kollagenolytischen und gelatinolytischen Aktivitäten sind nicht zwingend mit dem Antigensignal einzelner MMPs co-lokalisiert, was eine Prädominanz der MMP Aktivität in den Atemwegen und eine geringere Aktivität in den fibrotischen Arealen vermuten lässt, und somit eine mögliche Erklärung für den Umbau zur Honigwabenlunge (*honeycombing*) liefert. (d) die erhebliche Überexpression von MMP-13 in IPF Lungen und die gesteigerte Fibroseantwort bei MMP-13 *knockout* Mäusen nach Bleomycin Schädigung legt nahe, dass diese Kollagenase eine wichtige Rolle bei der Fibroseentwicklung spielt. Die hier gezeigten Daten belegen, dass MMP-13 eine wichtige, wenn nicht sogar eine Schlüsselrolle bei den Umbauprozessen im Rahmen einer IPF einnimmt, und zwar sowohl was die Deposition von Extrazellulärmatrix in

den Fibroseherden betrifft, wie auch im Hinblick auf die Bildung der Honigwaben Zysten (analog zur Induktion der Emphysembildung bei MMP-1 überexprimierenden Mäusen). Zur Aufklärung der Mechanismen, über die die MMP-13 Effekte vermittelt werden, sowie zur Identifizierung der beteiligten Mediatoren müssen weiterführende Studien durchgeführt werden.

8. ABBREVIATION

AECsII	Type II Aveolar epithelial cells
ANOVA	Analysis of variance
ARDS	Adult respiratory distress syndrome
BALF	Bronchoalveolar lavage fluid
BCA	Bicinchoninic acid
BOOP	Bronchiolitis obliterating organizing pneumonia
BSA	Bovine serum albumin
$CaCl_2$	Calcium chloride
cDNA	Complementary deoxyribonucleic acid
COMP	Cartilage oligomeric matrix protein
COPD	Chronic obstructive pulmonary disease
DAPI	4', 6-diamino-2-phenylindole
DPLD	Diffuse parenchymal lung disease
DQ	Dye-quenched
ECL	Enhanced Chemiluminescence
ECM	Extracellular matrix
EDTA	Ethylene diamine tetra-acetic acid
ELISA	Enzyme-linked immunosorbent assay
EMMPRIN	Extracellular matrix metalloproteinase inducer
Ex/Em	Excitation/Emission
FITC	Fluorescein isothiocyanate

FN	Fibronectin
GPI	Glycosylphosphatidyl inositol
H & E	Haematoxylin and eosin stain
HP	Hypersensitivity pneumonitis
HPS	Hermansky-Pudlack Syndrome
HRCT	High resolution computed tomography
IDV	Integrated density value
IgG	Immunoglobulin
IGFBP-3	Insulin growth factor binding protein-3
IHC	Immunohistochemistry
IIP	Idiopathic interstitial pneumonitis
IL1-β	Interleukin 1-beta
ILD	Interstitial lung disease
IPAH	Idiopathic pulmonary arterial hypertension
IPF	Idiopathic pulmonary fibrosis
ISZ	In situ zymography
kDa	Kilo Dalton
KO	Knockout
MCP-3	Monocyte chemoattractant protein-3
$MgCl_2$	Magnesium chloride
MMPs	Matrix metalloproteinases
mRNA	Messenger ribonucleic acid
MWM	Molecular weight marker

MT-MMP	Membrane type- matrix metalloproteinase
NaCl	Sodium chloride
NO	Nitric oxide
NSIP	Non-specific interstitial pneumonia
PAH	Pulmonary arterial hypertension
PAI -1	Plasminogen activator inhibitor-1
PBS	Phosphate buffered saine
PDGF	Platelet derived growth factor
PH	Pulmonary hypertension
ROS	Reactive oxygen species
RT-PCR	Reverse Transcription- Polymerase chain reaction
RV	Right ventricle
SDS-PAGE	Sodium dodecyl-sulphate - polyacrylamide gel electrophoresis
SEM	Standard error mean
SMC	Smooth muscle cell
SPARC	Secreted protein acidic and rich in cysteine
SP-C	Surfactant protein-C
TBS	Tris buffered saline
TBS/T	Tris buffered saline containing Tween-20
TELF	Tracheal epithelial lining fluid
TGF-β	Transforming growth factor-beta
TIMPs	Tissue inhibitors of metalloproteinases
TM	Transmembrane

TNF-α	Tissue necrosis factor-alpha
t-PA	Tissue-type plasminogen activator
UIP	Usual interstitial pneumonia
u-PA	Urokinase-type plasminogen activator
uPAR	Urokinase-type plasminogen activator receptor
VATS	Video-assisted thoracoscopic surgery
VEGF	Vascular endothelial growth factor
VN	Vitronectin
W.H.O	World Health Organization
WT	Wild type
$ZnCl_2$	Zinc chloride

9. Reference List

(1) Hayek H. *The Human Lung*. New York: Hafner; 1960.

(2) Ehrlich KC. Proteoglycan synthesis by rat lung cells cultured in vitro. *J Biol Chem* 1981;256(1):73-80.

(3) Kaplan NB, Grant MM, Brody JS. The lipid interstitial cell of the pulmonary alveolus. Age and species differences. *Am Rev Respir Dis* 1985;132(6):1307-12.

(4) Nixon W, Pack A. Effect of altered gas diffusivity on alveolar gas exchange-a theoretical study
1. *J Appl Physiol* 1980 January;48(1):147-53.

(5) Antic N, McEvoy RD. Primary alveolar hypoventilation and response to the respiratory stimulant almitrine
1. *Intern Med J* 2002 December;32(12):622-4.

(6) Agusti AG, Cardus J, Roca J, Grau JM, Xaubet A, Rodriguez-Roisin R. Ventilation-perfusion mismatch in patients with pleural effusion: effects of thoracentesis
1. *Am J Respir Crit Care Med* 1997 October;156(4 Pt 1):1205-9.

(7) Ng AW, Bidani A, Heming TA. Innate host defense of the lung: effects of lung-lining fluid pH
1. *Lung* 2004;182(5):297-317.

(8) Nicod LP. Pulmonary defence mechanisms
9. *Respiration* 1999;66(1):2-11.

(9) Schwarz MI. Infiltrative and Interstitial Lung Diseases. In: Murray JF, ed. *Textbook of Respiratory Medicine*. 2nd ed. Philadelphia: W.B. Saunders Company; 1988. p. 1803-26.

(10) Campbell EJ, Senior RM, Welgus HG. Extracellular matrix injury during lung inflammation. *Chest Chest* 1987;92(1):161-7.

(11) Clark JG, Kuhn C, III, McDonald JA, Mecham RP. Lung connective tissue. *Int Rev Connect Tissue Res* 1983;10:249-331.

(12) Katzenstein AL, Myers JL. Nonspecific interstitial pneumonia and the other idiopathic interstitial pneumonias: classification and diagnostic criteria. *Am J Surg Pathol* 2000;24(1):1-3.

(13) American Thoracic Society. Idiopathic pulmonary fibrosis: diagnosis and treatment. International consensus statement. American Thoracic Society (ATS), and the European Respiratory Society (ERS). *Am J Respir Crit Care Med* 2000;161(2 Pt 1):646-64.

(14) American Thoracic Society/European Respiratory Society International Multidisciplinary Consensus Classification of the Idiopathic Interstitial Pneumonias. This joint statement of the American Thoracic Society (ATS), and the European Respiratory Society (ERS) was adopted by the ATS board of directors, June 2001 and by the ERS Executive Committee, June 2001. *Am J Resp Crit Care Am J Resp Crit Care* 2002;165(2):277-304.

(15) Johnston ID, Prescott RJ, Chalmers JC, Rudd RM. British Thoracic Society study of cryptogenic fibrosing alveolitis: current presentation and initial management. Fibrosing Alveolitis Subcommittee of the Research Committee of the British Thoracic Society. *Thorax* 1997;52(1):38-44.

(16) Selman M, King TE, Pardo A. Idiopathic pulmonary fibrosis: prevailing and evolving hypotheses about its pathogenesis and implications for therapy. *Ann Intern Med* 2001;134(2):136-51.

(17) Horowitz JC, Thannickal VJ. Epithelial-mesenchymal interactions in pulmonary fibrosis. *Semin Respir Crit Care Med* 2006 December;27(6):600-12.

(18) White ES, Lazar MH, Thannickal VJ. Pathogenetic mechanisms in usual interstitial pneumonia/idiopathic pulmonary fibrosis. *J Pathol* 2003;201(3):343-54.

(19) Khalil N, O'Connor R. Idiopathic pulmonary fibrosis: current understanding of the pathogenesis and the status of treatment. *Can Med Assoc J Can Med Assoc J* 2004;171(2):153-60.

(20) Coultas DB, Zumwalt RE, Black WC, Sobonya RE. The epidemiology of interstitial lung diseases. *Am J Respir Crit Care Med* 1994;150(4):967-72.

(21) Hodgson U, Laitinen T, Tukiainen P. Nationwide prevalence of sporadic and familial idiopathic pulmonary fibrosis: evidence of founder effect among multiplex families in Finland. *Thorax* 2002;57(4):338-42.

(22) Pardo A, Selman M. Molecular mechanisms of pulmonary fibrosis. *Front Biosci Front Biosci* 2002;7:D1743-D1761.

(23) Katzenstein AL, Myers JL. Idiopathic pulmonary fibrosis: clinical relevance of pathologic classification. *Am J Respir Crit Care Med* 1998;157(4 Pt 1):1301-15.

(24) Panos RJ, Mortenson RL, Niccoli SA, King TE, Jr. Clinical deterioration in patients with idiopathic pulmonary fibrosis: causes and assessment 1. *Am J Med* 1990 April;88(4):396-404.

(25) Meyers BF, Patterson GA. Current status of lung transplantation 3. *Adv Surg* 2000;34:301-18.

(26) Meyers BF, Lynch JP, Trulock EP, Guthrie T, Cooper JD, Patterson GA. Single versus bilateral lung transplantation for idiopathic pulmonary fibrosis: a ten-year institutional experience 4. *J Thorac Cardiovasc Surg* 2000 July;120(1):99-107.

(27) Thabut G, Mal H, Castier Y, Groussard O, Brugiere O, Marrash-Chahla R, Leseche G, Fournier M. Survival benefit of lung transplantation for patients with idiopathic pulmonary fibrosis 3. *J Thorac Cardiovasc Surg* 2003 August;126(2):469-75.

(28) Flaherty KR, Martinez FJ. The role of pulmonary function testing in pulmonary fibrosis. *Curr Opin Pulm Med* 2000 September;6(5):404-10.

(29) Kazerooni EA. High-resolution CT of the lungs. *AJR Am J Roentgenol* 2001 September;177(3):501-19.

(30) Kazerooni EA, Martinez FJ, Flint A, Jamadar DA, Gross BH, Spizarny DL, Cascade PN, Whyte RI, Lynch JP, III, Toews G. Thin-section CT obtained at 10-mm increments versus limited three-level thin-section CT for idiopathic pulmonary fibrosis: correlation with pathologic scoring. *AJR Am J Roentgenol* 1997 October;169(4):977-83.

(31) Wells AU, Hansell DM, Rubens MB, Cullinan P, Black CM, du Bois RM. The predictive value of appearances on thin-section computed tomography in fibrosing alveolitis. *Am Rev Respir Dis* 1993 October;148(4 Pt 1):1076-82.

(32) Blewett CJ, Bennett WF, Miller JD, Urschel JD. Open lung biopsy as an outpatient procedure. *Ann Thorac Surg* 2001 April;71(4):1113-5.

(33) Miller JD, Urschel JD, Cox G, Olak J, Young JE, Kay JM, McDonald E. A randomized, controlled trial comparing thoracoscopy and limited thoracotomy for lung biopsy in interstitial lung disease. *Ann Thorac Surg* 2000 November;70(5):1647-50.

(34) Katzenstein AL, Zisman DA, Litzky LA, Nguyen BT, Kotloff RM. Usual interstitial pneumonia: histologic study of biopsy and explant specimens. *Am J Surg Pathol* 2002;26(12):1567-77.

(35) Katzenstein AL. Pathogenesis of "fibrosis" in interstitial pneumonia: an electron microscopic study. *Hum Pathol* 1985;16(10):1015-24.

(36) Selman M, Pardo A. Idiopathic pulmonary fibrosis: an epithelial/fibroblastic cross-talk disorder. *Respiratory research* 2002;3:3.

(37) Brody AR, Craighead JE. Interstitial associations of cells lining air spaces in human pulmonary fibrosis. *Virchows Arch A Pathol Anat Histol* 1976;372(1):39-49.

(38) Coalson JJ. The ultrastructure of human fibrosing alveolitis. *Virchows Arch A Pathol Anat Histol* 1982;395(2):181-99.

(39) Corrin B, Dewar A. Pathogenesis of idiopathic interstitial pulmonary fibrosis. *Ultrastruct Pathol* 1996;20(4):369-71.

(40) Nogee LM, Dunbar AE, III, Wert SE, Askin F, Hamvas A, Whitsett JA. A mutation in the surfactant protein C gene associated with familial interstitial lung disease. *N Engl J Med* 2001;344(8):573-9.

(41) Armanios MY, Chen JJ, Cogan JD, Alder JK, Ingersoll RG, Markin C, Lawson WE, Xie M, Vulto I, Phillips JA, III, Lansdorp PM, Greider CW, Loyd JE. Telomerase mutations in families with idiopathic pulmonary fibrosis. *N Engl J Med* 2007;356(13):1317-26.

(42) Korfei M, Ruppert C, Mahavadi P, Henneke I, Markart P, Koch M, Lang G, Fink L, Bohle RM, Seeger W, Weaver TE, Guenther A. Epithelial Endoplasmic Reticulum Stress and Apoptosis in Sporadic Idiopathic Pulmonary Fibrosis 1. *Am J Respir Crit Care Med* 2008 July 24.

(43) Raghu G, Brown KK, Bradford WZ, Starko K, Noble PW, Schwartz DA, King TE, Jr. A placebo-controlled trial of interferon gamma-1b in patients with idiopathic pulmonary fibrosis. *N Engl J Med* 2004;350(2):125-33.

(44) Endo M, Oyadomari S, Suga M, Mori M, Gotoh T. The ER stress pathway involving CHOP is activated in the lungs of LPS-treated mice. *J Biochem* 2005 October;138(4):501-7.

(45) Jordan R, Wang L, Graczyk TM, Block TM, Romano PR. Replication of a cytopathic strain of bovine viral diarrhea virus activates PERK and induces endoplasmic

reticulum stress-mediated apoptosis of MDBK cells. *J Virol* 2002 October;76(19):9588-99.

(46) Nakatani Y, Nakamura N, Sano J, Inayama Y, Kawano N, Yamanaka S, Miyagi Y, Nagashima Y, Ohbayashi C, Mizushima M, Manabe T, Kuroda M, Yokoi T, Matsubara O. Interstitial pneumonia in Hermansky-Pudlak syndrome: significance of florid foamy swelling/degeneration (giant lamellar body degeneration) of type-2 pneumocytes. *Virchows Arch* 2000 September;437(3):304-13.

(47) Perl AK, Whitsett JA. Molecular mechanisms controlling lung morphogenesis. *Clin Genet* 1999 July;56(1):14-27.

(48) Strieter RM, Gomperts BN, Keane MP. The role of CXC chemokines in pulmonary fibrosis. *J Clin Invest* 2007 March;117(3):549-56.

(49) Kolodsick JE, Peters-Golden M, Larios J, Toews GB, Thannickal VJ, Moore BB. Prostaglandin E2 inhibits fibroblast to myofibroblast transition via E. prostanoid receptor 2 signaling and cyclic adenosine monophosphate elevation. *Am J Respir Cell Mol Biol* 2003 November;29(5):537-44.

(50) Torday JS, Rehan VK. The evolutionary continuum from lung development to homeostasis and repair. *American journal of physiology Lung cellular and molecular physiology* 2007 March;292(3):L608-L611.

(51) Scotton CJ, Chambers RC. Molecular targets in pulmonary fibrosis: the myofibroblast in focus. *Chest Chest* 2007 October;132(4):1311-21.

(52) Marchand-Adam S, Marchal J, Cohen M, Soler P, Gerard B, Castier Y, Leseche G, Valeyre D, Mal H, Aubier M, Dehoux M, Crestani B. Defect of hepatocyte growth factor secretion by fibroblasts in idiopathic pulmonary fibrosis. *Am J Respir Crit Care Med* 2003 November 15;168(10):1156-61.

(53) King TE, Jr., Schwarz MI, Brown K, Tooze JA, Colby TV, Waldron JA, Jr., Flint A, Thurlbeck W, Cherniack RM. Idiopathic pulmonary fibrosis: relationship between histopathologic features and mortality. *Am J Respir Crit Care Med* 2001;164(6):1025-32.

(54) Kelly M, Kolb M, Bonniaud P, Gauldie J. Re-evaluation of fibrogenic cytokines in lung fibrosis. *Curr Pharm Des* 2003;9(1):39-49.

(55) Strieter RM. Pathogenesis and natural history of usual interstitial pneumonia: the whole story or the last chapter of a long novel. *Chest Chest* 2005 November;128(5 Suppl 1):526S-32S.

(56) Hashimoto N, Jin H, Liu T, Chensue SW, Phan SH. Bone marrow-derived progenitor cells in pulmonary fibrosis. *J Clin Invest* 2004 January;113(2):243-52.

(57) Moore BB, Murray L, Das A, Wilke CA, Herrygers AB, Toews GB. The role of CCL12 in the recruitment of fibrocytes and lung fibrosis. *Am J Respir Cell Mol Biol* 2006 August;35(2):175-81.

(58) Phillips RJ, Burdick MD, Hong K, Lutz MA, Murray LA, Xue YY, Belperio JA, Keane MP, Strieter RM. Circulating fibrocytes traffic to the lungs in response to CXCL12 and mediate fibrosis. *J Clin Invest* 2004 August;114(3):438-46.

(59) Thiery JP. Epithelial-mesenchymal transitions in development and pathologies. *Curr Opin Cell Biol* 2003 December;15(6):740-6.

(60) Willis BC, duBois RM, Borok Z. Epithelial origin of myofibroblasts during fibrosis in the lung. *Proc Am Thorac Soc* 2006 June;3(4):377-82.

(61) Ikegami T, Zhang Y, Matsuzaki Y. Liver fibrosis: possible involvement of EMT 2. *Cells Tissues Organs* 2007;185(1-3):213-21.

(62) Wynn TA. Cellular and molecular mechanisms of fibrosis 7. *J Pathol* 2008 January;214(2):199-210.

(63) Huber MA, Kraut N, Beug H. Molecular requirements for epithelial-mesenchymal transition during tumor progression 1. *Curr Opin Cell Biol* 2005 October;17(5):548-58.

(64) Selman M, Pardo A, Kaminski N. Idiopathic pulmonary fibrosis: aberrant recapitulation of developmental programs? 2. *PLoS Med* 2008 March 4;5(3):e62.

(65) Zavadil J, Bottinger EP. TGF-beta and epithelial-to-mesenchymal transitions. *Oncogene* 2005 August 29;24(37):5764-74.

(66) Gunther A, Mosavi P, Ruppert C, Heinemann S, Temmesfeld B, Velcovsky HG, Morr H, Grimminger F, Walmrath D, Seeger W. Enhanced tissue factor pathway activity and fibrin turnover in the alveolar compartment of patients with interstitial lung disease. *Thromb Haemost* 2000 June;83(6):853-60.

(67) Kotani I, Sato A, Hayakawa H, Urano T, Takada Y, Takada A. Increased procoagulant and antifibrinolytic activities in the lungs with idiopathic pulmonary fibrosis. *Thromb Res* 1995 March 15;77(6):493-504.

(68) Wygrecka M, Markart P, Ruppert C, Petri K, Preissner KT, Seeger W, Guenther A. Cellular origin of pro-coagulant and (anti)-fibrinolytic factors in bleomycin-injured lungs
4. *Eur Respir J* 2007 June;29(6):1105-14.

(69) Kobayashi H, Gabazza EC, Taguchi O, Wada H, Takeya H, Nishioka J, Yasui H, Kobayashi T, Hataji O, Suzuki K, Adachi Y. Protein C anticoagulant system in patients with interstitial lung disease. *Am J Respir Crit Care Med* 1998 June;157(6 Pt 1):1850-4.

(70) McDonald JA. The yin and yang of fibrin in the airways. *N Engl J Med* 1990 March 29;322(13):929-31.

(71) Chambers RC, Dabbagh K, McAnulty RJ, Gray AJ, Blanc-Brude OP, Laurent GJ. Thrombin stimulates fibroblast procollagen production via proteolytic activation of protease-activated receptor 1. *Biochem J* 1998 July 1;333 (Pt 1):121-7.

(72) Eitzman DT, McCoy RD, Zheng X, Fay WP, Shen T, Ginsburg D, Simon RH. Bleomycin-induced pulmonary fibrosis in transgenic mice that either lack or overexpress the murine plasminogen activator inhibitor-1 gene. *J Clin Invest* 1996 January 1;97(1):232-7.

(73) Sisson TH, Hanson KE, Subbotina N, Patwardhan A, Hattori N, Simon RH. Inducible lung-specific urokinase expression reduces fibrosis and mortality after lung injury in mice. *American journal of physiology Lung cellular and molecular physiology* 2002 November;283(5):L1023-L1032.

(74) Gunther A, Lubke N, Ermert M, Schermuly RT, Weissmann N, Breithecker A, Markart P, Ruppert C, Quanz K, Ermert L, Grimminger F, Seeger W. Prevention of bleomycin-induced lung fibrosis by aerosolization of heparin or urokinase in rabbits. *Am J Respir Crit Care Med* 2003 December 1;168(11):1358-65.

(75) Chapman HA. Disorders of lung matrix remodeling. *J Clin Invest* 2004 January;113(2):148-57.

(76) Chua F, Gauldie J, Laurent GJ. Pulmonary fibrosis: searching for model answers. *Am J Respir Cell Mol Biol* 2005 July;33(1):9-13.

(77) Keane MP, Strieter RM, Belperio JA. Mechanisms and mediators of pulmonary fibrosis. *Crit Rev Immunol* 2005;25(6):429-63.

(78) Selman M, Thannickal VJ, Pardo A, Zisman DA, Martinez FJ, Lynch JP, III. Idiopathic pulmonary fibrosis: pathogenesis and therapeutic approaches. *Drugs* 2004;64(4):405-30.

(79) Sime PJ, Xing Z, Graham FL, Csaky KG, Gauldie J. Adenovector-mediated gene transfer of active transforming growth factor-beta1 induces prolonged severe fibrosis in rat lung. *J Clin Invest* 1997 August 15;100(4):768-76.

(80) Giri SN, Hyde DM, Hollinger MA. Effect of antibody to transforming growth factor beta on bleomycin induced accumulation of lung collagen in mice 1. *Thorax* 1993 October;48(10):959-66.

(81) Broekelmann TJ, Limper AH, Colby TV, McDonald JA. Transforming growth factor beta 1 is present at sites of extracellular matrix gene expression in human pulmonary fibrosis. *Proc Natl Acad Sci U S A* 1991 August 1;88(15):6642-6.

(82) Selman M, Ruiz V, Cabrera S, Segura L, Ramirez R, Barrios R, Pardo A. TIMP-1, -2, -3, and -4 in idiopathic pulmonary fibrosis. A prevailing nondegradative lung microenvironment? *American journal of physiology Lung cellular and molecular physiology* 2000;279(3):L562-L574.

(83) Tan RJ, Fattman CL, Niehouse LM, Tobolewski JM, Hanford LE, Li Q, Monzon FA, Parks WC, Oury TD. Matrix metalloproteinases promote inflammation and fibrosis in asbestos-induced lung injury in mice 2. *Am J Respir Cell Mol Biol* 2006 September;35(3):289-97.

(84) Corbel M, Belleguic C, Boichot E, Lagente V. Involvement of gelatinases (MMP-2 and MMP-9) in the development of airway inflammation and pulmonary fibrosis. *Cell Biol Toxicol* 2002;18(1):51-61.

(85) Cosgrove GP, Schwarz MI, Geraci MW, Brown KK, Worthen GS. Overexpression of matrix metalloproteinase-7 in pulmonary fibrosis 1. *Chest Chest* 2002 March;121(3 Suppl):25S-6S.

(86) Zuo FR, Kaminski N, Eugui E, Allard J, Yakhini Z, Ben-Dor A, Lollini L, Morris D, Kim Y, DeLustro B, Sheppard D, Pardo A, Selman M, Heller RA. Gene expression analysis reveals matrilysin as a key regulator of pulmonary fibrosis in mice and humans. *P Natl Acad Sci USA P Natl Acad Sci USA* 2002;99(9):6292-7.

(87) Huh JW, Kim DS, Oh YM, Shim TS, Lim CM, Lee SD, Koh Y, Kim WS, Kim WD, Kim KR. Is metalloproteinase-7 specific for idiopathic pulmonary fibrosis? 1. *Chest Chest* 2008 May;133(5):1101-6.

(88) Cosgrove GP, du Bois RM. Matrix metalloproteinase-7 expression in fibrosing lung disease: restoring the balance
1. *Chest Chest* 2008 May;133(5):1058-60.

(89) Betsuyaku T, Fukuda Y, Parks WC, Shipley JM, Senior RM. Gelatinase B is required for alveolar bronchiolization after intratracheal bleomycin. *Am J Pathol Am J Pathol* 2000;157(2):525-35.

(90) Manoury B, Nenan S, Guenon I, Boichot E, Planquois JM, Bertrand CP, Lagente V. Macrophage metalloelastase (MMP-12) deficiency does not alter bleomycin-induced pulmonary fibrosis in mice. *J Inflamm (Lond)* 2006;3:2.

(91) Pardo A, Selman M. Matrix metalloproteases in aberrant fibrotic tissue remodeling. *Proc Am Thorac Soc* 2006;3(4):383-8.

(92) Lawson WE, Loyd JE. The genetic approach in pulmonary fibrosis: can it provide clues to this complex disease? *Proc Am Thorac Soc* 2006 June;3(4):345-9.

(93) Loyd JE. Pulmonary fibrosis in families. *Am J Respir Cell Mol Biol* 2003 September;29(3 Suppl):S47-S50.

(94) Ruppert C, Markart P, Schmidt R, Grimminger F, Seeger W, Lehr CM, Gunther A. Chemical crosslinking of urokinase to pulmonary surfactant protein B for targeting alveolar fibrin
3. *Thromb Haemost* 2003 January;89(1):53-64.

(95) Markart P, Ruppert C, Grimminger F, Seeger W, Gunther A. Fibrinolysis-inhibitory capacity of clot-embedded surfactant is enhanced by SP-B and SP-C
5. *American journal of physiology Lung cellular and molecular physiology* 2003 January;284(1):L69-L76.

(96) Amin RS, Wert SE, Baughman RP, Tomashefski JF, Jr., Nogee LM, Brody AS, Hull WM, Whitsett JA. Surfactant protein deficiency in familial interstitial lung disease. *J Pediatr* 2001 July;139(1):85-92.

(97) Thomas AQ, Lane K, Phillips J, III, Prince M, Markin C, Speer M, Schwartz DA, Gaddipati R, Marney A, Johnson J, Roberts R, Haines J, Stahlman M, Loyd JE. Heterozygosity for a surfactant protein C gene mutation associated with usual interstitial pneumonitis and cellular nonspecific interstitial pneumonitis in one kindred. *Am J Respir Crit Care Med* 2002 May 1;165(9):1322-8.

(98) Greider CW, Blackburn EH. Identification of a specific telomere terminal transferase activity in Tetrahymena extracts. *Cell* 1985 December;43(2 Pt 1):405-13.

(99) Nakamura TM, Morin GB, Chapman KB, Weinrich SL, Andrews WH, Lingner J, Harley CB, Cech TR. Telomerase catalytic subunit homologs from fission yeast and human. *Science* 1997 August 15;277(5328):955-9.

(100) Armanios M, Chen JL, Chang YP, Brodsky RA, Hawkins A, Griffin CA, Eshleman JR, Cohen AR, Chakravarti A, Hamosh A, Greider CW. Haploinsufficiency of telomerase reverse transcriptase leads to anticipation in autosomal dominant dyskeratosis congenita. *Proc Natl Acad Sci U S A* 2005 November 1;102(44):15960-4.

(101) Flaherty KR, Toews GB, Lynch JP, III, Kazerooni EA, Gross BH, Strawderman RL, Hariharan K, Flint A, Martinez FJ. Steroids in idiopathic pulmonary fibrosis: a prospective assessment of adverse reactions, response to therapy, and survival 2. *Am J Med* 2001 March;110(4):278-82.

(102) Moeller A, Ask K, Warburton D, Gauldie J, Kolb M. The bleomycin animal model: a useful tool to investigate treatment options for idiopathic pulmonary fibrosis? 1. *Int J Biochem Cell Biol* 2008;40(3):362-82.

(103) Park SH, Saleh D, Giaid A, Michel RP. Increased endothelin-1 in bleomycin-induced pulmonary fibrosis and the effect of an endothelin receptor antagonist 1. *Am J Respir Crit Care Med* 1997 August;156(2 Pt 1):600-8.

(104) Moore BB, Hogaboam CM. Murine models of pulmonary fibrosis. *American journal of physiology Lung cellular and molecular physiology* 2008 February;294(2):L152-L160.

(105) Birkedal-Hansen H, Moore WG, Bodden MK, Windsor LJ, Birkedal-Hansen B, DeCarlo A, Engler JA. Matrix metalloproteinases: a review. *Crit Rev Oral Biol Med* 1993;4(2):197-250.

(106) Nagase H, Woessner JF, Jr. Matrix metalloproteinases. *J Biol Chem* 1999;274(31):21491-4.

(107) Parks WC. *Matrix Metalloproteinases*. San Diego: Academic Press; 1998.

(108) Woessner JF, Jr. The family of matrix metalloproteinases. *Ann N Y Acad Sci* 1994;732:11-21.

(109) Overall CM, Lopez-Otin C. Strategies for MMP inhibition in cancer: Innovations for the post-trial era. *Nat Rev Cancer Nat Rev Cancer* 2002;2(9):657-72.

(110) Stocker W, Grams F, Baumann U, Reinemer P, Gomis-Ruth FX, McKay DB, Bode W. The metzincins--topological and sequential relations between the astacins, adamalysins, serralysins, and matrixins (collagenases) define a superfamily of zinc-peptidases. *Protein Sci* 1995;4(5):823-40.

(111) Bode W, Gomis-Ruth FX, Stockler W. Astacins, serralysins, snake venom and matrix metalloproteinases exhibit identical zinc-binding environments (HEXXHXXGXXH and Met-turn) and topologies and should be grouped into a common family, the 'metzincins'. *FEBS Lett* 1993;331(1-2):134-40.

(112) Stocker W, Bode W. Structural features of a superfamily of zinc-endopeptidases: the metzincins. *Curr Opin Struct Biol* 1995;5(3):383-90.

(113) Gross J, Lapiere CM. Collagenolytic activity in amphibian tissues: a tissue culture assay. *Proc Natl Acad Sci U S A* 1962;48:1014-22.

(114) Lohi J, Wilson CL, Roby JD, Parks WC. Epilysin, a novel human matrix metalloproteinase (MMP-28) expressed in testis and keratinocytes and in response to injury. *J Biol Chem* 2001;276(13):10134-44.

(115) Marchenko GN, Strongin AY. MMP-28, a new human matrix metalloproteinase with an unusual cysteine-switch sequence is widely expressed in tumors. *Gene* 2001;265(1-2):87-93.

(116) Parks WC, Wilson CL, Lopez-Boado YS. Matrix metalloproteinases as modulators of inflammation and innate immunity. *Nat Rev Immunol* 2004;4(8):617-29.

(117) Greenlee KJ, Werb Z, Kheradmand F. Matrix metalloproteinases in lung: Multiple, multifarious, and multifaceted. *Physiol Rev Physiol Rev* 2007;87(1):69-98.

(118) Nagase H, Visse R, Murphy G. Structure and function of matrix metalloproteinases and TIMPs. *Cardiovasc Res Cardiovasc Res* 2006;69(3):562-73.

(119) Woessner JF, Jr. Matrix metalloproteinases and their inhibitors in connective tissue remodeling. *Faseb J* 1991;5(8):2145-54.

(120) Visse R, Nagase H. Matrix metalloproteinases and tissue inhibitors of metalloproteinases - Structure, function, and biochemistry. *Circ Res Circ Res* 2003;92(8):827-39.

(121) d'Ortho MP, Will H, Atkinson S, Butler G, Messent A, Gavrilovic J, Smith B, Timpl R, Zardi L, Murphy G. Membrane-type matrix metalloproteinases 1 and 2 exhibit

broad-spectrum proteolytic capacities comparable to many matrix metalloproteinases. *Eur J Biochem* 1997;250(3):751-7.

(122) Itoh Y, Binner S, Nagase H. Steps involved in activation of the complex of pro-matrix metalloproteinase 2 (progelatinase A) and tissue inhibitor of metalloproteinases (TIMP)-2 by 4-aminophenylmercuric acetate. *Biochem J* 1995;308 (Pt 2):645-51.

(123) Knauper V, Cowell S, Smith B, Lopez-Otin C, O'Shea M, Morris H, Zardi L, Murphy G. The role of the C-terminal domain of human collagenase-3 (MMP-13) in the activation of procollagenase-3, substrate specificity, and tissue inhibitor of metalloproteinase interaction. *J Biol Chem* 1997;272(12):7608-16.

(124) Marchenko GN, Ratnikov BI, Rozanov DV, Godzik A, Deryugina EI, Strongin AY. Characterization of matrix metalloproteinase-26, a novel metalloproteinase widely expressed in cancer cells of epithelial origin. *Biochem J* 2001;356(Pt 3):705-18.

(125) Murphy G, Segain JP, O'Shea M, Cockett M, Ioannou C, Lefebvre O, Chambon P, Basset P. The 28-kDa N-terminal domain of mouse stromelysin-3 has the general properties of a weak metalloproteinase. *J Biol Chem* 1993;268(21):15435-41.

(126) Ochieng J, Fridman R, Nangia-Makker P, Kleiner DE, Liotta LA, Stetler-Stevenson WG, Raz A. Galectin-3 is a novel substrate for human matrix metalloproteinases-2 and -9. *Biochemistry* 1994;33(47):14109-14.

(127) Patterson ML, Atkinson SJ, Knauper V, Murphy G. Specific collagenolysis by gelatinase A, MMP-2, is determined by the hemopexin domain and not the fibronectin-like domain. *FEBS Lett* 2001;503(2-3):158-62.

(128) Pei D. CA-MMP: a matrix metalloproteinase with a novel cysteine array, but without the classic cysteine switch. *FEBS Lett* 1999;457(2):262-70.

(129) Shimada T, Nakamura H, Ohuchi E, Fujii Y, Murakami Y, Sato H, Seiki M, Okada Y. Characterization of a truncated recombinant form of human membrane type 3 matrix metalloproteinase. *Eur J Biochem* 1999;262(3):907-14.

(130) Stix B, Kahne T, Sletten K, Raynes J, Roessner A, Rocken C. Proteolysis of AA amyloid fibril proteins by matrix metalloproteinases-1, -2, and -3. *Am J Pathol* 2001;159(2):561-70.

(131) Stolow MA, Bauzon DD, Li J, Sedgwick T, Liang VC, Sang QA, Shi YB. Identification and characterization of a novel collagenase in Xenopus laevis: possible roles during frog development. *Mol Biol Cell* 1996;7(10):1471-83.

(132) Stracke JO, Fosang AJ, Last K, Mercuri FA, Pendas AM, Llano E, Perris R, Di Cesare PE, Murphy G, Knauper V. Matrix metalloproteinases 19 and 20 cleave aggrecan and cartilage oligomeric matrix protein (COMP). *FEBS Lett* 2000;478(1-2):52-6.

(133) Stracke JO, Hutton M, Stewart M, Pendas AM, Smith B, Lopez-Otin C, Murphy G, Knauper V. Biochemical characterization of the catalytic domain of human matrix metalloproteinase 19. Evidence for a role as a potent basement membrane degrading enzyme. *J Biol Chem* 2000;275(20):14809-16.

(134) Uria JA, Lopez-Otin C. Matrilysin-2, a new matrix metalloproteinase expressed in human tumors and showing the minimal domain organization required for secretion, latency, and activity. *Cancer Res* 2000;60(17):4745-51.

(135) Wang X, Yi J, Lei J, Pei D. Expression, purification and characterization of recombinant mouse MT5-MMP protein products. *FEBS Lett* 1999;462(3):261-6.

(136) Yang M, Kurkinen M. Cloning and characterization of a novel matrix metalloproteinase (MMP), CMMP, from chicken embryo fibroblasts. CMMP, Xenopus XMMP, and human MMP19 have a conserved unique cysteine in the catalytic domain. *J Biol Chem* 1998;273(28):17893-900.

(137) Balbin M, Fueyo A, Knauper V, Lopez JM, Alvarez J, Sanchez LM, Quesada V, Bordallo J, Murphy G, Lopez-Otin C. Identification and enzymatic characterization of two diverging murine counterparts of human interstitial collagenase (MMP-1) expressed at sites of embryo implantation
1. *J Biol Chem* 2001 March 30;276(13):10253-62.

(138) Ugwu F, Van Hoef B, Bini A, Collen D, Lijnen HR. Proteolytic cleavage of urokinase-type plasminogen activator by stromelysin-1 (MMP-3). *Biochemistry* 1998;37(20):7231-6.

(139) Lijnen HR, Arza B, Van Hoef B, Collen D, Declerck PJ. Inactivation of plasminogen activator inhibitor-1 by specific proteolysis with stromelysin-1 (MMP-3). *J Biol Chem* 2000;275(48):37645-50.

(140) English WR, Puente XS, Freije JM, Knauper V, Amour A, Merryweather A, Lopez-Otin C, Murphy G. Membrane type 4 matrix metalloproteinase (MMP17) has tumor necrosis factor-alpha convertase activity but does not activate pro-MMP2. *J Biol Chem* 2000;275(19):14046-55.

(141) Wang Y, Johnson AR, Ye QZ, Dyer RD. Catalytic activities and substrate specificity of the human membrane type 4 matrix metalloproteinase catalytic domain. *J Biol Chem* 1999;274(46):33043-9.

(142) Bode W, Fernandez-Catalan C, Tschesche H, Grams F, Nagase H, Maskos K. Structural properties of matrix metalloproteinases. *Cell Mol Life Sci* 1999;55(4):639-52.

(143) Becker JW, Marcy AI, Rokosz LL, Axel MG, Burbaum JJ, Fitzgerald PM, Cameron PM, Esser CK, Hagmann WK, Hermes JD. Stromelysin-1: three-dimensional structure of the inhibited catalytic domain and of the C-truncated proenzyme. *Protein Sci* 1995;4(10):1966-76.

(144) Van Wart HE, Birkedal-Hansen H. The cysteine switch: a principle of regulation of metalloproteinase activity with potential applicability to the entire matrix metalloproteinase gene family. *Proc Natl Acad Sci U S A* 1990;87(14):5578-82.

(145) Gururajan R, Grenet J, Lahti JM, Kidd VJ. Isolation and characterization of two novel metalloproteinase genes linked to the Cdc2L locus on human chromosome 1p36.3. *Genomics* 1998;52(1):101-6.

(146) Pei D, Weiss SJ. Furin-dependent intracellular activation of the human stromelysin-3 zymogen. *Nature* 1995;375(6528):244-7.

(147) Pei D, Weiss SJ. Transmembrane-deletion mutants of the membrane-type matrix metalloproteinase-1 process progelatinase A and express intrinsic matrix-degrading activity. *J Biol Chem* 1996;271(15):9135-40.

(148) Springman EB, Angleton EL, Birkedal-Hansen H, Van Wart HE. Multiple modes of activation of latent human fibroblast collagenase: evidence for the role of a Cys73 active-site zinc complex in latency and a "cysteine switch" mechanism for activation. *Proc Natl Acad Sci U S A* 1990 January;87(1):364-8.

(149) Briknarova K, Gehrmann M, Banyai L, Tordai H, Patthy L, Llinas M. Gelatin-binding region of human matrix metalloproteinase-2: solution structure, dynamics, and function of the COL-23 two-domain construct1. *J Biol Chem* 2001 July 20;276(29):27613-21.

(150) Cha H, Kopetzki E, Huber R, Lanzendorfer M, Brandstetter H. Structural basis of the adaptive molecular recognition by MMP9. *J Mol Biol* 2002;320(5):1065-79.

(151) Overall CM. Molecular determinants of metalloproteinase substrate specificity: matrix metalloproteinase substrate binding domains, modules, and exosites. *Mol Biotechnol* 2002;22(1):51-86.

(152) Page-McCaw A, Ewald AJ, Werb Z. Matrix metalloproteinases and the regulation of tissue remodelling. *Nat Rev Mol Cell Biol* 2007;8(3):221-33.

(153) Smith TF, Gaitatzes C, Saxena K, Neer EJ. The WD repeat: a common architecture for diverse functions
1. *Trends Biochem Sci* 1999 May;24(5):181-5.

(154) Allan JA, Docherty AJ, Barker PJ, Huskisson NS, Reynolds JJ, Murphy G. Binding of gelatinases A and B to type-I collagen and other matrix components. *Biochem J* 1995;309 (Pt 1):299-306.

(155) Steffensen B, Wallon UM, Overall CM. Extracellular matrix binding properties of recombinant fibronectin type II-like modules of human 72-kDa gelatinase/type IV collagenase. High affinity binding to native type I collagen but not native type IV collagen. *J Biol Chem* 1995;270(19):11555-66.

(156) Massova I, Kotra LP, Fridman R, Mobashery S. Matrix metalloproteinases: structures, evolution, and diversification
3. *Faseb J* 1998 September;12(12):1075-95.

(157) Shapiro SD. Matrix metalloproteinase degradation of extracellular matrix: biological consequences. *Curr Opin Cell Biol* 1998;10(5):602-8.

(158) Park AJ, Matrisian LM, Kells AF, Pearson R, Yuan ZY, Navre M. Mutational analysis of the transin (rat stromelysin) autoinhibitor region demonstrates a role for residues surrounding the "cysteine switch". *J Biol Chem* 1991 January 25;266(3):1584-90.

(159) Caterina JJ, Yamada S, Caterina NC, Longenecker G, Holmback K, Shi J, Yermovsky AE, Engler JA, Birkedal-Hansen H. Inactivating mutation of the mouse tissue inhibitor of metalloproteinases-2(Timp-2) gene alters proMMP-2 activation. *J Biol Chem* 2000 August 25;275(34):26416-22.

(160) Hernandez-Barrantes S, Toth M, Bernardo MM, Yurkova M, Gervasi DC, Raz Y, Sang QA, Fridman R. Binding of active (57 kDa) membrane type 1-matrix metalloproteinase (MT1-MMP) to tissue inhibitor of metalloproteinase (TIMP)-2 regulates MT1-MMP processing and pro-MMP-2 activation. *J Biol Chem* 2000 April 21;275(16):12080-9.

(161) Strongin AY, Collier I, Bannikov G, Marmer BL, Grant GA, Goldberg GI. Mechanism of cell surface activation of 72-kDa type IV collagenase. Isolation of the activated form of the membrane metalloprotease. *J Biol Chem* 1995 March 10;270(10):5331-8.

(162) Wang Z, Juttermann R, Soloway PD. TIMP-2 is required for efficient activation of proMMP-2 in vivo. *J Biol Chem* 2000 August 25;275(34):26411-5.

(163) Fu X, Kassim SY, Parks WC, Heinecke JW. Hypochlorous acid generated by myeloperoxidase modifies adjacent tryptophan and glycine residues in the catalytic domain of matrix metalloproteinase-7 (matrilysin): an oxidative mechanism for restraining proteolytic activity during inflammation. *J Biol Chem* 2003 August 1;278(31):28403-9.

(164) Gu Z, Kaul M, Yan B, Kridel SJ, Cui J, Strongin A, Smith JW, Liddington RC, Lipton SA. S-nitrosylation of matrix metalloproteinases: signaling pathway to neuronal cell death. *Science* 2002 August 16;297(5584):1186-90.

(165) Foronjy RF, Mirochnitchenko O, Propokenko O, Lemaitre V, Jia Y, Inouye M, Okada Y, D'Armiento JM. Superoxide dismutase expression attenuates cigarette smoke- or elastase-generated emphysema in mice. *Am J Respir Crit Care Med* 2006;173(6):623-31.

(166) Lemaitre V, D'Armiento J. Matrix metalloproteinases in development and disease. *Birth Defects Res C Embryo Today* 2006;78(1):1-10.

(167) Sternlicht MD, Werb Z. How matrix metalloproteinases regulate cell behavior. *Annu Rev Cell Dev Bi Annu Rev Cell Dev Bi* 2001;17:463-516.

(168) Clark IM, Swingler TE, Sampieri CL, Edwards DR. The regulation of matrix metalloproteinases and their inhibitors. *Int J Biochem Cell Biol* 2007.

(169) Barmina OY, Walling HW, Fiacco GJ, Freije JM, Lopez-Otin C, Jeffrey JJ, Partridge NC. Collagenase-3 binds to a specific receptor and requires the low density lipoprotein receptor-related protein for internalization. *J Biol Chem* 1999 October 15;274(42):30087-93.

(170) Brooks PC, Stromblad S, Sanders LC, von Schalscha TL, Aimes RT, Stetler-Stevenson WG, Quigley JP, Cheresh DA. Localization of matrix metalloproteinase MMP-2 to the surface of invasive cells by interaction with integrin alpha v beta 3. *Cell* 1996 May 31;85(5):683-93.

(171) Dumin JA, Dickeson SK, Stricker TP, Bhattacharyya-Pakrasi M, Roby JD, Santoro SA, Parks WC. Pro-collagenase-1 (matrix metalloproteinase-1) binds the alpha(2)beta(1) integrin upon release from keratinocytes migrating on type I collagen. *J Biol Chem* 2001 August 3;276(31):29368-74.

(172) Stricker TP, Dumin JA, Dickeson SK, Chung L, Nagase H, Parks WC, Santoro SA. Structural analysis of the alpha(2) integrin I domain/procollagenase-1 (matrix metalloproteinase-1) interaction. *J Biol Chem* 2001 August 3;276(31):29375-81.

(173) Yu Q, Stamenkovic I. Cell surface-localized matrix metalloproteinase-9 proteolytically activates TGF-beta and promotes tumor invasion and angiogenesis. *Genes Dev* 2000 January 15;14(2):163-76.

(174) Yu WH, Woessner JF, Jr. Heparan sulfate proteoglycans as extracellular docking molecules for matrilysin (matrix metalloproteinase 7). *J Biol Chem* 2000 February 11;275(6):4183-91.

(175) Yu WH, Woessner JF, Jr., McNeish JD, Stamenkovic I. CD44 anchors the assembly of matrilysin/MMP-7 with heparin-binding epidermal growth factor precursor and ErbB4 and regulates female reproductive organ remodeling. *Genes Dev* 2002 February 1;16(3):307-23.

(176) Egeblad M, Werb Z. New functions for the matrix metalloproteinases in cancer progression. *Nat Rev Cancer* 2002 March;2(3):161-74.

(177) Corry DB, Kiss A, Song LZ, Song L, Xu J, Lee SH, Werb Z, Kheradmand F. Overlapping and independent contributions of MMP2 and MMP9 to lung allergic inflammatory cell egression through decreased CC chemokines. *Faseb J* 2004 June;18(9):995-7.

(178) Oh J, Takahashi R, Adachi E, Kondo S, Kuratomi S, Noma A, Alexander DB, Motoda H, Okada A, Seiki M, Itoh T, Itohara S, Takahashi C, Noda M. Mutations in two matrix metalloproteinase genes, MMP-2 and MT1-MMP, are synthetic lethal in mice. *Oncogene* 2004 June 24;23(29):5041-8.

(179) Stickens D, Behonick DJ, Ortega N, Heyer B, Hartenstein B, Yu Y, Fosang AJ, Schorpp-Kistner M, Angel P, Werb Z. Altered endochondral bone development in matrix metalloproteinase 13-deficient mice. *Development Development* 2004;131(23):5883-95.

(180) Uchinami H, Seki E, Brenner DA, D'Armiento J. Loss of MMP 13 attenuates murine hepatic injury and fibrosis during Cholestasis. *Hepatology Hepatology* 2006;44(2):420-9.

(181) Inada M, Wang Y, Byrne MH, Miyaura C, Krane SM. Mice with null mutation in collagenase-3 (matrix metalloproteinase[MMP]-13) exhibit altered bone remodeling and increased bone mass. *J Bone Miner Res J Bone Miner Res* 2001;16:S149.

(182) Inada M, Wang Y, Byrne MH, Miyaura C, Krane SM. Loss of function of matrix metalloproteinase-13 (MMP-13) affects collagen accumulation and bone formation. *J Bone Miner Res J Bone Miner Res* 2002;17:S171.

(183) Inada M, Wang Y, Byrne MH, Miyaura C, Krane SM. The collagenase, matrix metalloproteinase-13 (MMP-13), is required for osteoclast formation and function. *J Bone Miner Res J Bone Miner Res* 2003;18:S195.

(184) Inada M, Wang YM, Byrne MH, Rahman MU, Miyaura C, Lopez-Otin C, Krane SM. Critical roles for collagenase-3 (Mmp13) in development of growth and in endochondral plate cartilage ossification. *P Natl Acad Sci USA P Natl Acad Sci USA* 2004;101(49):17192-7.

(185) Brew K, Dinakarpandian D, Nagase H. Tissue inhibitors of metalloproteinases: evolution, structure and function. *Biochim Biophys Acta* 2000;1477(1-2):267-83.

(186) Morgunova E, Tuuttila A, Bergmann U, Tryggvason K. Structural insight into the complex formation of latent matrix metalloproteinase 2 with tissue inhibitor of metalloproteinase 2. *Proc Natl Acad Sci U S A* 2002;99(11):7414-9.

(187) Olson MW, Gervasi DC, Mobashery S, Fridman R. Kinetic analysis of the binding of human matrix metalloproteinase-2 and -9 to tissue inhibitor of metalloproteinase (TIMP)-1 and TIMP-2. *J Biol Chem* 1997;272(47):29975-83.

(188) Bode W, Fernandez-Catalan C, Grams F, Gomis-Ruth FX, Nagase H, Tschesche H, Maskos K. Insights into MMP-TIMP interactions
1. *Ann N Y Acad Sci* 1999 June 30;878:73-91.

(189) Murphy G, Houbrechts A, Cockett MI, Williamson RA, O'Shea M, Docherty AJ. The N-terminal domain of tissue inhibitor of metalloproteinases retains metalloproteinase inhibitory activity. *Biochemistry* 1991;30(33):8097-102.

(190) Williamson RA, Marston FA, Angal S, Koklitis P, Panico M, Morris HR, Carne AF, Smith BJ, Harris TJ, Freedman RB. Disulphide bond assignment in human tissue inhibitor of metalloproteinases (TIMP)
1. *Biochem J* 1990 June 1;268(2):267-74.

(191) Williamson RA, Martorell G, Carr MD, Murphy G, Docherty AJ, Freedman RB, Feeney J. Solution structure of the active domain of tissue inhibitor of metalloproteinases-2. A new member of the OB fold protein family
1. *Biochemistry* 1994 October 4;33(39):11745-59.

(192) Gomis-Ruth FX, Maskos K, Betz M, Bergner A, Huber R, Suzuki K, Yoshida N, Nagase H, Brew K, Bourenkov GP, Bartunik H, Bode W. Mechanism of inhibition of the human matrix metalloproteinase stromelysin-1 by TIMP-1. *Nature* 1997;389(6646):77-81.

(193) Fernandez-Catalan C, Bode W, Huber R, Turk D, Calvete JJ, Lichte A, Tschesche H, Maskos K. Crystal structure of the complex formed by the membrane type 1-matrix metalloproteinase with the tissue inhibitor of metalloproteinases-2, the soluble progelatinase A receptor. *EMBO J* 1998;17(17):5238-48.

(194) Gasson JC, Golde DW, Kaufman SE, Westbrook CA, Hewick RM, Kaufman RJ, Wong GG, Temple PA, Leary AC, Brown EL. Molecular characterization and expression of the gene encoding human erythroid-potentiating activity. *Nature* 1985;315(6022):768-71.

(195) Fujimoto N, Zhang J, Iwata K, Shinya T, Okada Y, Hayakawa T. A one-step sandwich enzyme immunoassay for tissue inhibitor of metalloproteinases-2 using monoclonal antibodies. *Clin Chim Acta* 1993;220(1):31-45.

(196) Stetler-Stevenson WG, Liotta LA, Kleiner DE, Jr. Extracellular matrix 6: role of matrix metalloproteinases in tumor invasion and metastasis. *Faseb J* 1993;7(15):1434-41.

(197) Ritter LM, Garfield SH, Thorgeirsson UP. Tissue inhibitor of metalloproteinases-1 (TIMP-1) binds to the cell surface and translocates to the nucleus of human MCF-7 breast carcinoma cells. *Biochemical and biophysical research communications* 1999;257(2):494-9.

(198) Zhao WQ, Li H, Yamashita K, Guo XK, Hoshino T, Yoshida S, Shinya T, Hayakawa T. Cell cycle-associated accumulation of tissue inhibitor of metalloproteinases-1 (TIMP-1) in the nuclei of human gingival fibroblasts. *J Cell Sci* 1998;111 (Pt 9):1147-53.

(199) Stetler-Stevenson WG, Bersch N, Golde DW. Tissue inhibitor of metalloproteinase-2 (TIMP-2) has erythroid-potentiating activity. *FEBS Lett* 1992;296(2):231-4.

(200) Hayakawa T, Yamashita K, Tanzawa K, Uchijima E, Iwata K. Growth-promoting activity of tissue inhibitor of metalloproteinases-1 (TIMP-1) for a wide range of cells. A possible new growth factor in serum. *FEBS Lett* 1992;298(1):29-32.

(201) Guedez L, Courtemanch L, Stetler-Stevenson M. Tissue inhibitor of metalloproteinase (TIMP)-1 induces differentiation and an antiapoptotic phenotype in germinal center B cells. *Blood* 1998;92(4):1342-9.

(202) Guedez L, Martinez A, Zhao S, Vivero A, Pittaluga S, Stetler-Stevenson M, Raffeld M, Stetler-Stevenson WG. Tissue inhibitor of metalloproteinase 1 (TIMP-1) promotes plasmablastic differentiation of a Burkitt lymphoma cell line: implications in the pathogenesis of plasmacytic/plasmablastic tumors. *Blood* 2005;105(4):1660-8.

(203) Valente P, Fassina G, Melchiori A, Masiello L, Cilli M, Vacca A, Onisto M, Santi L, Stetler-Stevenson WG, Albini A. TIMP-2 over-expression reduces invasion and angiogenesis and protects B16F10 melanoma cells from apoptosis. *Int J Cancer* 1998;75(2):246-53.

(204) Murphy AN, Unsworth EJ, Stetler-Stevenson WG. Tissue inhibitor of metalloproteinases-2 inhibits bFGF-induced human microvascular endothelial cell proliferation. *J Cell Physiol* 1993;157(2):351-8.

(205) Ruiz A, Brett P, Bok D. TIMP-3 is expressed in the human retinal pigment epithelium. *Biochemical and biophysical research communications* 1996;226(2):467-74.

(206) Kishnani NS, Staskus PW, Yang TT, Masiarz FR, Hawkes SP. Identification and characterization of human tissue inhibitor of metalloproteinase-3 and detection of three additional metalloproteinase inhibitor activities in extracellular matrix. *Matrix Biol* 1995;14(6):479-88.

(207) Butler GS, Will H, Atkinson SJ, Murphy G. Membrane-type-2 matrix metalloproteinase can initiate the processing of progelatinase A and is regulated by the tissue inhibitors of metalloproteinases. *Eur J Biochem* 1997;244(2):653-7.

(208) Langton KP, McKie N, Curtis A, Goodship JA, Bond PM, Barker MD, Clarke M. A novel tissue inhibitor of metalloproteinases-3 mutation reveals a common molecular phenotype in Sorsby's fundus dystrophy. *J Biol Chem* 2000;275(35):27027-31.

(209) Tabata Y, Isashiki Y, Kamimura K, Nakao K, Ohba N. A novel splice site mutation in the tissue inhibitor of the metalloproteinases-3 gene in Sorsby's fundus dystrophy with unusual clinical features. *Hum Genet* 1998;103(2):179-82.

(210) Weber BH, Vogt G, Pruett RC, Stohr H, Felbor U. Mutations in the tissue inhibitor of metalloproteinases-3 (TIMP3) in patients with Sorsby's fundus dystrophy. *Nat Genet* 1994;8(4):352-6.

(211) Ahonen M, Poukkula M, Baker AH, Kashiwagi M, Nagase H, Eriksson JE, Kahari VM. Tissue inhibitor of metalloproteinases-3 induces apoptosis in melanoma cells by stabilization of death receptors. *Oncogene* 2003;22(14):2121-34.

(212) Bond M, Murphy G, Bennett MR, Newby AC, Baker AH. Tissue inhibitor of metalloproteinase-3 induces a Fas-associated death domain-dependent type II apoptotic pathway. *J Biol Chem* 2002;277(16):13787-95.

(213) Gomez DE, Alonso DF, Yoshiji H, Thorgeirsson UP. Tissue inhibitors of metalloproteinases: structure, regulation and biological functions. *Eur J Cell Biol* 1997;74(2):111-22.

(214) Greene J, Wang M, Liu YE, Raymond LA, Rosen C, Shi YE. Molecular cloning and characterization of human tissue inhibitor of metalloproteinase 4. *J Biol Chem* 1996;271(48):30375-80.

(215) Kai HS, Butler GS, Morrison CJ, King AE, Pelman GR, Overall CM. Utilization of a novel recombinant myoglobin fusion protein expression system to characterize the tissue inhibitor of metalloproteinase (TIMP)-4 and TIMP-2 C-terminal domain and tails by mutagenesis. The importance of acidic residues in binding the MMP-2 hemopexin C-domain. *J Biol Chem* 2002;277(50):48696-707.

(216) Liu YE, Wang M, Greene J, Su J, Ullrich S, Li H, Sheng S, Alexander P, Sang QA, Shi YE. Preparation and characterization of recombinant tissue inhibitor of metalloproteinase 4 (TIMP-4)
1. *J Biol Chem* 1997 August 15;272(33):20479-83.

(217) Wang M, Liu YE, Greene J, Sheng S, Fuchs A, Rosen EM, Shi YE. Inhibition of tumor growth and metastasis of human breast cancer cells transfected with tissue inhibitor of metalloproteinase 4
2. *Oncogene* 1997 June 12;14(23):2767-74.

(218) Foronjy RF, Okada Y, Cole R, D'Armiento J. Progressive adult-onset emphysema in transgenic mice expressing human MMP-1 in the lung. *Am J Physiol Lung Cell Mol Physiol* 2003 May;284(5):L727-L737.

(219) Ikeda M, Sorimachi K, Akimoto K, Yasumura Y. Reversed-phase high-performance liquid chromatographic analysis of hydroxyproline and proline from collagen by derivatization with dabsyl chloride. *J Chromatogr* 1993 November 24;621(2):133-8.

(220) Sormiachi K, Ikeda M, Akimoto K, Niwa A. Rapid determination of dabsylated hydroxyproline from cultured cells by reversed-phase high-performance liquid chromatography. *J Chromatogr B Biomed Appl* 1995 February 17;664(2):435-9.

(221) Goodson WH, III, Hunt TK. Development of a new miniature method for the study of wound healing in human subjects. *J Surg Res* 1982 November;33(5):394-401.

(222) Woessner JF. Determination of Hydroxyproline in Tissue and Protein Samples Containing Small Proportions of This Imino Acid. *Arch Biochem Biophys Arch Biochem Biophys* 1961;93(2):440.

(223) Mook OR, Van Overbeek C, Ackema EG, Van Maldegem F, Frederiks WM. In situ localization of gelatinolytic activity in the extracellular matrix of metastases of colon cancer in rat liver using quenched fluorogenic DQ-gelatin. *J Histochem Cytochem* 2003;51(6):821-9.

(224) Snoek-van Beurden PA, Von den Hoff JW. Zymographic techniques for the analysis of matrix metalloproteinases and their inhibitors. *Biotechniques* 2005;38(1):73-83.

(225) Kirk JME, Dacosta PE, Turnerwarwick M, Littleton RJ, Laurent GJ. Biochemical-Evidence for an Increased and Progressive Deposition of Collagen in Lungs of Patients with Pulmonary Fibrosis. *Clin Sci Clin Sci* 1986;70(1):39-45.

(226) Carmeliet P. Proteinases in cardiovascular aneurysms and rupture: targets for therapy? *J Clin Invest* 2000;105(11):1519-20.

(227) Longo GM, Xiong W, Greiner TC, Zhao Y, Fiotti N, Baxter BT. Matrix metalloproteinases 2 and 9 work in concert to produce aortic aneurysms. *J Clin Invest* 2002;110(5):625-32.

(228) Parks WC. A confederacy of proteinases. *J Clin Invest* 2002;110(5):613-4.

(229) Pyo R, Lee JK, Shipley JM, Curci JA, Mao D, Ziporin SJ, Ennis TL, Shapiro SD, Senior RM, Thompson RW. Targeted gene disruption of matrix metalloproteinase-9 (gelatinase B) suppresses development of experimental abdominal aortic aneurysms. *J Clin Invest* 2000;105(11):1641-9.

(230) Gough PJ, Gomez IG, Wille PT, Raines EW. Macrophage expression of active MMP-9 induces acute plaque disruption in apoE-deficient mice. *J Clin Invest* 2006;116(1):59-69.

(231) Janssens S, Lijnen HR. What has been learned about the cardiovascular effects of matrix metalloproteinases from mouse models? *Cardiovasc Res* 2006;69(3):585-94.

(232) Lemaitre V, O'Byrne TK, Borczuk AC, Okada Y, Tall AR, D'Armiento J. ApoE knockout mice expressing human matrix metalloproteinase-1 in macrophages have less advanced atherosclerosis. *J Clin Invest J Clin Invest* 2001;107(10):1227-34.

(233) Takaishi H, Kimura T, Dalal S, Okada Y, D'Armiento J. Joint diseases and matrix metalloproteinases: a role for MMP-13. *Curr Pharm Biotechnol* 2008;9(1):47-54.

(234) Burrage PS, Mix KS, Brinckerhoff CE. Matrix metalloproteinases: role in arthritis. *Front Biosci* 2006;11:529-43.

(235) McMillan JI, Riordan JW, Couser WG, Pollock AS, Lovett DH. Characterization of a glomerular epithelial cell metalloproteinase as matrix metalloproteinase-9 with enhanced expression in a model of membranous nephropathy. *J Clin Invest* 1996;97(4):1094-101.

(236) Schanstra JP, Neau E, Drogoz P, revalo Gomez MA, Lopez Novoa JM, Calise D, Pecher C, Bader M, Girolami JP, Bascands JL. In vivo bradykinin B2 receptor activation reduces renal fibrosis. *J Clin Invest* 2002;110(3):371-9.

(237) Schubert C. Remodeling in the kidney. *Nat Med* 2006;12(4):391.

(238) Zeisberg M, Khurana M, Rao VH, Cosgrove D, Rougier JP, Werner MC, Shield CF, III, Werb Z, Kalluri R. Stage-specific action of matrix metalloproteinases influences progressive hereditary kidney disease. *PLoS Med* 2006;3(4):e100.

(239) Crawford HC, Scoggins CR, Washington MK, Matrisian LM, Leach SD. Matrix metalloproteinase-7 is expressed by pancreatic cancer precursors and regulates acinar-to-ductal metaplasia in exocrine pancreas. *J Clin Invest* 2002;109(11):1437-44.

(240) Gurlek A, Karavitaki N, Ansorge O, Wass JA. What are the markers of aggressiveness in prolactinomas? Changes in cell biology, extracellular matrix components, angiogenesis and genetics. *Eur J Endocrinol* 2007;156(2):143-53.

(241) Vargo-Gogola T, Fingleton B, Crawford HC, Matrisian LM. Matrilysin (matrix metalloproteinase-7) selects for apoptosis-resistant mammary cells in vivo. *Cancer Res* 2002;62(19):5559-63.

(242) Saarialho-Kere UK, Chang ES, Welgus HG, Parks WC. Distinct localization of collagenase and tissue inhibitor of metalloproteinases expression in wound healing associated with ulcerative pyogenic granuloma. *J Clin Invest* 1992;90(5):1952-7.

(243) Toriseva MJ, Ala-aho R, Karvinen J, Baker AH, Marjomaki VS, Heino J, Kahari VM. Collagenase-3 (MMP-13) enhances remodeling of three-dimensional collagen and promotes survival of human skin fibroblasts. *J Invest Dermatol* 2007;127(1):49-59.

(244) Gomez DE, De Lorenzo MS, Alonso DF, Andrade ZA. Expression of metalloproteinases (MMP-1, MMP-2, and MMP-9) and their inhibitors (TIMP-1 and TIMP-2) in schistosomal portal fibrosis. *Am J Trop Med Hyg Am J Trop Med Hyg* 1999;61(1):9-13.

(245) Iimuro Y, Brenner DA. Matrix metalloproteinase gene delivery for liver fibrosis. *Pharm Res* 2008;25(2):249-58.

(246) Lanone S, Zheng T, Zhu Z, Liu W, Lee CG, Ma B, Chen Q, Homer RJ, Wang J, Rabach LA, Rabach ME, Shipley JM, Shapiro SD, Senior RM, Elias JA. Overlapping and enzyme-specific contributions of matrix metalloproteinases-9 and -12 in IL-13-induced inflammation and remodeling. *J Clin Invest* 2002;110(4):463-74.

(247) Matute-Bello G, Wurfel MM, Lee JS, Park DR, Frevert CW, Madtes DK, Shapiro SD, Martin TR. Essential role of MMP-12 in Fas-induced lung fibrosis. *Am J Respir Cell Mol Biol* 2007;37(2):210-21.

(248) Ra HJ, Parks WC. Control of matrix metalloproteinase catalytic activity. *Matrix Biol* 2007;26(8):587-96.

(249) Hayashi T, Stetler-Stevenson WG, Fleming MV, Fishback N, Koss MN, Liotta LA, Ferrans VJ, Travis WD. Immunohistochemical study of metalloproteinases and their tissue inhibitors in the lungs of patients with diffuse alveolar damage and idiopathic pulmonary fibrosis
32. *Am J Pathol* 1996 October;149(4):1241-56.

(250) Pardo A, Selman M. Idiopathic pulmonary fibrosis: new insights in its pathogenesis. *Int J Biochem Cell B Int J Biochem Cell B* 2002;34(12):1534-8.

(251) Ruiz V, Ordâoänez RM, Berumen J, Ramâirez R, Uhal B, Becerril C, Pardo A, Selman M, Instituto Nacional de Enfermedades Respiratorias MC. Unbalanced collagenases/TIMP-1 expression and epithelial apoptosis in experimental lung fibrosis. *American journal of physiology Lung cellular and molecular physiology* 2003;285(5):L1026-L1036.

(252) Lemjabbar H, Gosset P, Lamblin C, Tillie I, Hartmann D, Wallaert B, Tonnel AB, Lafuma C. Contribution of 92 kDa gelatinase/type IV collagenase in bronchial inflammation during status asthmaticus. *Am J Respir Crit Care Med* 1999;159(4 Pt 1):1298-307.

(253) Suga M, Iyonaga K, Okamoto T, Gushima Y, Miyakawa H, Akaike T, Ando M. Characteristic elevation of matrix metalloproteinase activity in idiopathic interstitial pneumonias. *Am J Resp Crit Care Am J Resp Crit Care* 2000;162(5):1949-56.

(254) Fukuda Y, Ishizaki M, Kudoh S, Kitaichi M, Yamanaka N. Localization of matrix metalloproteinases-1, -2, and -9 and tissue inhibitor of metalloproteinase-2 in interstitial lung diseases
59. *Lab Invest* 1998 June;78(6):687-98.

(255) Henry MT, McMahon K, Mackarel AJ, Prikk K, Sorsa T, Maisi P, Sepper R, FitzGerald MX, O'Connor CM. Matrix metalloproteinases and tissue inhibitor of

metalloproteinase-1 in sarcoidosis and IPF. *Eur Respir J Eur Respir J* 2002;20(5):1220-7.

(256) Rosas IO, Richards TJ, Konishi K, Zhang Y, Gibson K, Lokshin AE, Lindell KO, Cisneros J, Macdonald SD, Pardo A, Sciurba F, Dauber J, Selman M, Gochuico BR, Kaminski N. MMP1 and MMP7 as potential peripheral blood biomarkers in idiopathic pulmonary fibrosis
1. *PLoS Med* 2008 April 29;5(4):e93.

(257) D'Armiento J, Dalal SS, Okada Y, Berg RA, Chada K. Collagenase expression in the lungs of transgenic mice causes pulmonary emphysema. *Cell* 1992;71(6):955-61.

(258) Foronjy R, Nkyimbeng T, Wallace A, Thankachen J, Okada Y, Lemaitre V, D'Armiento J. Transgenic expression of matrix metalloproteinase-9 causes adult-onset emphysema in mice associated with the loss of alveolar elastin. *American journal of physiology Lung cellular and molecular physiology* 2008 June;294(6):L1149-L1157.

(259) Imai K, Dalal SS, Chen ES, Downey R, Schulman LL, Ginsburg M, D'Armiento J. Human collagenase (matrix metalloproteinase-1) expression in the lungs of patients with emphysema. *Am J Respir Crit Care Med* 2001;163(3 Pt 1):786-91.

(260) Hautamaki RD, Kobayashi DK, Senior RM, Shapiro SD. Requirement for macrophage elastase for cigarette smoke-induced emphysema in mice. *Science* 1997;277(5334):2002-4.

(261) Vincenti MP, Brinckerhoff CE. Transcriptional regulation of collagenase (MMP-1, MMP-13) genes in arthritis: integration of complex signaling pathways for the recruitment of gene-specific transcription factors. *Arthritis Res Arthritis Res* 2002;4(3):157-64.

(262) Yan L, Zucker S, Toole BP. Roles of the multifunctional glycoprotein, emmprin (basigin; CD147), in tumour progression. *Thromb Haemost* 2005;93(2):199-204.

(263) Woessner JF, Jr. Quantification of matrix metalloproteinases in tissue samples. *Methods Enzymol* 1995;248:510-28.

(264) Yan SJ, Blomme EA. In situ zymography: a molecular pathology technique to localize endogenous protease activity in tissue sections. *Vet Pathol* 2003;40(3):227-36.

(265) Campbell EJ, Campbell MA. Pericellular proteolysis by neutrophils in the presence of proteinase inhibitors: effects of substrate opsonization. *J Cell Biol* 1988;106(3):667-76.

(266) Berbescu EA, Katzenstein AL, Snow JL, Zisman DA. Transbronchial biopsy in usual interstitial pneumonia. *Chest Chest* 2006;129(5):1126-31.

(267) Hunninghake GW, Lynch DA, Galvin JR, Gross BH, Muller N, Schwartz DA, King TE, Lynch JP, Hegele R, Waldron J, Colby TV, Hogg JC. Radiologic findings are strongly associated with a pathologic diagnosis of usual interstitial pneumonia. *Chest Chest* 2003;124(4):1215-23.

(268) Katzenstein AL, Fiorelli RF. Nonspecific interstitial pneumonia/fibrosis. Histologic features and clinical significance. *Am J Surg Pathol* 1994;18(2):136-47.

(269) Ortiz LA, Lasky J, Gozal E, Ruiz V, Lungarella G, Cavarra E, Brody AR, Friedman M, Pardo A, Selman M. Tumor necrosis factor receptor deficiency alters matrix metalloproteinase 13/tissue inhibitor of metalloproteinase 1 expression in murine silicosis. *Am J Respir Crit Care Med* 2001;163(1):244-52.

(270) Deguchi JO, Aikawa E, Libby P, Vachon JR, Inada M, Krane SM, Whittaker P, Aikawa M. Matrix metalloproteinase-13/collagenase-3 deletion promotes collagen accumulation and organization in mouse atherosclerotic plaques. *Circulation Circulation* 2005;112(17):2708-15.

(271) Swiderski RE, Dencoff JE, Floerchinger CS, Shapiro SD, Hunninghake GW. Differential expression of extracellular matrix remodeling genes in a murine model of bleomycin-induced pulmonary fibrosis. *Am J Pathol Am J Pathol* 1998;152(3):821-8.

(272) Balbin M, Fueyo A, Tester AM, Pendas AM, Pitiot AS, Astudillo A, Overall CM, Shapiro SD, Lopez-Otin C. Loss of collagenase-2 confers increased skin tumor susceptibility to male mice. *Nat Genet* 2003 November;35(3):252-7.

(273) Rovai LE, Herschman HR, Smith JB. The murine neutrophil-chemoattractant chemokines LIX, KC, and MIP-2 have distinct induction kinetics, tissue distributions, and tissue-specific sensitivities to glucocorticoid regulation in endotoxemia. *J Leukoc Biol* 1998 October;64(4):494-502.

(274) Raulo SM, Sorsa TA, Kiili MT, Maisi PS. Evaluation of collagenase activity, matrix metalloproteinase-8, and matrix metalloproteinase-13 in horses with chronic obstructive pulmonary disease. *Am J Vet Res Am J Vet Res* 2001;62(7):1142-8.

(275) Dozier S, Escobar GP, Lindsey ML. Matrix metalloproteinase (MMP)-7 activates MMP-8 but not MMP-13. *Med Chem* 2006;2(5):523-6.

(276) Foronjy RF, Okada Y, Cole R, D'Armiento J, Department of Medicine DoMM, Pulmonary Medicine CUNYNY. Progressive adult-onset emphysema in transgenic mice expressing human MMP-1 in the lung. *American journal of physiology Lung cellular and molecular physiology* 2003;284(5):L727-L737.

10. ERKLÄRUNG

“Ich erkläre: Ich habe die vorgelegte Dissertation selbständig, ohne unerlaubte fremde Hilfe und nur mit den Hilfen angefertigt, die ich in der Dissertation angegeben habe. AlleTextstellen, die wörtlich oder sinngemäß aus veröffentlichten oder nicht veröffentlichten Schriften entnommen sind, und alle Angaben, die auf mündlichen Auskünften beruhen, sind als solche kenntlich gemacht. Bei den von mir durchgeführten und in der Dissertation erwähnten Untersuchungen habe ich die Grundsätze guter wissenschaftlicher Praxis, wie sie in der „Satzung der Justus-Liebig-Universität Gießen zur Sicherung guter wissenschaftlicher Praxis“ niedergelegt sind, eingehalten.”

_____ _____

Eusebius Henry Nkyimbeng Takwi Datum

11. ACKNOWLEDGEMENT

I would like to express my profound gratitude to Prof. Dr. Werner Seeger for giving me the opportunity to learn not only science in the International Graduate program but train to become a good scientist. Professor Seeger, you have positively changed my future.I have drawn enormous inspiration from your steadfastness in science, medicine, management and life.

I would like to express my sincere appreciation to Dr. Oliver Eickelberg, Director of the International Graduate Program, Signalling Mechanisms in Lung Physiology and Disease (SMLPD) and Molecular Biology and Medicine of the Lung (MBML) and the MBML faculty for their enormous efforts in making the program progress successfully. Oli, thank you so much for the countless times you have given me academic and moral support, especially during the period of my exhange training in New York.

I would like to sincerely thank Prof. Dr. Andreas Günther, my PI, for his efforts and contribution to my learning, and for enormous patience and guidance. I learnt as much as I could from his scientific insight and optimism I would also like to express my sincere gratitude to Prof. Dr. Jeanine D'Armiento of Columbia University, my Co-PI, for her profound support, guidance and scientific motivation during my stay in her laboratory.

I sincerely thank the postdoctoral fellows and technical staff in the Gunther and D'Armiento laboratories, and Dr. Karin Endres for all their support. My special thanks go to my colleagues in MBML for their contribution to make the study an interactive, interesting and enjoying of its kind. Bhola, Fotini and Markus, thank you for always being there.

Finally, I am indebted to my parents and family (in particular Mami ANN, MaAwah, Aunty Ben, Uncle Sulle, WNK, Ndia Che, Nche, Anye), family and friends for their enormous support throughout my training.

I dedicate this thesis to Joseph Ndeh Nkyimbeng, my father, of blessed memory.

12. CURRICULUM VITAE

Eusebius Henry, Nkyimbeng-Takwi

Current Address
Columbia University,
College of Physicians and Surgeons,
630 West 168th Street, P&S 9-449 ,
New York, NY 10032, U.S.A

Permanent Address
Ntarinkon, Mankon
P.O.Box 883 Mankon
North West Province
Cameroon

takwi.nkyimbeng@uglc.de
tn2182@columbia.edu
takwi.nkyimbeng@gmail.com

EDUCATION

Oct. 2004 – Aug 2008: **Doctor of Philosophy of Science (PhD)**, University of Giessen and Marburg, Germany/Columbia University, New York.

Dissertation: *Extracellular matrix remodeling by Matrix Metalloproteinases in the lung.*

Oct. 2004 - Sep.2006: **Certificate of completion**. International Graduate Program, "Molecular Biology and Medicine of the Lung (MBML), University of Giessen Lung Centre, Giessen, Germany.

Oct.2003 -Sep.2004: Research Assisitant, Vrije Universiteit Brussel, Belgium.

Project: *The effects of macrophage alternative activation marker FIZZ1 on the molecular and functional properties of macrophages and the underlying mechanisms.*

2003: **Master of Science**, Molecular Biology (Distinction)
Sep.2001 - Sep.2003: Interuniversity Program Molecular Biology (IPMB)
Vrije Universiteit Brussel, Brussel, Belgium.

Dissertation: *Cloning, expression and purification of mouse FIZZ1 and generation of anti-FIZZ1 monoclonal antibodies.*

1990 - 1995: **Bachelor of Science**, Biochemistry (1st Class Hons)
University of Calabar, Nigeria.

Dissertation: *In vitro studies on ascorbic acid deficient guinea pigs treated with ivermectin.*

HONORS

2004 -2008: DFG/SMLPD Scholarship for PhD training, Giessen, Germany

2001-2003: Flemish Interuniversity Council (VLIR) Scholarship for Master of Science studies, Brussels, Belgium

12/1996: Professor Dunstan Akintonwa Prize for Best graduand in Biochemistry (Convocation prizes & awards, University of Calabar, Nigeria)

12/1996: Elder Chief Grace A. Edet Prize for Best Graduand in Biochemistry (Convocation prizes & awards, University of Calabar, Nigeria)

1994/95: Certificate of Honor from Calabar University Biochemistry Students Association (CUBSA)

1992/93: Certificate of Honor from Calabar University Biochemistry Students Association (CUBSA).

JOB EXPERIENCE

2001 : McHenry Rural Health Care, Gelli Ddyfod, Wales, U. K.
Co -founder and trustee. Organized field training on health education and sensitization on HIV/AIDS/TB

1996 - 2001: Capitol Health Services, Bamenda, Cameroon.
Assistant Coordinator in charge of internship and training of community nurses.

1996 - 2000: International University, Bamenda, Cameroon
(Part-time) Facilitator of problem-based learning sessions in Biochemistry to 1st and 2nd year medical students.

1996 -1996: General Hospital, Bamenda, North West Province, Cameroon
Specimen collection and analysis: Clinical chemistry unit and Blood bank /HIV screening laboratory.

1995 -1996: Institute of Veterinary Research, Mankon Center, Cameroon.
Assistant, Biochemistry Department.
Supervisor: Fabian Ekue (DVM, PhD).

PUBLICATIONS

Utu Baku B, Umoh IB, Ebong PE, **Nkyimbeng HT,** Abara AE.
Influence of low ascorbic acid on RNA/Protein ratio and hepatic lipids in ivermectin (Mectizan) treated guinea pigs. Global Journal of Pure and Applied Sciences 1999 5(4):513-518.

Foronjy RF, **Nkyimbeng T**, Wallace AM, Thankachen J, Okada Y, Lemaitre V, D'Armiento JM. The Transgenic Expression of Matrix Metalloproteinase-9 Causes Adult-Onset Emphysema in Mice Associated with the Loss of Alveolar Elastin.
Am J Physiol Lung Cell Mol Physiol. 2008 Apr 11.

POSTER PRESENTATIONS

Nkyimbeng, T., Shiomi, T., Okada, Y., Seeger, W., Günther A., D'Armiento J. (2008)
Role of MMP-13 in Bleomycin induced pulmonary fibrosis in mice.
Annual Congress of the American Thoracic Society, Toronto, Canada, 16-22 May 2008.

Nkyimbeng, T., Ruppert, C., Lang, G., Seeger W., Günther A. (2007)
Characterization of matrix metalloproteinase (MMP) expression and activity in the lungs of patients with Idiopathic Pulmonary Fibrosis (IPF). *Annual Congress of the American Thoracic Society, San Francisco, California, U.S.A, 18-23 May 2007*

Nkyimbeng, T., Ruppert, C., Seeger, W., and Günther, A. (2007)
Characterization of matrix metalloproteinase (MMP) expression and activity in the lungs of patients with Idiopathic Pulmonary Fibrosis (IPF). *Keystone Symposium: Molecular Mechanisms of Fibrosis: From Bench to Bedside, Tahoe City, California, U.S.A., 11-15 March 2007*

Nkyimbeng T., Ruppert C., Klepetko W., Seeger W., Günther A. (2006)
Characterization of matrix metalloproteinase (MMP) expression and activity in the lungs of patients with Idiopathic Pulmonary Fibrosis (IPF). *14th International Colloquium on Lung Fibrosis (ICLF), Etville-Erbach, Germany, 7-10 September 2006.*

ORAL PRESENTATIONS

Nkyimbeng T., Ruppert C., Markart P., Korfei M., Schmidt R., Seeger W., Günther A. (2006) Characterization of matrix metalloproteinase (MMP) expression and activity in the lungs of patients with Idiopathic Pulmonary Fibrosis (IPF). *47th Congress of German Society for Pneumology, Nürnberg, Germany, 29 March – 1 April, 2006.*

Nkyimbeng T., Ruppert C., Markart P., Korfei M., Schmidt R., Seeger W., Günther A. (2008) Characterization of matrix metalloproteinase (MMP) expression and activity in the lungs of patients with Idiopathic Pulmonary Fibrosis (IPF). *German Society for Pneumology /Cell Biology, Bonn, Germany, 14- 15 October 2005*